ORNL/TM-2024/3248

Current State of Benchmark Applicability for Commercial-Scale HALEU Fuel Transport

Lisa Fassino
Mathieu N. Dupont
Iyad Al-Qasir
William A. Wieselquist
William B.J. Marshall

March 2024

OAK RIDGE
National Laboratory

ORNL IS MANAGED BY UT-BATTELLE LLC FOR THE US DEPARTMENT OF ENERGY

ORNL/TM-2024/3248

Nuclear Energy and Fuel Cycle Division

CURRENT STATE OF BENCHMARK APPLICABILITY FOR COMMERCIAL-SCALE HALEU FUEL TRANSPORT

Lisa Fassino
Mathieu N. Dupont
Iyad Al-Qasir
William A. Wieselquist
William B. J. Marshall

March 2024

Prepared by
OAK RIDGE NATIONAL LABORATORY
Oak Ridge, TN 37831
managed by
UT-BATTELLE LLC
for the
US DEPARTMENT OF ENERGY
under contract DE-AC05-00OR22725

CONTENTS

LIST OF TABLES

LIST OF FIGURES

ABBREVIATIONS

ACU	Abilene Christian University
AGN-201M	Aerojet General Nucleonics Model 201
AGR	advanced gas reactor
ARC	advanced reactor concepts
ARC-100	Advanced Reactor Concepts 100-MWe SFR SMR
ARDP	Advanced Reactor Demonstration Program
BANR	BWXT Advanced Nuclear Reactor
BISO	bi-structural isotropic
BMR	Brazilian Multipurpose Reactor
BWR	boiling water reactor
BWXT	BWX Technologies
CCR	criticality control rod
CCV	cask containment vessel
CE	continuous energy
C/E	calculated over expected k_{eff}
CLUTCH	contributon-linked eigenvalue sensitivity/uncertainty estimation via track-length importance characterization
CNPS	Compact Nuclear Power Source
CoC	Certificate of Compliance
DICE	Database for the International Handbook of Evaluated Criticality Safety Benchmark Experiments
DoD	U.S. Department of Defense
DOE	U.S. Department of Energy
DARPA	Defense Advanced Research Projects Agency
DNCSH	US Department of Energy and Nuclear Regulatory Commission Collaboration for Criticality Safety Support for Commercial-Scale HALEU Fuel Cycles and Transportation
DRACO	Demonstration Rocket for Agile Cislunar Operations
EALF	energy corresponding to the average lethargy causing fission
EBR-II	Experimental Breeder Reactor II
eV	electron volt
FCA	fast critical assembly
FCC	face-centered cubic
FCM®	Fully Ceramic Microencapsulated
FFTF	Fast Flux Test Facility
FHR	fluoride salt-cooled high-temperature reactor
FMR	fast modular reactor
GA-EMS	General Atomics Electromagnetic Systems
GCFR	gas-cooled fast reactor
GNDS	Generalised Nuclear Database Structure
GNF-A	Global Nuclear Fuel-Americas
HALEU	High-Assay Low-Enriched Uranium
HC-HTGR	Horizontal Compact-High-Temperature Gas-cooled Reactor
HEU	highly enriched uranium
HTGR	high-temperature gas-cooled reactor
HTP	HALEU Transport Package
HTTR	High-Temperature Test Reactor

ICSBEP	International Criticality Safety Benchmark Evaluation Project
IDAT	International Reactor Physics Evaluation project Database and Analysis Tool
IFP	iterated fission probability
INL	Idaho National Laboratory
IRPhE	International Reactor Physics Evaluation project
JAEA	Japan Atomic Energy Agency
KP-FHR	Kairos Power Fluoride Salt-Cooled High-Temperature Reactor
KUCA	Kyoto University Critical Assembly
LANL	Los Alamos National Laboratory
LEU	low-enriched uranium
LLNL	Lawrence Livermore National Laboratory
LMFR	liquid metal-cooled fast reactor
LMT	Low-enriched-uranium-Metal-Thermal (LEU-MET-THERM)
LST	Low-enriched-uranium-Solution-Thermal (LEU-SOL-THERM)
LWR	light-water reactor
MARVEL	Microreactor Applications Research Validation and Evaluation
MCFR	Molten Chloride Fast Reactor
MCRE	Molten Chloride Reactor Experiment
MFC	Materials and Fuels Complex
MIGHTR	Modular Integrated Gas-Cooled High-Temperature Reactor
MIT	Massachusetts Institute of Technology
MG	multigroup
MMR	micro modular reactor
MOU	Memorandum of Understanding
MOS	Margin of Subcriticality
MSRE	Molten Salt Reactor Experiment
MSR	molten salt reactor
MSRR	Molten Salt Research Reactor
MURR	Missouri University Research Reactor
NASA	National Aeronautics and Space Administration
NCERC	National Criticality Experiments Research Center
NEUP	Nuclear Energy University Program
NEXT Lab	Nuclear Energy eXperimental Testing Laboratory
NEXTRA	Nuclear Energy eXperimental Research Alliance
NFS	Nuclear Fuel Services
NNSS	Nevada National Security Sites
NRC	US Nuclear Regulatory Commission
NTS	Nuclear Transport Solutions
N/A	Not Applicable
OP	Outer Packaging
OPTIMUS®	OPTImal Modular Universal Shipping package
ORNL	Oak Ridge National Laboratory
pcm	Percent mille
PDOS	phonon density of states
PSI	Paul Scherrer Institute
PWR	pressurized water reactor
RCF	reactor critical facility
RPI	Rensselaer Polytechnic Institute
$S(\alpha,\beta)$	thermal neutron scattering law

SANS	small-angle neutron scattering
SFR	sodium-cooled fast reactor
SMR	small modular reactor
SMR-160	Holtec International's 160-MW SMR
SNL	Sandia National Laboratory
SNS	Spallation Neutron Source
SPRF/CX	Sandia Pulsed Reactor Facility – Critical Experiments
STACY	Static Experiment Critical Facility
S/U	sensitivity/uncertainty
TF3	TRISO-X Fuel Fabrication Facility
TRISO	Tri-structural Isotropic
TRISO-X	X-Energy's Proprietary TRISO particle fuel
TSL	Thermal neutron Scattering Law
USL	upper subcritical limit
USNC	Ultra Safe Nuclear Corporation
WPEC	Working Party on International Nuclear Data Evaluation Cooperation
WPNCS	Working Party on Nuclear Criticality Safety
VADER	Validation Analysis Data Evaluation Resource
VALID	ORNL Verified, Archived Library of Inputs and Data
VHTRC	Very High Temperature Reactor Critical assembly
VP-55	55-Gallon Versa Pac
VP-110	110-Gallon Versa Pac
ZED-2	Zero Energy Deuterium-2 reactor
ZPPR	Zero-Power Physics Reactor

ABSTRACT

Safe and economical operations within new HALEU-based fuel cycles may require new benchmarks to support criticality safety. Recognizing this need, congress has authorized funding for the US Department of Energy (DOE) and Nuclear Regulatory Commission (NRC) Collaboration for Criticality Safety Support for Commercial-Scale HALEU Fuel Cycles and Transportation (DNCSH), a project with scope to streamline future criticality safety-related applications to the NRC, regarding the quality of relevant benchmark data for the front-end and back-end of HALEU-based fuel cycles. These activities support industry as well, as reductions in bias and uncertainty may enable more economical activities without compromising safety, e.g. the ability to transport a larger amount of fresh fuel on one conveyance.

For background, this report provides a single-source summary of: i) reactor fuel forms currently designed to utilize HALEU fuel, focusing on DOE-supported Advanced Reactor Demonstration Program (ARDP) designs; ii) facilities for HALEU production or fuel fabrication; and iii) NRC-approved HALEU transportation packages. With respect to fresh fuel transportation, we can remark that transportation packages exist for potential increases in enrichment in commercial light water reactor (LWR) fuel of up to 8%. Advanced reactors with TRISO particle fuel and graphite are prevalent. There is the ability today to transport HALEU, but not yet at commercial-scale or for upcoming advanced reactor fuel forms (e.g. full-sized sodium-fast reactor assemblies), with the exception of the DN-30X UF_6 transportation package. Based on this survey, there appears to be potential needs for nuclear data and benchmarks to support criticality safety applications.

In the remaining sections, we survey existing criticality safety evaluations for HALEU, facilities suitable for new critical experiments, and nuclear data aspects relevant for HALEU-based fuel cycles. There are enough gaps in quality and quantity of experiments and data to warrant the development of application models which can more precisely highlight gaps in the validation basis, e.g. a large-scale pebble transport package to investigate the validation basis for graphite and TRISO particle fuel systems. Notably, the readiness assessment reveals that while benchmark coverage in the HALEU enrichment range is good across energy spectrums, there is a diversity of fuel forms, moderators, and potentially transportation strategies that warrants development of generic front-end and back-end application models with neutronically relevant materials that can uncover gaps across all HALEU ARDP, and potentially other, advanced reactor designs.

1. INTRODUCTION

The Inflation Reduction Act of 2022 (H.R. 5376) includes several sections that bolster support for the nuclear industry and the development of advanced reactor technology and fuels. Section 50173 secures funding to support the availability of high-assay low-enriched uranium (HALEU) through FY 2026 [1]. HALEU fuel is a classification within the low-enriched uranium (LEU) range, and it spans enrichments between 5 and 20 wt% ^{235}U, making them applicable in reactors with higher energy densities compared to those of typical commercial nuclear fuels enriched to 3–5 wt% ^{235}U [2]. The next wave of advanced fission reactors relies heavily on HALEU in various forms for their designs. Ten such designs are currently supported under the Advanced Reactor Demonstration Program (ARDP), a US Department of Energy (DOE)–sponsored initiative to speed up the demonstration of advanced fission reactors through cost-shared partnerships with US industry [3]. The ten reactors are split into three categories based on technological maturity: demonstration (operational within 5–7 years), risk reduction (support demonstration within 10–14 years), and concept development (potential demonstration by mid-2030s) [4]. A comprehensive, up-to-date review of benchmark applicability for HALEU transport spanning the multitude of upcoming advanced reactor fuel forms as well as pathways to address gaps is essential to ensure that key stakeholders in regulatory bodies, research, and industry are prepared for the integration of these advanced reactor fuels.

Comprehensive nuclear criticality safety analysis is paramount to the integration of HALEU fuels for advanced reactor fuel cycles in compliance with 10 CFR Parts 70 and 71. New safety analyses must justify where the current validation basis is applicable for the higher enrichments, different materials, fuel forms, and storage configurations inherent to these advanced reactor designs, and any gaps in applicability must be identified and addressed. This report provides a scoping assessment to collect key insights on recent HALEU fuel–related analyses and activities, including a summary of relevant and available design characteristics for the ten ARDP reactors; facilities known to be involved in production or management of HALEU and transportation packages suitable for HALEU; benchmark experiments applicable for HALEU designs, detailing completed evaluations as well as in-progress experiments and evaluations; existing facilities capable of performing new experiments for HALEU validation; and current and upcoming thermal neutron scattering law (TSL) libraries applicable for HALEU modeling and simulation.

2. HALEU IN ADVANCED REACTOR DESIGNS

Despite the barriers to its integration, HALEU is a crucial aspect of many advanced reactor concepts. Its utility lies in supporting longer lifetimes with smaller footprints compared to those in most traditional LEU-fueled designs through higher target burnups and higher energy densities. Identifying the key characteristics of these advanced reactor designs that intend to utilize HALEU is an essential first step in predicting potential validation gaps, which could make licensing transportation packages a challenge. Of the ten ARDP awardees, nine require HALEU fuel. Each of the ten reactors in the ARDP is listed below in their respective pathways.

The two reactors in the demonstration pathway are the following:

1. TerraPower's Natrium: a sodium-cooled fast reactor (SFR)
2. X-energy's Xe-100: a pebble-bed high-temperature gas-cooled reactor (HTGR)

The designs in the risk reduction category include the following:

3. The Kairos Power Fluoride salt-cooled High-temperature Reactor (KP-FHR): a pebble-fueled FHR
4. Westinghouse Nuclear's eVinci™ heat-pipe microreactor
5. The Molten Chloride Fast Reactor (MCFR) by Southern Company and TerraPower: a molten salt reactor (MSR) with dissolved fuel
6. The BWX Technologies (BWXT) Advanced Nuclear Reactor (BANR): an HTGR
7. Holtec International's Small Modular Reactor-160 (SMR-160): an LEU-fueled light-water reactor (LWR)

Lastly, the designs in the concept development stage include the following:

8. Advanced Reactor Concepts' (ARC's) advanced sodium-cooled reactor facility, which will house the ARC-100 SFR/SMR
9. Fast Modular Reactor (FMR) by General Atomics Electromagnetic Systems (GA-EMS): a gas-cooled fast reactor (GCFR) design
10. Horizontal Compact High-Temperature Gas Reactor (HC-HGTR) by the Massachusetts Institute of Technology (MIT)

Not only is HALEU essential to the majority of ARDP awardees, but its utility spans numerous other designs for experimental, demonstration, and power generation purposes. Some of these designs include the following:

- The Project Pele microreactor by the US Department of Defense (DoD) and BWXT
- The Aurora microreactor by Oklo
- The MARVEL microreactor by DOE
- The Demonstration Rocket for Agile Cislunar Operations (DRACO) by the Defense Advanced Research Projects Agency (DARPA) in collaboration with the National Aeronautics and Space Administration (NASA)
- The Hermes test reactor and Hermes 2 SMR by Kairos Power
- The Molten Salt Research Reactor (MSRR) by the Nuclear Energy eXperimental Testing Laboratory (NEXT Lab) at Abilene Christian University (ACU)
- The Ultra Safe Nuclear Corporation (USNC) micro modular reactor (MMR)
- The Lightbridge helically twisted HALEU fuel for current commercial reactors

Although the scope of all HALEU applications is quite large, a great deal of information pertaining to the usage of HALEU in advanced reactor designs can be gathered from examining the ARDP designs. A summary of the most up-to-date publicly available ARDP design information is provided in Table 2-1, but some of this information is expected to change as the designs mature. More information on each reactor design and the applicable sources for the information in Table 2-1 can be found in their relevant subsections below. Details that are not known are kept blank, and details that do not apply are labeled "not applicable" (N/A) in the table.

The latest details on each of these ARDP designs using HALEU are provided below. Relevant experiments and demonstration reactors designed to support licensing are also included. Available information regarding the fabrication and transportation of the fuel types is provided where possible.

Table 2-1. Reactor characteristics for ARDP awardees using HALEU

Lead	Reactor Name	Reactor Type	Neutron Spectrum	Fuel Type	Power	Enrichment (wt% ^{235}U)	Moderator	Reflector	Coolant
TerraPower	Natrium	SFR	Fast	Sodium-bonded Metallic Alloy U-10Zr Pins	345 MWe	19.75	N/A	—	Sodium
X-energy	Xe-100	Pebble Bed HTGR	Thermal	UCO TRISO Particle Spherical Graphite Compacts	80 MWe	15.5	Graphite	Graphite	Helium
Kairos Power	KP-FHR	Pebble Bed FHR	Thermal	UCO TRISO Particle Annular Spherical Graphite Compacts with Low-Density Graphite Cores	140 MWe	19.55	Pyrolytic Graphite, FLiBe	Graphite	FLiBe
Westinghouse Nuclear	eVinci	Heat-pipe Microreactor	Thermal	UCO TRISO Particle Cylindrical Graphite Compacts	5 MWe	19.75	Graphite	—	Sodium Heat Pipes
Southern Company and TerraPower	MCFR	MSR	Fast	Dissolved Uranium in Salt ($NaCl-UCl_3$)	800 MWe	HALEU	N/A	—	Salt
BWXT	BANR	HTGR	Thermal	UN TRISO in SiC/Carbon Matrix Compact, Additively Manufactured	50 MWth	19.75 (Baseline Design)	Graphite	—	Helium
ARC	ARC-100	SFR	Fast	Sodium-bonded U-10Zr pins	100 MWe	20 Max.; 13.1 Avg.	N/A	Stainless Steel	Sodium
GA-EMS	FMR	GFR	Fast	UO_2 Pellets	44 MWe	19.75	N/A	Zr_3Si_2 and Graphite	Helium
MIT	HC-HTGR	HTGR	Thermal	TRISO Particle Graphite Compact	~58 MWth	—	Graphite	—	Helium

2.1 NATRIUM™ BY TERRAPOWER

The Natrium™ reactor design is a pool-type, sodium-cooled fast reactor with a molten salt energy storage system [5]. It is fueled with sodium-bonded metallic fuel pins using uranium enriched up to 19.75 wt% ^{235}U [6]. The reactor will start up using their "Type 1" fuel design and transition to "Type 1B" fuel afterward. The Type 1 fuel is a U-10Zr alloy with a sodium bond to the HT9 cladding, and it is approximately 5 m in length overall, including the shield slug, plenum, and structural components. The material used for the shield slug is not specified. Type 1B fuel is a mechanically bonded "U-0Zr" design, which is formed in an annulus filled with helium and surrounded by a fuel–cladding chemical interaction barrier [7]. A 345 MWe demonstration Natrium™ reactor is planned in Kemmerer, Wyoming, and it will include a molten salt–based energy storage system [8]. Figure 2-1 reproduces a schematic from a presentation to the US Nuclear Regulatory Commission (NRC) by TerraPower [6], and it illustrates some of the differences between the Type 1 and Type 1B fuels.

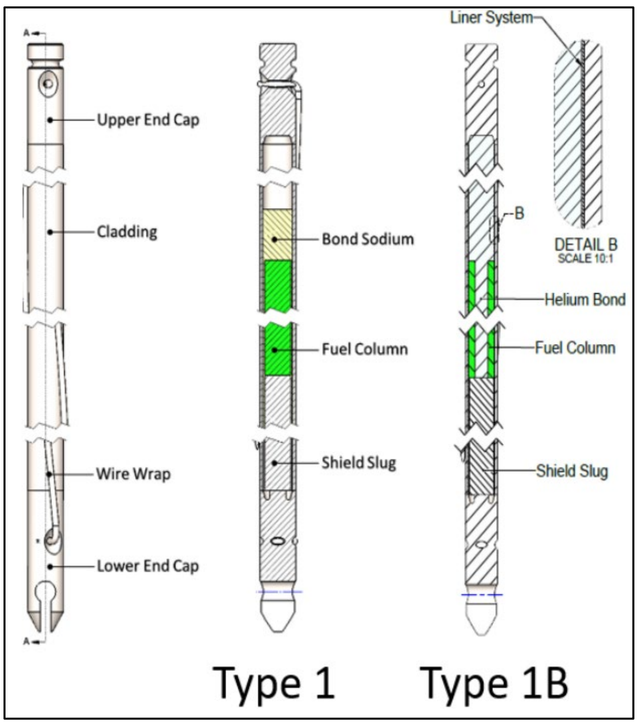

Figure 2-1. Schematic of Type 1 and Type 1B Natrium™ reactor fuels, sourced directly from [6].

In October 2022, Global Nuclear Fuel–Americas (GNF-A) (a GE–Hitachi Nuclear Energy joint venture) and TerraPower announced their agreement to build the Natrium™ Fuel Facility in Wilmington, North Carolina. Construction was expected to begin in 2023, but delays in the HALEU supply chain have postponed most construction plans. However, Centrus and TerraPower maintain a contract to support domestic enrichment capabilities [9].

TerraPower has stated that GNF-A will design and test a new shipping container for unirradiated Natrium™ fuel assemblies that will be suitable for transport via truck. The spent fuel path TerraPower has detailed is similar to that of an LWR, but analysis is underway to investigate how the Type 1–specific fuel characteristics will impact storage requirements [6]. The design similarities to Experimental Breeder

Reactor-II (EBR-II) and Fast Flux Test Facility (FFTF) sodium-bonded metallic U-10Zr fuel pins are expected to support licensing.

2.2 XE-100 BY X-ENERGY

The Xe-100 is a high-temperature, gas-cooled SMR designed by X-energy rated at 80 MWe alone, or 320 MWe in the scaled-up four-pack power plant. A single reactor circulates 220,000 graphite pebbles containing tri-structural isotropic (TRISO) particle fuel. The pebbles are cooled by pressurized helium at 750°C, and control rods of an unspecified material are used for reactivity control [10]. There are approximately 19,000 TRISO particles per 60 mm diameter pebble, and the particles contain UCO kernels enriched to 15.5 wt% ^{235}U [11]. The spherical fuel element contains a 5 mm fuel-free zone at the perimeter of the compact [12].

The Xe-100 fuel is proprietary TRISO-X fuel fabricated from TRISO-X, LLC, a subsidiary company of X-energy [10]. An X-energy news release from April of 2022 announced that X-energy's TRISO-X selected the Oak Ridge Horizon Center for its first advanced reactor fuel fabrication facility in North America. The TRISO-X Fuel Fabrication Facility (TF3) will initially produce 8 MTU/year of fuel, which can support approximately twelve Xe-100 reactors. The TF3 is expected to double that capacity by the early 2030s [13]. The reference design specifications for the TRISO-X pebbles from their 2021 fuel pebble qualification methodology report [12] are reproduced in Figure 2-2 below. No details pertaining to the transport of HALEU material to the TF3 or the transportation of TRISO-X particle compacts from the TF3 were found.

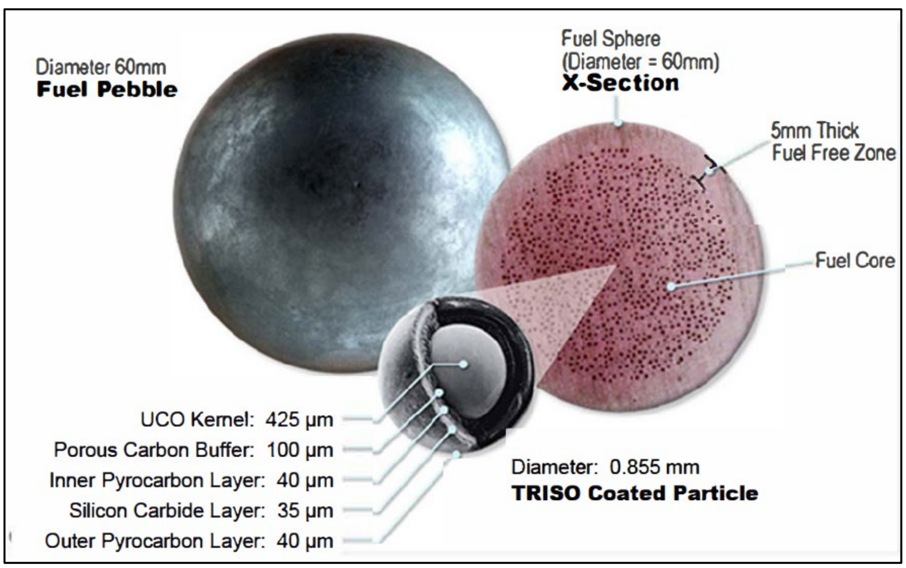

Figure 2-2. Reference fuel element design, taken directly from [12].

2.3 THE KP-FHR AND HERMES REACTOR BY KAIROS POWER

The Kairos Power FHR is a graphite-moderated and FLiBe ($2LiF\text{-}BeF_2$)–cooled reactor that will utilize TRISO particles in graphite pebble compacts for fuel. The rated power output is 140 MWe and 320 MW_{th} with a reactor outlet temperature of 650°C. The Hermitage Center Industrial Park in Oak Ridge, TN, will host the low-power demonstration reactor supporting this design, Hermes, a prototype FHR that will achieve a thermal power of 35 MW_{th} [14]. This reactor will share many design features of the full KP-FHR design. The 4 cm diameter KP-FHR pebble uses a three-region annular design consisting of the innermost sphere, a low-density carbon matrix; the surrounding fuel annulus of TRISO-coated fuel particles in a carbon matrix; and the exterior fuel-free carbon matrix shell. The carbon for the fuel is specifically noted to be pyrolytic graphite, which has different material features than typical nuclear graphite. The TRISO particles used in the fuel features 425 µm UCO kernels enriched to 19.55% ^{235}U, and they are formed using UO_2, UC_2, and UC with a carbon-to-uranium ratio of about 0.1–0.4 [15]. While not known for the KP-FHR yet, the average power per pebble in the Hermes core design is ~1,000 W with a 190-day average residence time that will make 4–6 passes through the core and discharge at 6–8% fissions per initial metal atom. Likewise, the control and shutdown elements are specified for Hermes: B_4C annular elements clad in SS-316H [16]. Although the FLiBe is reported to contribute to 50% of the neutron moderation in the reactor, the pebbles are not expected to be stored or transported in FLiBe [17]. A rendering of their fuel pebble design with the TRISO particle fuel annulus is provided in Figure 2-3.

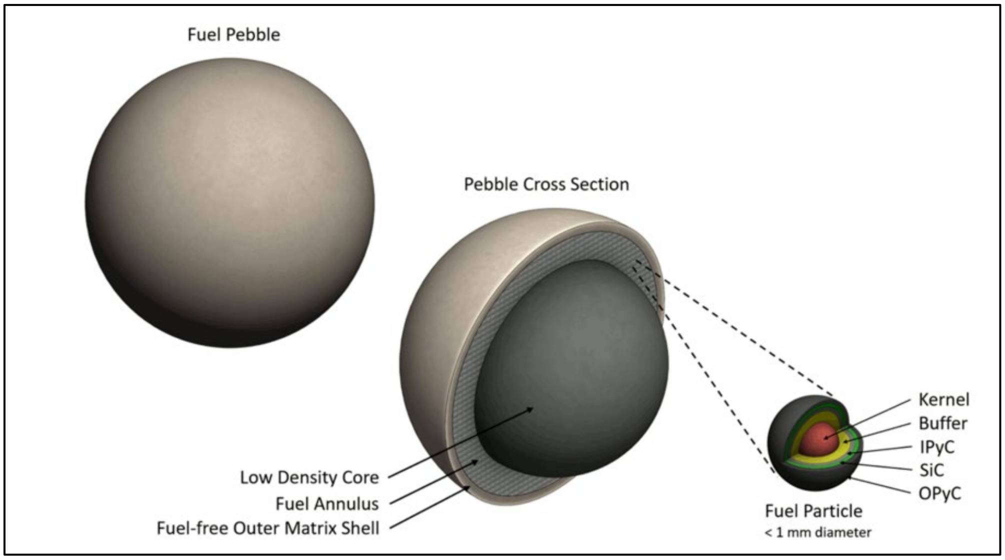

Figure 2-3. Rendering of the Kairos Power fuel pebble, taken directly from [15].

Kairos Power will manufacture the HALEU TRISO particles and annular pebble compacts at the Atlas Fuel Fabrication Facility in the Oak Ridge, TN, East Tennessee Technology Park near the Hermes demonstration test. This facility will be a Category II facility under 10 CFR 70 regulations [15].

The spent fuel storage system consists of stainless-steel storage canisters designed to hold 1,900 to 2,100 pebbles. The canisters will be sealed and transported to a water-filled cooling pool for initial storage, followed by air-cooling [18]. A 2021 presentation by Kairos Power describes the KP-X used fuel canister design as consisting of 38 canisters of 12 in. diameter and 72 in. height arranged inside a 68 in. inner diameter overpack compatible with existing NAC-LWT transport casks [17], and their provided rendering of this design is reproduced in Figure 2-4.

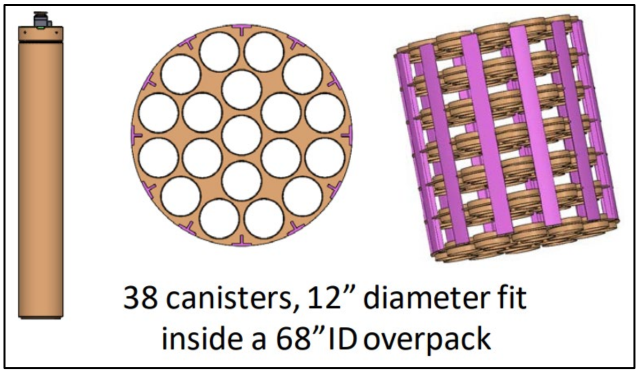

Figure 2-4. KP-FHR used fuel canister design, taken directly from [17].

2.4 WESTINGHOUSE NUCLEAR'S EVINCI REACTOR

The Westinghouse eVinci reactor is a 15 MW_{th} / 5 MWe thermal spectrum reactor that uses heat pipes to transfer high-temperature energy out of the core. The core comprises hexagonal graphite blocks with channels for fuel, burnable absorbers, sodium heat pipes, and shutdown rods. The steel canister enclosing the core is filled with helium, and it is surrounded with a thick radial reflector that includes the control drums [19]. The fuel is UCO HALEU TRISO particles enriched to 19.75% ^{235}U [19, 20]. Figure 2-5 below provides a rendering of the microreactor design from a recent Westinghouse pre-submittal meeting with the NRC [21]. Information for the TRISO particle fabrication could not be found.

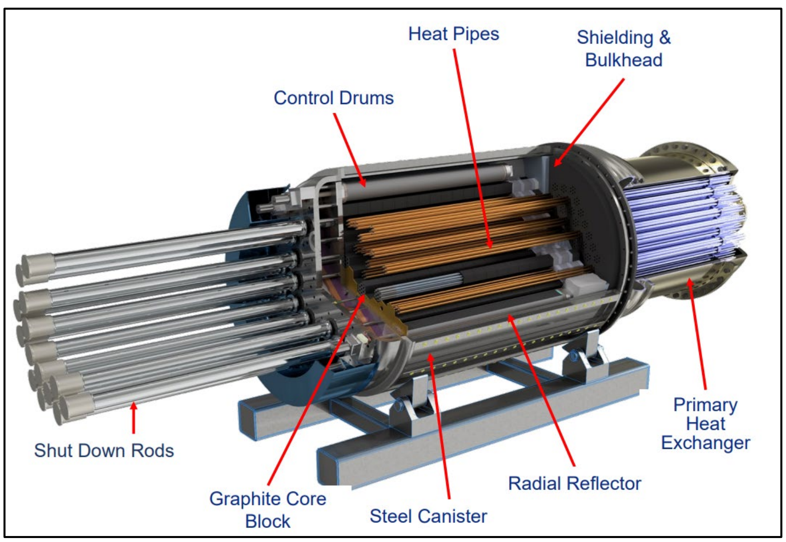

Figure 2-5. eVinci microreactor rendering, taken directly from [21]

The full microreactor system is transported in three parts: the reactor container, instrumentation and control container, and power conversion container [22]; the available rendering of these containers is reproduced in Figure 2-6.

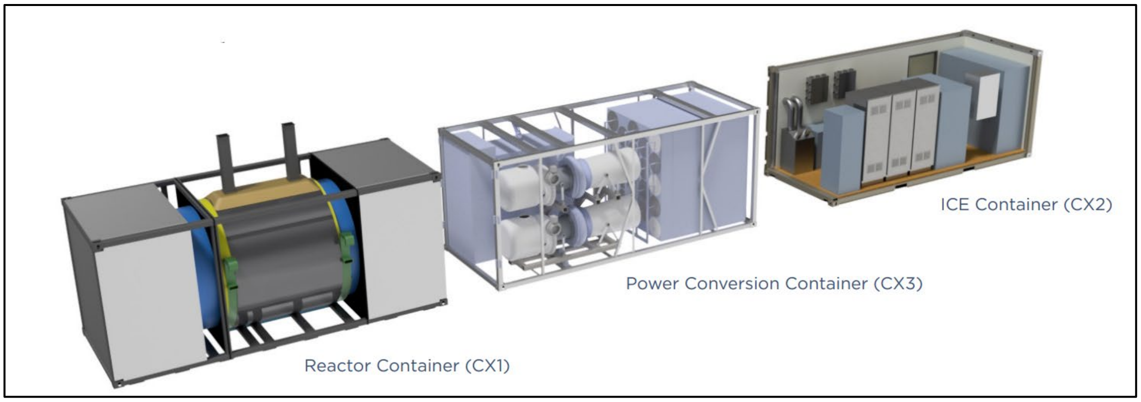

Figure 2-6. eVinci microreactor containers, taken directly from [22].

2.5 THE MOLTEN CHLORIDE FAST REACTOR BY TERRAPOWER AND SOUTHERN COMPANY

The MCFR is a fast-spectrum, molten chloride salt reactor designed by TerraPower to be fueled with dissolved HALEU. Many of the final design parameters for the MCFR are not yet publicly available, and are likely to come after completion of their upcoming experiment, the Molten Chloride Reactor Experiment (MCRE). The MCRE is part of an ARDP award, where TerraPower and Southern Company have partnered to develop the facility and tests which will support licensing of the MCFR. This experiment will use HEU fuel instead of HALEU to minimize the size of the experiment. The conceptual design parameters for the MCRE include a thermal power of 200 kW, maximum fuel salt temperature of 600–700°C, SS-316H structural materials, and Inconel 600/625 cladding materials. The fuel salt for the MCRE is an eutectic mixture of NaCl and UCL_3. The HEU fuel will come from the Zero-Power Physics Reactor (ZPPR) feedstock and will be synthesized into UCl_3 in a fuel salt synthesis line established at the Materials and Fuels Complex (MFC) at Idaho National Laboratory (INL), where the experiment will take place [23]. Beyond a 2021 presentation that notes minor aspects of the MCFR such as the 800 MWe plant power, little information is available on the design [24].

2.6 THE BWXT ADVANCED NUCLEAR REACTOR

BWXT has been developing designs for both a baseline microreactor and the BANR [25]. The baseline design is a thermal spectrum, high-temperature, helium gas–cooled microreactor that can provide 50 MWth using UCO TRISO particle fuel enriched to 19.75% ^{235}U pressed into a graphite matrix [25]. Cladding and moderator for the system are also graphite [25]. The baseline reactor and BANR are expected to ship as a whole unit on a commercial shipping truck flatbed, as seen in Figure 2-7, taken from their 2021 presentation [25].

Figure 2-7. BWXT transport design for their baseline microreactor, taken directly from [25].

Per the BWXT website, the BANR is also a 50MW$_{th}$ design [26]. In contrast to the baseline design that has been noted to have a higher technological/manufacturing readiness level, the BANR is still in the risk-reduction phase [25]. A key distinction is the use of UN TRISO fuel particles for the BANR as well the implementation of advanced manufacturing methods and instrumentation [25]. One such example of the advanced manufacturing method includes additive manufacturing of fuel elements that will be filled with UN TRISO particles, packed with SiC powder, and then densified [27].

As of 2021, BWXT had plans to downblend HEU to HALEU for their HALEU supply, citing the availability of HEU and the desire to avoid transporting UF_6 HALEU [25]. Additionally, they re-started their TRISO particle facility and began establishing a capacity to manufacture TRISO particles to support the needs of their own design as well as that of DoD and NASA for Project Pele and DRACO, respectively [25]. Not limited to BANR, BWXT announced in August of 2023 that they would be producing over two metric tons of 19.75% enriched HALEU fuel over the next five years from government-owned scrap material containing uranium [28]. Though it was not explicitly stated that the BANR will have the same 19.75% enrichment as the baseline design, it is a reasonable expectation given the similarities between the design and current fuel manufacturing efforts.

2.7 ADVANCED REACTOR CONCEPTS' ARC-100

The ARC-100 is a HALEU-fueled, sodium-cooled fast reactor designed for 286 MW$_{th}$/100 MWe. It uses a metal U-10Zr sodium-bonded fuel for power, and it uses a natural convection sodium pool for cooling with an outlet temperature of 510°C. The fuel is expected to have a maximum enrichment of 20 wt% and average enrichment of 13.1% over the 99 hexagonal assemblies, which each consist of 217 pins. The reactor is surrounded by 42 steel reflector assemblies, and it includes six primary and three secondary control assemblies [29]. A core diagram and fuel schematic for the design is provided in Figure 2-8.

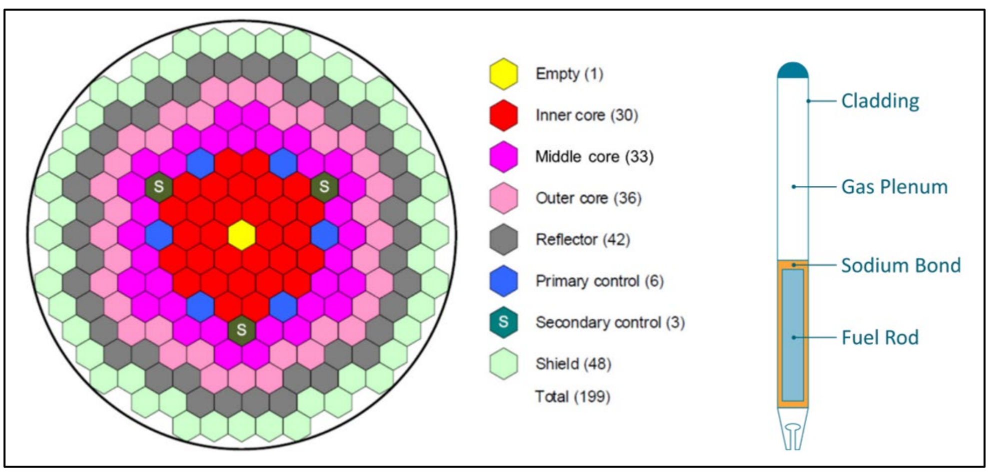

Figure 2-8. ARC-100 core diagram (left) and fuel schematic (right), taken directly from [29].

Details on the transport containers for new fuel could not be found, but spent fuel storage is part of the vessel design. The vessel is designed to have capacity for an entire core of fuel assemblies, as shown in Figure 2-9, where the spent fuel is expected to stay until ready for dry storage modules of unspecified design.

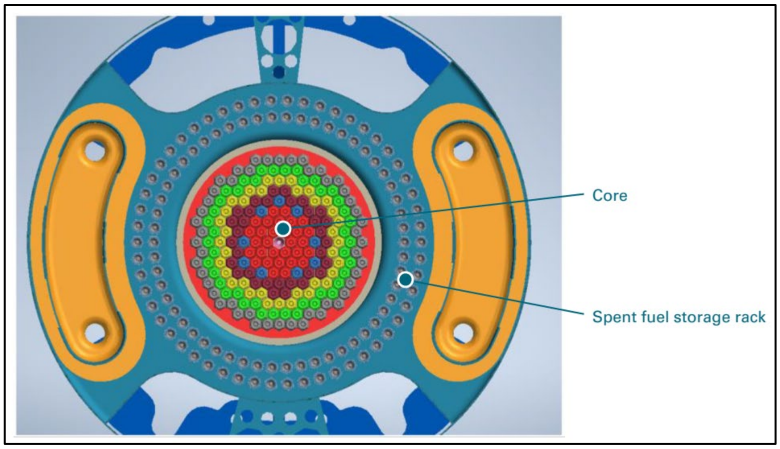

Figure 2-9. ARC-100 in-vessel spent fuel storage design, taken directly from [29].

2.8 THE GA-EMS FAST METAL REACTOR

The GA-EMS FMR is a helium gas–cooled fast reactor designed for operation at 509–800°C with a power output of 44 MWe. It is fueled with SiC-clad, 19.75 wt% enriched UO_2 pellet pins arranged in triangular pitch to form a hexagonal fuel assembly [30]. Each assembly, as shown in Figure 2-10, contains 120 fuel rods and a central support tube [30]. The core is annular and is surrounded by solid reflector blocks of Zr_3Si_2 and graphite [30]. Information about where the HALEU fuel will be sourced, fabricated, or transported could not be found.

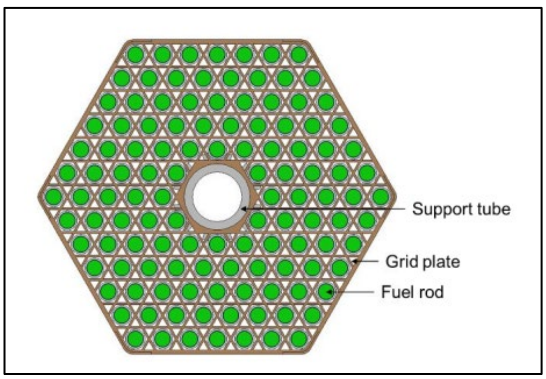

Figure 2-10. GA-EMS FMR fuel assembly diagram, taken directly from [30].

2.9 THE HORIZONTAL COMPACT-HIGH TEMPERATURE GAS-COOLED REACTOR BY MIT

The HC-HTGR is a helium gas-cooled thermal spectrum reactor. Based on available documentation, it is expected that the HC-HTGR will use HALEU TRISO fuel particles in graphite compacts for fuel. Much of the HC-HTGR design is still underway and changing constantly, as it is in a very preliminary stage of development [31]. A rendering of the integrated reactor pressure vessel and steam generator is provided in Figure 2-11.

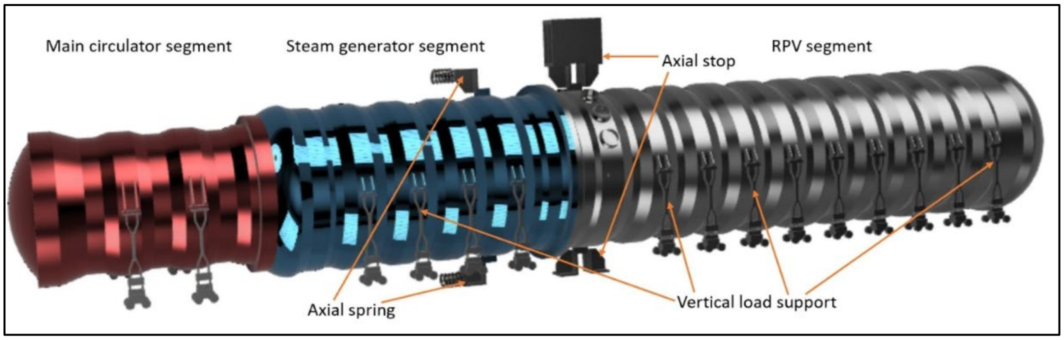

Figure 2-11. HC-HTGR integrated reactor pressure vessel and steam generator rendering, taken directly from [31].

3. FUEL CYCLE FACILITY DISCUSSION

Government initiative has spurred rapid growth in domestic enrichment capabilities, and multiple entities are pursuing down-blending activities to convert existing HEU fuel and feedstock into HALEU fuel. Until recently, Russian state-owned enrichment capabilities were the predominant supplier of HALEU fuel, and efforts on the domestic and global scale are attempting to increase HALEU production capabilities to eliminate dependence on Russian-produced HALEU. Listed below are five such organizations with current and/or planned capabilities for HALEU production. These capabilities include both increased enrichment capabilities to support enrichment above LEU as well as down-blending activities to utilize existing HEU for HALEU production.

3.1 CENTRUS ENERGY CORPORATION

Centrus Energy Corporation currently leads the United States in HALEU enrichment capabilities, having recently made their first HALEU delivery to DOE in November of 2023 [32]. This 20 kg delivery of HALEU comes from the Centrus Energy Corp. American Centrifuge Plant in Piketon, Ohio, which only began production in October of 2023 [32] following their initial testing and demonstration cascade in February of the same year [33]. The American Centrifuge Plant increased production to 900 kg/yr following the initial 20 kg delivery [32]. Centrus is expected to be an essential component of the domestic HALEU supply chain, and they currently have a memorandum of understanding (MOU) with TerraPower and Oklo. Their MOU with Oklo conveys their partnership to supply Oklo with HALEU fuel in the future [34], and their MOU with Terrapower was to cooperatively establish a cost-competitive and timely source of HALEU enrichment capacity [35].

3.2 URENCO USA

Urenco USA declared that they plan to expand their enrichment facility in Eunice, New Mexico, for HALEU production in 2019 [36]. This desire was reemphasized again in February of 2023, but no public commitments or plans to expand enrichment capabilities have been finalized since then [37]. Also in February of 2023, Kairos Power announced their MOU with Urenco USA to collaborate on securing a HALEU supply for their KP-FHR fuel program [38]. Urenco USA is also expected to supply USNC with uranium enriched to under 10 wt% ^{235}U for their TRISO particle fuel fabrication factory, which will produce their Fully Ceramic Microencapsulated (FCM®) fuel [39].

3.3 BWX TECHNOLOGIES

BWXT currently leads in the domestic down-blending of HEU: current efforts are underway to produce over two metric tons of 19.75% enriched HALEU in five years, sourced from government-owned scrap material containing uranium [28]. BWXT's Category II facility in Lynchburg, Virginia, is their site for down-blending activities as well as current and upcoming fabrication activities. BWXT began production of TRISO particle fuel for the Project Pele microreactor in December of 2022 [40], and in addition to fabricating the Project Pele microreactor for the DoD, they will also be fabricating the DRACO thermal propulsion reactor for DARPA [41]. As of 2021, the BWXT TRISO particle production facility has demonstrated capabilities to manufacture uranium kernels in oxide, carbide, alloy, nitride, and oxi-carbide forms, with ceramic, graphitic, and refractory coatings [25]. BWXT subsidiary Nuclear Fuel Services (NFS) also holds a contract for HEU conversion and purification services for their Category I nuclear facility in Erwin, Tennessee [42].

3.4 NATRIUM FUEL FACILITY

The Natrium Fuel Facility at the GNF-A site in Wilmington, North Carolina, is a joint TerraPower and GNF-A planned enrichment facility which will be funded through TerraPower and the ARDP. Construction for this facility was anticipated to begin in 2023, and it is expected produce reliable source of HALEU fuel required for the Natrium demonstration plant and additional Natrium plants in the future [43].

3.5 ORANO

French company Orano plans to extend uranium enrichment capacity at their Georges Besse II plant in Bollène, France, but only within the LEU+ range of HALEU enrichment (5–8 wt% ^{235}U) [44]. This can service the increased enrichment needs of existing LWR designs, but it is not expected that the increased enrichment capacity will satisfy the needs of advanced reactor fuels in the 10–20 wt% ^{235}U HALEU range.

3.6 IDAHO NATIONAL LABORATORY

A small number of 15% enriched HALEU pellets have been fabricated at Idaho National Laboratory to support HALEU testing for General Electric, but fabrication of less than 200 pellets in total is planned for the experiments [45]. The production of these pellets was limited for experimental purposes, and this facility is not expected to be pursue to larger-scale production.

4. TRANSPORTATION PACKAGES

The demand for HALEU fuel in advanced reactor designs necessitates the development of new transportation packages for its transport. Before the fuel fabrication stage, fuel transportation typically concerns UF_6, and only recent approvals from the NRC have certified transportation packages suitable for HALEU fuel, as transportation package design must balance enrichment and capacity. After fuel fabrication, both the higher enrichment as well as the variety of forms present additional licensing challenges. Additional transportation challenges will likely arise for the transportation of the spent fuel, but little information is available on what that will look like. As of January 2024, the NRC lists the following transportation packages and their respective organizations as involved in increased enrichment (between 5 and 20 wt%) licensing activities:

- Traveller by Westinghouse,
- MAP-12 and MAP-13 by Framatome,
- RAJ-II by GNF-A,
- TN-B1 by Framatome,
- OPTIMUS®-L by NAC,
- DN30-X by Orano, and
- Versa-Pac by Orano (formerly TN Americas, LLC) [46].

However, not all the increased enrichment licensing activities are intended for enrichments in the 10–20 wt% range necessary for many advanced reactor fuels. Additionally, the ES-3100 by Consolidated Nuclear Security is considered since it is suitable for HEU transport. A summary of the approved enrichments for these designs is provided in Table 4-1, and additional information on each is provided in their respective sections below.

Table 4-1. Summary of HALEU transportation packages

Transportation Package	Owner	Fuel Type	Current Approved Enrichment (wt% ^{235}U)	Relevant Contents per Package	Approximate Outer Dimensions (m)	Certificate of Compliance Date	NRC Docket Number
Traveller STD	Westinghouse	Fresh or slightly contaminated PWR assemblies; PWR or BWR UO_2 fuel rods	Up to 6% for assemblies or up to 7% for fuel rods	One assembly or one container of rods	5.0 × 0.7 × 1.0 (L × W × H)	1/26/2023 [47]	07109380
Traveller XL					5.7 × 0.7 × 1.0 (L × W × H)		
MAP-12	Framatome	Fresh UO_2 PWR assemblies	Up to 8%	Two assemblies	5.3 × 1.1 × 0.8 (L × W × H)	2/6/2021 [48]	07109319
MAP-13					5.6 × 1.1 × 0.8 (L × W × H)		
RAJ-II	GNF-A	Fresh BWR fuel assemblies (8x8 to 10x10); BWR, CANDU, or PWR rods	Up to 8% for UO_2 fuel types	Two assemblies or rod containers	4.7 × 0.5 × 0.3 (L × W × H)	7/24/2023 [49]	07109309
TN-B1	Framatome	Fresh BWR fuel assemblies (8x8 to 11x11); BWR, CANDU, or PWR rods	Up to 5%, with request to extend to 8%	Two assemblies or rod containers	4.7 × 0.5 × 0.3 (L × W × H)	10/23/2023 [50]	07109372
OPTIMUS®-L	NAC	Certain waste materials; unirradiated TRISO particle solid right circular cylindrical compacts	Up to 20% for TRISO particle compacts	≤ 68 kgU for TRISO particle compacts	1.2 × 1.8 (D × H)	2/6/2024 [51]	07109390
DN30-10	Orano	UF_6	Up to 10%	1,460 kg UF_6; 98 kgU	2.4 × 1.2 × 1.3 (D × L × H)	3/27/2023 [52]	07109388
DN30-20			Up to 20%	1,271 kg UF_6; 170 kgU			
Versa-Pac 55 (VP-55)	Orano	Uranium oxides, uranium metal, uranyl nitrate crystals, other uranium compounds, and TRISO particle fuel	Up to 100% with additional HALEU-range specific limits	1-2 6.4 L containers	0.6 × 0.9 (D × H)	4/12/2023 [53]	07109342
Versa-Pac 110 (VP-110)				~0.5 kg^{235}U for up to 20 wt% ^{235}U	0.8 × 1.1 (D × H)		
ES-3100	Consolidated Nuclear Security	Uranium oxides, nitrides, and metals; TRIGA fuel (UZrH)	Up to 100%	Up to approx. 35 kg^{235}U in metals and 12 kg^{235}U in oxides or nitrides	0.5 × 1.1 (D × H)	1/5/2021 [54]	07109315

4.1 TRAVELLER BY WESTINGHOUSE

The Traveller transportation package comes in both Standard (STD) and XL models, and they are used for transporting a single PWR assembly as well as loose PWR or BWR UO_2 fuel rods. A 2020 Oak Ridge National Laboratory (ORNL) report that assessed the feasibility of existing transportation packages for HALEU use determined that the Traveller package could potentially support transportation of pressurized water reactor (PWR) and boiling water reactor (BWR) UO_2 fuel rods up to 10 wt% [55], and as of January 2023, the Traveller STD and XL packages were approved for increased enrichments up to 6 wt% for fresh uranium or slightly contaminated PWR fuel assemblies, or UO_2 rods with enrichments up to 7 wt% [47]. The Traveller package consists of an outerpack, clamshell, and fuel assembly or rod pipe container, and the Traveller XL is distinguished from the Traveller STD model by its ability to accommodate both standard and long length fuel assemblies and rod pipe as opposed to only standard length. The Traveller STD has an approximate outer length, width, and height of 5.0 m, 0.7 m, and 1.0 m, respectively, and the Traveller XL has an approximate outer length, width, and height of 5.7 m, 0.7 m, and 1.0 m, respectively [47]. From their safety evaluation report, Figure 4-1 reproduces a rendering of the Traveller outerpack, and Figure 4-2 reproduces a cross section of the outerpack and clamshell [56]. Further information for this package is available under NRC docket number 71-9380 (07109380).

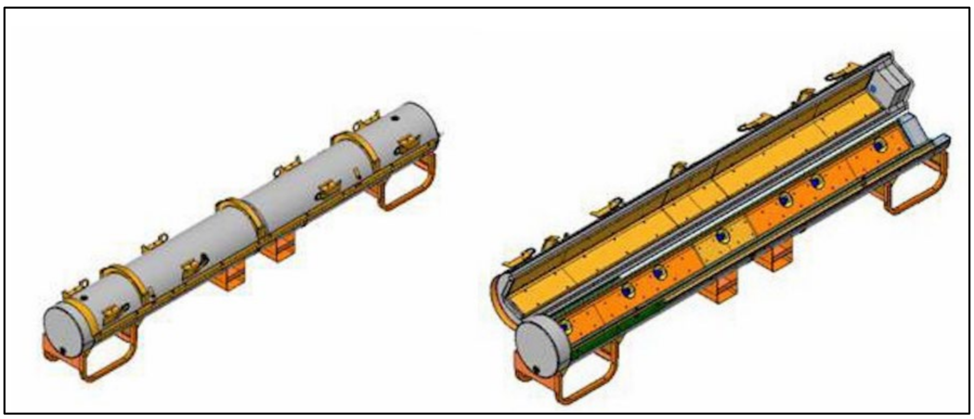

Figure 4-1. Closed (left) and open (right) Traveller outerpack, taken directly from [56].

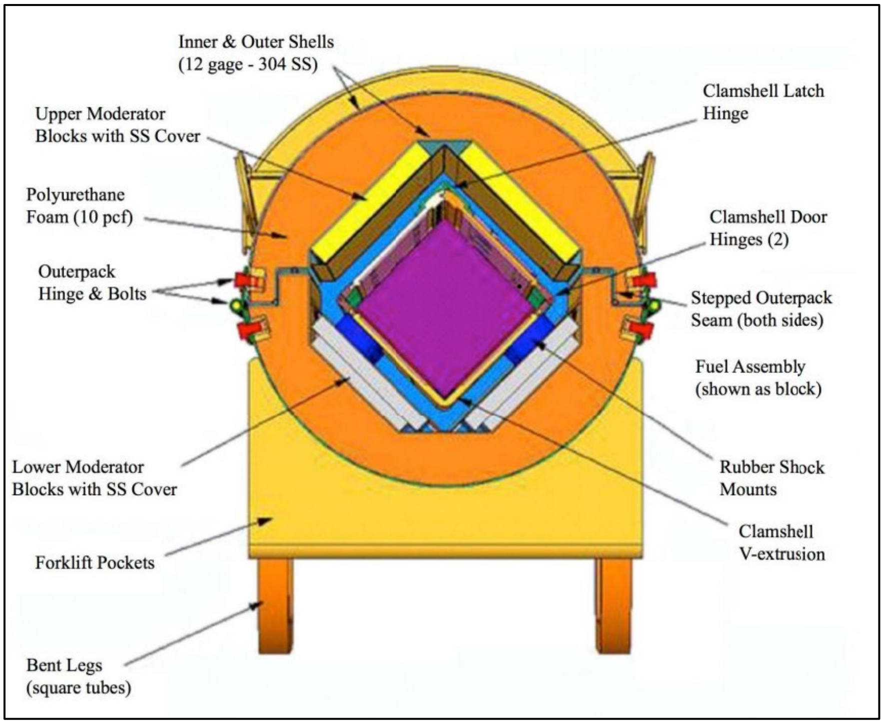

Figure 4-2. Traveller outerpack and clamshell cross section, taken directly from [56].

4.2 MAP-12 AND MAP-13 BY FRAMATOME

The MAP-12 and MAP-13 packages are designed to transport unirradiated PWR assemblies, and Framatome recently received NRC approval to include content enrichments up to 8 wt%. The package consists of a base and lid, with capacity for two assemblies. The permitted fuel configuration in the 5-8 wt% range includes only uranium oxide rods in a 17x17 array. The MAP-12 package accommodates a 144 in. maximum nominal active fuel length, and the package has an outer length, width, and height of approximately 5.3 m, 1.1 m, and 0.8 m, respectively. The MAP-13 package accommodates a slightly larger 150 in. nominal active fuel length, and the package has an outer length, width, and height of approximately 5.6 m, 1.1 m, and 0.8 m, respectively [48]. A rendering of the MAP package is provided in their latest Certificate of Compliance (CoC) application [57], and it is reproduced below in Figure 4-3. Two cross-sectional views from the same report are reproduced in Figure 4-4 and Figure 4-5, showing the width- and length-wise cross sections, respectively. Further information for this package is available under NRC docket number 71-9319 (07109319).

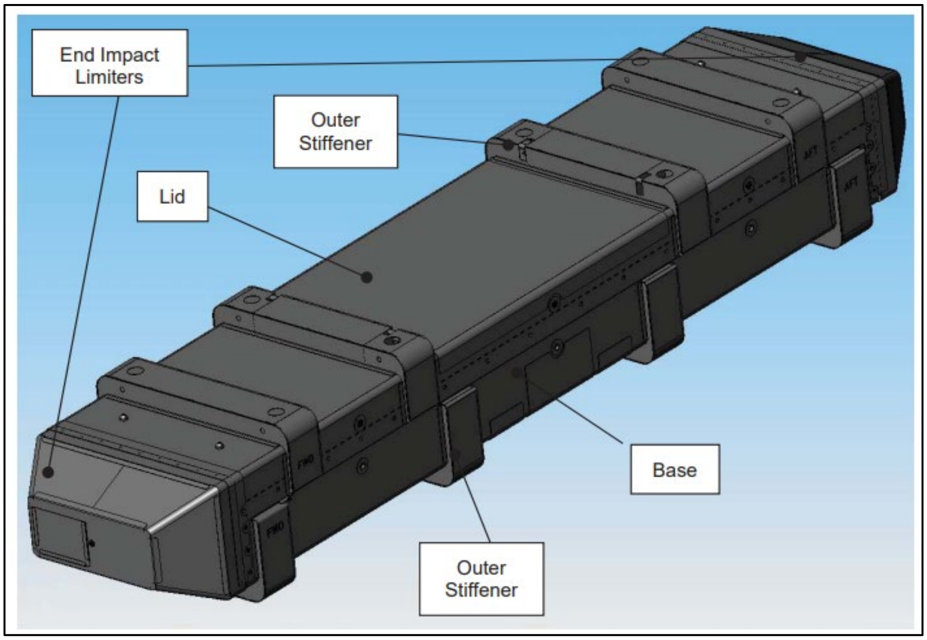

Figure 4-3. MAP package rendering, taken directly from [57].

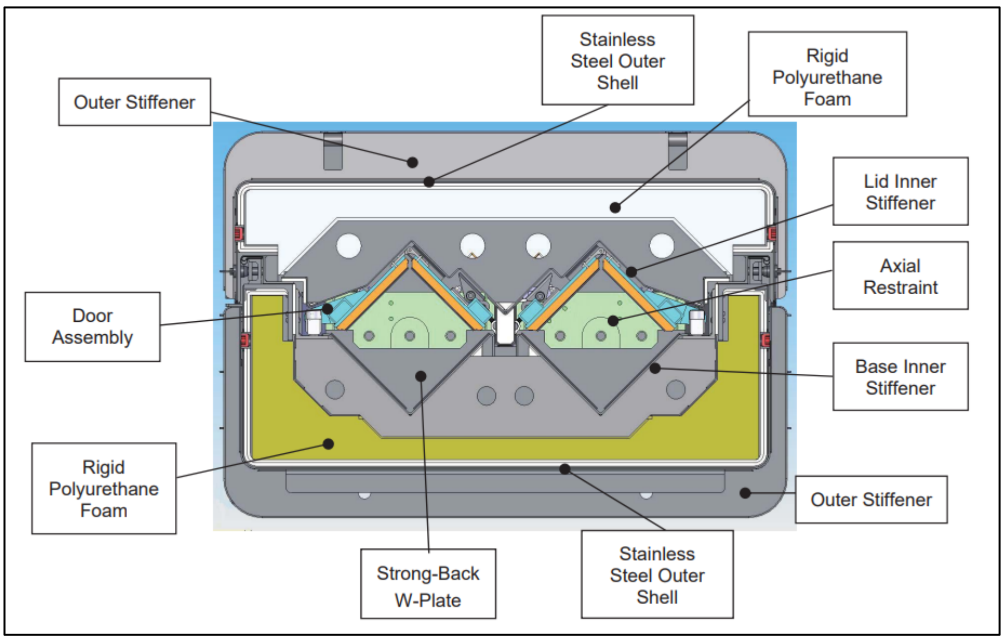

Figure 4-4. MAP cross-sectional view, taken directly from [57].

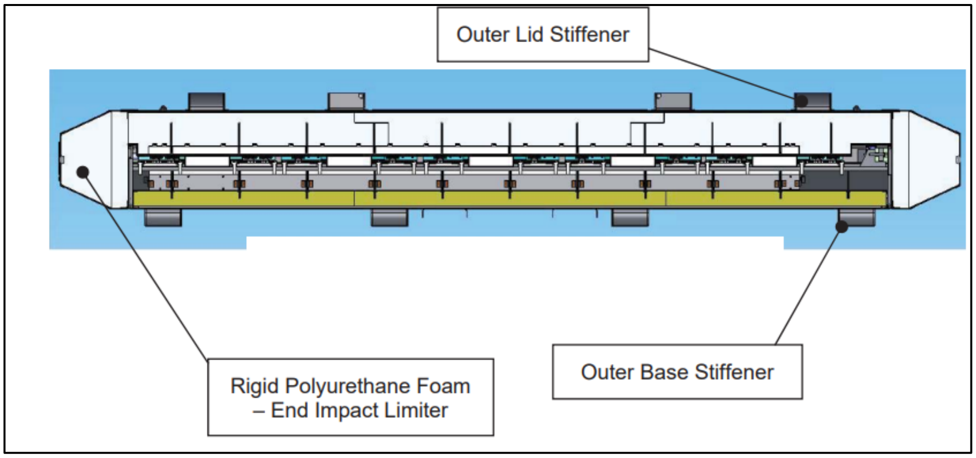

Figure 4-5. Lengthwise cross section view of the map package, taken directly from [57].

4.3 RAJ-II BY GLOBAL NUCLEAR FUEL - AMERICAS

The RAJ-II package is designed for transporting BWR fuel assemblies, but it can also transport certain configurations of UO_2 or UC rods designed for use in PWR, BWR, or CANDU reactors. As of July 2023, GNF-A received approval for their RAJ-II package to extend enrichment limits up to 8 wt% ^{235}U for certain configurations. The package has an outer length, width, and height of approximately 4.7 m, 0.5 m, and 0.3 m, respectively. In the HALEU enrichment range, the contents must be either a constructed UO_2 GNF 10x10 BWR fuel assembly or rods of the same type. At 8 wt% ^{235}U, the contents are limited to either one assembly or up to 30 individual rods per compartment, of which there are two per package [49]. A diagram of the RAJ-II package, seen in Figure 4-6, was provided in their safety report [58]. Further information for this package is available under NRC docket number 71-9309 (07109309).

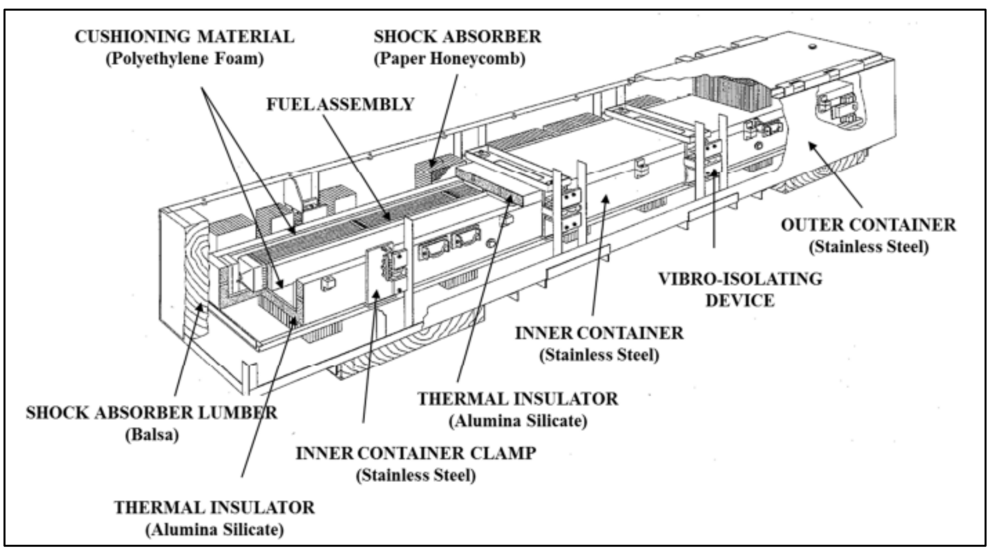

Figure 4-6. RAJ-II package diagram, taken directly from [58].

4.4 TN-B1 PACKAGE BY FRAMATOME

The TN-B1 package is physically identical to the RAJ-II package described in Section 4.3, but it is licensed separately from the RAJ-II for transporting the ATRIUM 11x11 fuel assembly and rods not covered under the RAJ-II license. Although the Framatome TN-B1 package does not currently support enrichments higher than 5% [50], the 2020 HALEU feasibility assessment determined the TN-B1 package by Framatome could potentially support up to an average BWR fuel assembly enrichment of 10 wt% [55]. Framatome recently submitted a safety analysis report supporting their amendment request for increased enrichment values up to 8% [59]. A diagram of the package is reproduced from that report in Figure 4-7. Further information for this package is available under NRC docket number 71-9372 (07109372).

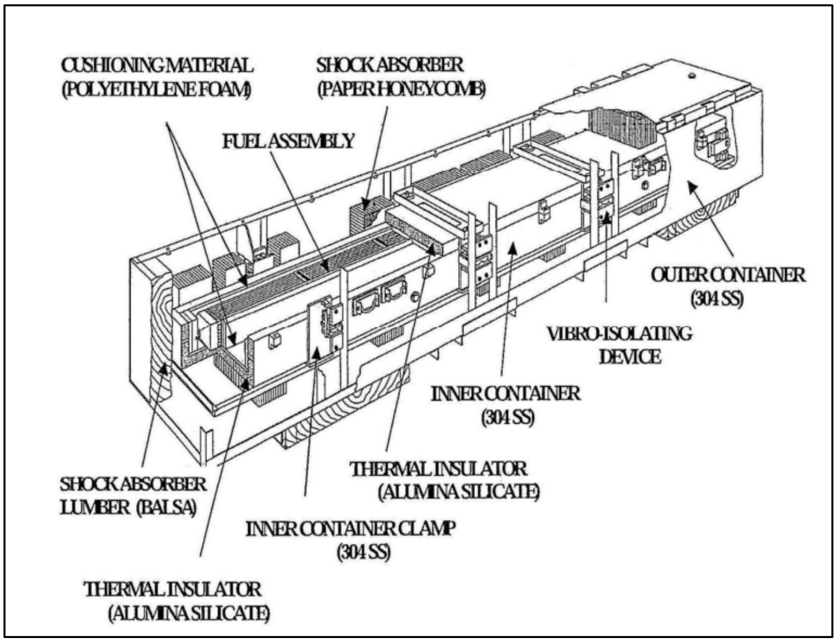

Figure 4-7. TN-B1 package drawing, taken directly from [59].

4.5 OPTIMUS®-L BY NAC

NAC International is currently developing a number of packages in their OPTImal Modular Universal Shipping (OPTIMUS®) package product line to support the transportation of HALEU material in a variety of advanced reactor fuel forms, including licensing of inserts for TRISO particle compacts, microreactor transportation, and extra-large payloads [60]. As of May 2023, NAC International expected they would make their first HALEU shipment in the first quarter of 2024 using an OPTIMUS®-L package system, designed for use in low-activity applications [61]. An expanded view of the OPTIMUS®-L from an NAC brochure [62] is provided in Figure 4-8 below. The package consists of a cask containment vessel (CCV) with bottom support plate, the outer packaging (OP), and optional shield insert assemblies. It can contain a variety of contents, including certain waste forms but more relevantly, unirradiated TRISO particle compacts in solid right circular cylinders. As specified in their latest CoC, the TRISO particle compacts can have a maximum enrichment of 20% ^{235}U, with a mean uranium loading of up to 68 kgU and maximum mean matrix density of 1.8 g/cc [51]. The OP has outer dimensions of approximately 1.2 m diameter and 1.8 m height. The interior of the CCV is approximately 0.8 m diameter and 1.2 m height. Further information for this package is available under NRC docket number 71-9390 (07109390).

Figure 4-8. OPTIMUS®-L component view, taken directly from [62].

4.6 DN30-X BY ORANO

Orano currently holds a consortium agreement with Urenco to develop and test their 30B-X cylinder for LEU+ and HALEU transport [63]. This new cylinder would be used inside the DN30-X package which was approved by the NRC in March of 2023 [52]. The DN30-X package consists of both the DN30 package and the 30B-X cylinder together, and the X can be replaced by "10" or "20" to indicate maximum enrichments of 10 or 20 wt%, respectively. These packages also contain criticality control rods (CCRs) of boron carbide, including 33 CCRs for the 30B-10 and 44 CCRs for the 30B-20 cylinders. For DN30-10, the maximum mass of UF_6 is 1,460 kg, and for the DN30-20, the maximum is 1,271 kg. This corresponds to fissile material quantities of 98 kg and 170 kg, respectively. Both cylinder types have an approximate length of 2.1 m and diameter of 0.8 m. The exterior packaging is oriented horizontally, and the entire package including feet has an approximate length of 2.4 m, diameter of 1.2 m, and height of 1.3 m [52]. As seen in the safety analysis report submitted to the NRC, Figure 4-9 and Figure 4-10 show the interior and exterior of the 30B-X cylinders, respectively. Figure 4-11 shows the exploded diagram of the DN30-X package, and Figure 4-12 shows a rendering of the assembled package with one of the transport options [64]. Further information for this package is available under NRC docket number 71-9388 (07109388).

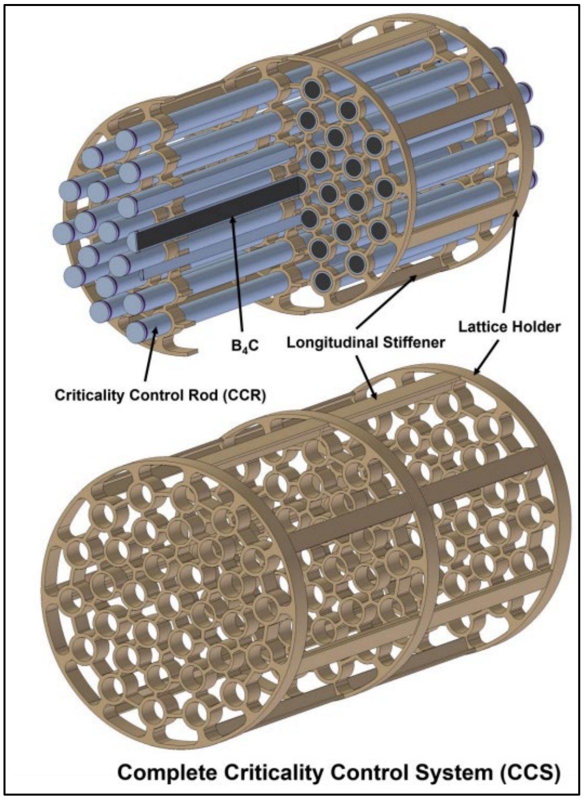

Figure 4-9. 30B-X cylinder interior, taken directly from [64].

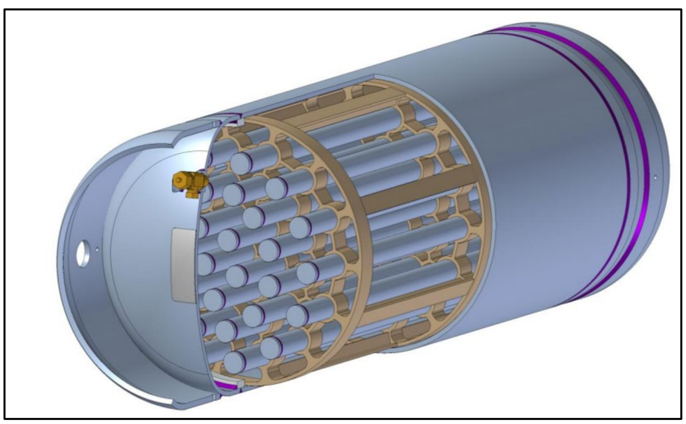

Figure 4-10. 30B-X cylinder exterior and cutaway, taken directly from [64].

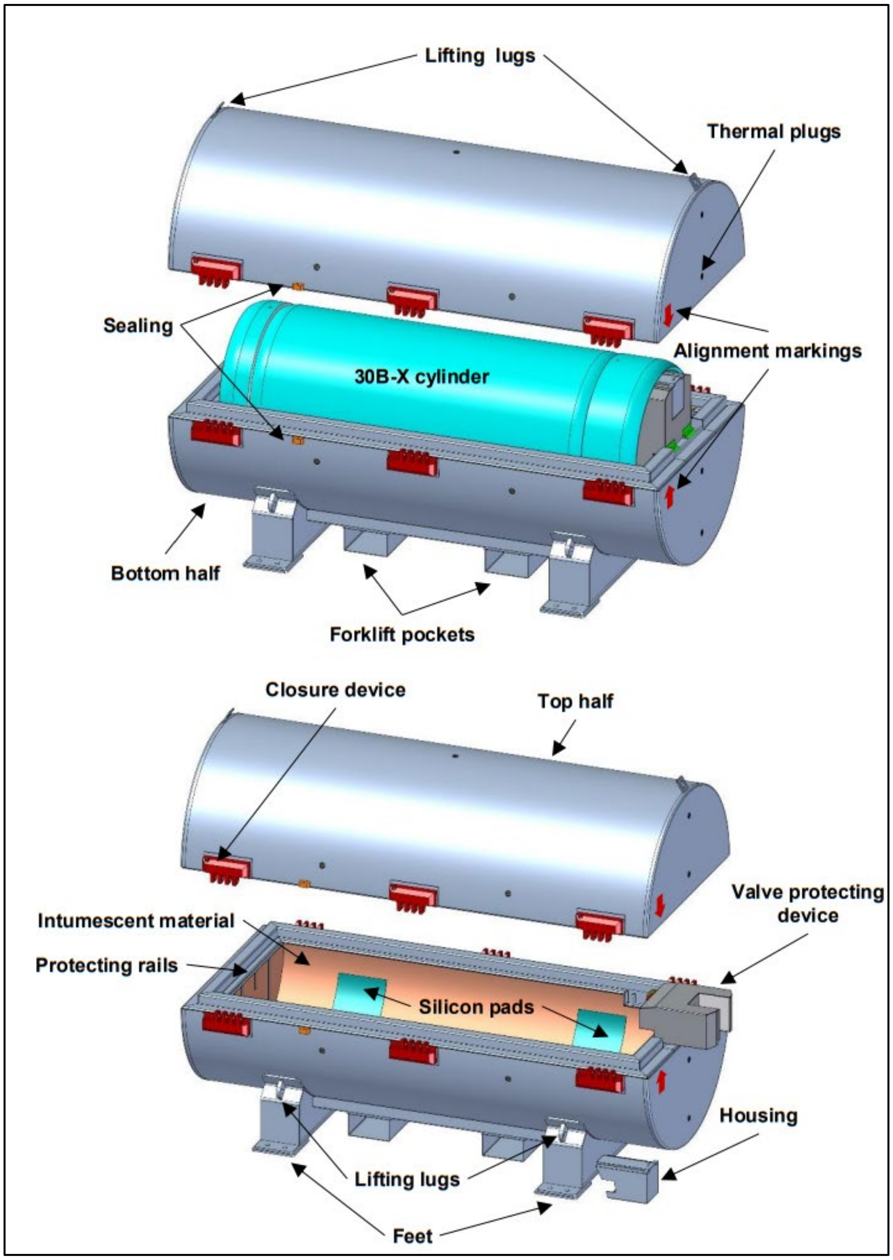

Figure 4-11. DN30-X exploded view, taken directly from [64].

Figure 4-12. Assembled DN30-X package, taken directly from [64].

4.7 VERSA-PAC BY ORANO

The Versa-Pac is a multipurpose transport package licensed to transport up to 100 wt% ^{235}U in both their 55-gallon (VP-55) and 110-gallon (VP-110) variants. The Versa-Pac accommodates a wide variety of materials. These include solid uranium materials such as uranium oxides, some uranyl nitrate crystals, some uranium compounds, uranium metals or alloys, and natural thorium. It may also include TRISO fuel and compacts with kernels made of oxides, carbides, and/or nitrides. There are no restrictions on the TRISO particle size, density, and uranium content per particle. The TRISO particles may be loose or pressed into various compact forms. UF_6 is also permitted for Versa-Pac designs under specific constraints [53].

The uranium mass limits are set by ^{235}U enrichment depending on whether there are limits on hydrogenous packing material for the contents included or whether certain interior containers are used. For simplicity, only ground/vessel limits are described herein, but air limits are detailed in the CoC. For the VP-55 and VP-110, the fissile material limit is 0.505 kg ^{235}U for enrichments up to 10 wt% ^{235}U and 0.445 kg^{235}U for enrichments up to 20 wt% ^{235}U for any of the listed permitted contents, but larger mass limits exist for the VP-55 given certain packing material or container limitations. With some hydrogenous packing limitations and for uranium compounds not containing hydrogen, the ^{235}U mass limit increases to 0.685 kg and 0.605 kg for 10 and 20 wt% ^{235}U, respectively. When the volume of the contents is restricted by a 5 in. (6.4 L) pipe container, there may be up to 1.215 kg^{235}U at 20 wt% ^{235}U, and there is no limit for 10 wt% ^{235}U. The limiting factor for the contents without mass limits is the theoretical densities of the contents, corresponding to 122 kg uranium metal, 60 kg UO_2, and 45 kg U_3O_8. Lastly, if there are both volume restrictions from using 5 in. pipe containers as well as hydrogenous packing material limitations, there are no mass limits for contents up to 20 wt% ^{235}U. Instead under these restrictions, there may be one pipe for up to 20 wt% ^{235}U contents for all compounds and uranium metals. Alternatively, there may be two pipes in a high-capacity basket for up to 20 wt% ^{235}U for uranium compounds only. For enrichments up to 10 wt% ^{235}U, there may be two pipes for uranium oxides, compounds, and metals. Lastly, 1S and 2S type cylinders for UF_6 are permitted to contain up to nearly 0.430 kg and 0.601 kg^{235}U, respectively, for enrichments up to 20 wt% ^{235}U [53].

In terms of scale, the VP-55 has an approximate outer diameter and height of 0.6 m and 0.9 m, respectively, whereas the VP-110 has an approximate outer diameter and height of 0.8 m and 1.1 m, respectively. The approximate inner diameter and height are 0.4 m and 0.7 m, respectively for the VP-55 and 0.5 m and 0.8 m, respectively for the VP-110 [53]. A component diagram of the Versa-Pac design is provided in Figure 4-13, sourced from revision 13 of the Versa-Pac CoC application report [65]. Orano has been developing transportation packages for LEU+ and HALEU, and the aforementioned high-capacity basket for their Versa-Pac VP-55 enriched uranium transport package received NRC approval in September of 2023, seen in Figure 4-14 [66]. Further information for this package is available under NRC docket number 71-9342 (07109342).

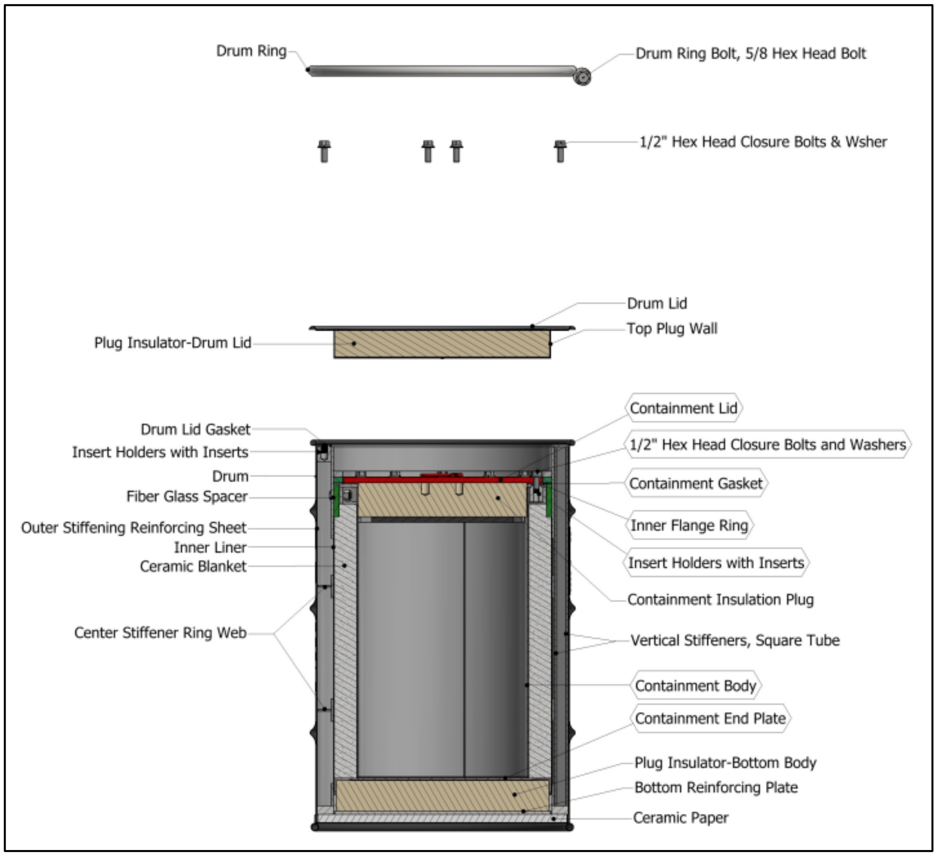

Figure 4-13. Versa-Pac component diagram, taken directly from [65].

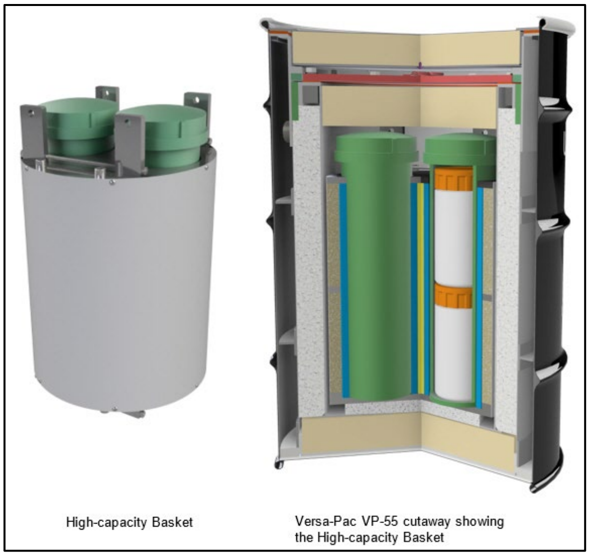

Figure 4-14. Orano high-capacity basket and cutaway in the VP-55, sourced directly from [66].

4.8 ES-3100 BY CONSOLIDATED NUCLEAR SECURITY

The ES-3100 packaging is designed for transporting various material forms enriched up to 100 wt% ^{235}U. It is a 30-gallon cylindrical drum approximately 0.5 m in diameter and 1.1 m in height, with an inner containment vessel with a diameter and height of approximately 0.1 m and 0.8 m, respectively. The package may contain a wide variety of contents. When it includes uranium as solid metal or alloy, mass limits range from approximately 15 to 35 kg^{235}U per package for enrichments up to 100 wt% ^{235}U. These mass limits are lower for each enrichment range if the metal is categorized as broken metal. If the contents are uranium oxide, which may include UO_2, UO_3, and U_3O_8, there may be up to approximately 15 kg of oxide with a maximum ^{235}U mass limit of approximately 10 kg with carbon or 12 kg without carbon, respectively. Uranium nitride contents have a UN_x mass limit ranging from approximately 5 kg to 12 kg depending on the value of x in UN_x and seal time. When the contents are unirradiated TRIGA fuel elements and pellets, there is a maximum of approximately 0.4 kg^{235}U for enrichments up to 100 wt% ^{235}U [54]. A cutaway diagram of the ES-3100 cask from the latest safety analysis report is reproduced in Figure 4-15 [67]. Further information for this package is available under NRC docket number 71-9315 (07109315).

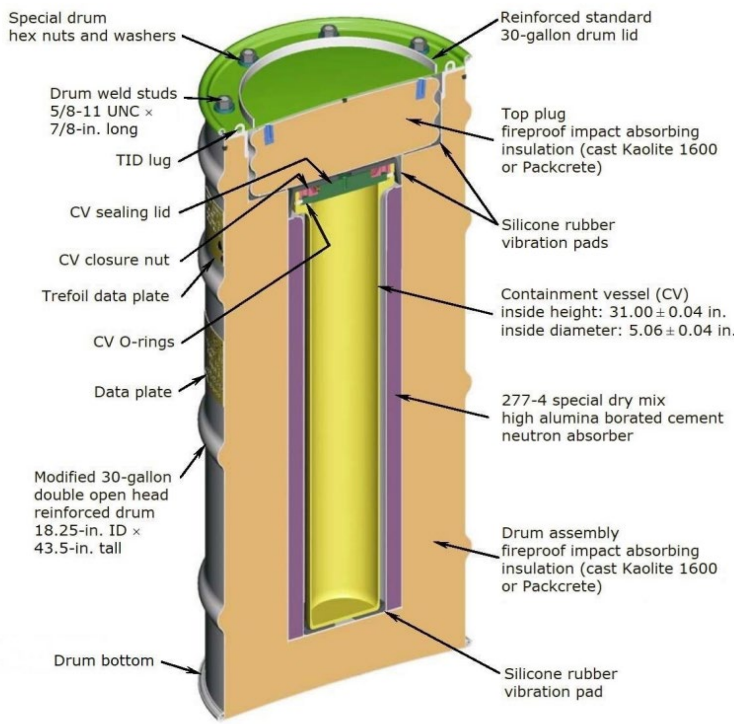

Figure 4-15. Cutaway diagram of ES-3100 packaging, taken directly from [67].

5. AVAILABILITY OF HALEU EVALUATIONS

5.1 SUMMARY OF HALEU DATA IN ICSBEP HANDBOOK

The International Criticality Safety Benchmark Evaluation Project (ICSBEP) Handbook [68] has historically focused on low-enriched and high-enriched uranium and plutonium for commercial and military applications, but some critical experiments already exist in the 5–20 wt% ^{235}U enrichment range and from different fuel forms and moderators that could be potentially relevant for the validation of the HALEU fuel types, as noted in recently published work [69]. The Database for the International Criticality safety benchmark Evaluation program handbook (DICE) [70] can be used to classify the available experiments by different parameters, such as fuel type, fuel enrichment, and energy corresponding to the average lethargy causing fission (EALF). It should be noted however that the values reported from DICE may correspond to an average of fissile material spanning an assembly or one of multiple fissile materials present in an experiment. Thus, the evaluations detailed herein should be used as a starting point for similarity assessments, as the enrichments provided by DICE may not be wholly representative of the evaluation. Some evaluation listings presented herein include additional enrichment values where there is evidently more than one significant contributor to the fissile material of the evaluation (i.e., both enrichment values for the UO_2 and uranyl nitrate solution fuel in several LEU-MISC-THERM evaluations are listed).

As described in the previous sections, most of the ARDP awardees plan to use HALEU fuel enriched around 19.75 wt% ^{235}U, close to the upper bound of the 5–20 wt% range, so experiments with fuel enriched between 9 and 21 wt% ^{235}U are potentially more relevant than experiments with fuel enriched between 5 and 9 wt% ^{235}U. Therefore, the available experiments from the ICSBEP Handbook and those potentially applicable to HALEU fuel when looking at the ^{235}U enrichment (5 to 21 wt% ^{235}U) are separated into two categories, 5 to 9 wt% ^{235}U in Table 5-1 and 9 to 21 wt% ^{235}U in Table 5-2. In total, there are 448 critical experiments from 77 evaluations are available in the ICSBEP Handbook spanning the 5–21 wt% ^{235}U, showing that a large pool of validation candidates already exist when considering only the fuel enrichment. Among those 448 experiments, 266 have a fuel enrichment between 5 and 9 wt% ^{235}U, and 182 have a fuel enrichment between 9 and 21 wt% ^{235}U. Of the experiments in the 9–21 wt% ^{235}U enrichment range, 40 have fuel enrichments between 18 and 21 wt% ^{235}U, and those are expected to be more relevant to the upper enrichment bound of HALEU fuel. Some experiments have a high experimental uncertainty and/or a high/low calculational over expected (C/E) ratio, so caution should be exercised when using those evaluations—such as IEU-COMP-THERM-009-001 with an experimental uncertainty of 600 pcm and IEU-COMP-MIXED-002-008 with a C/E of 1.044. Because the DICE enrichment data for a given experiment may represent one of multiple or an average of different nuclear material enrichments used in the experiment, it is possible that some of the experiments listed are from mixed LEU and HEU fuel experiments. An additional study would be needed to determine the impact of using mixed LEU and HEU fuel experiments on validation in comparison to experiments using fuel entirely within the HALEU enrichment range.

Table 5-1. ICSBEP evaluations with 5–9 wt% ^{235}U-enriched fuel, from DICE

Evaluation ID	# of cases	Fuel wt% ^{235}U	Fuel type	Moderator	Spectrum
IEU-MET-FAST-010	1	8.88	U Metal	None	Fast
IEU-MET-FAST-011	1	6.01	U Metal	Graphite	Fast
LEU-SOL-THERM-005	3	5.64	$UO_2(NO_3)_2$	Water	Thermal
LEU-SOL-THERM-011	13	6.01	$UO_2(NO_3)_2$	Water	Thermal
LEU-COMP-THERM-018	1	7.00	UO_2	Water	Thermal
LEU-COMP-THERM-019	3	5.19	UO_2	Water	Thermal
LEU-COMP-THERM-020	7	5.00	UO_2	Water	Thermal
LEU-COMP-THERM-021	6	5.00	UO_2	Water	Thermal
LEU-COMP-THERM-025	4	7.41	UO_2	Water	Thermal
LEU-COMP-THERM-031	6	5.00	UO_2	Water	Thermal
LEU-COMP-THERM-047	2	7.00	UO_2	Water	Thermal
LEU-COMP-THERM-070	12	6.50	UO_2	Water	Thermal
LEU-COMP-THERM-075	6	6.50	UO_2	Water	Thermal
LEU-COMP-THERM-076	3	7.00	UO_2	Water	Thermal
LEU-COMP-THERM-078	15	6.90	UO_2	Water	Thermal
LEU-COMP-THERM-080	11	6.90	UO_2	Water	Thermal
LEU-COMP-THERM-081	1	6.60	UO_2	Water	Thermal
LEU-COMP-THERM-085	13	6.50	UO_2	Water	Thermal
LEU-COMP-THERM-094	11	6.50	UO_2	Water	Thermal
LEU-COMP-THERM-096	19	6.90	UO_2	Water	Thermal
LEU-COMP-THERM-097	24	6.90	UO_2	Water	Thermal
LEU-COMP-THERM-098	7	5.74	UO_2	Water	Thermal
LEU-COMP-THERM-101	22	6.90	UO_2	Water	Thermal
LEU-COMP-THERM-102	27	6.90	UO_2	Water	Thermal
LEU-MISC-THERM-001	5	4.98, 6.02	UO_2, $UO_2(NO_3)_2$	Water	Thermal
LEU-MISC-THERM-002	6	4.98, 6.02	UO_2, $UO_2(NO_3)_2$	Water	Thermal
LEU-MISC-THERM-003	15	4.98, 5.99	UO_2, $UO_2(NO_3)_2$	Water	Thermal
LEU-MISC-THERM-006	10	4.98, 6.00	UO_2, $UO_2(NO_3)_2$	Water	Thermal
LEU-MISC-THERM-007	12	4.98, 6.00	UO_2, $UO_2(NO_3)_2$	Water	Thermal
Total number of evaluations:	**29**		**Total number of experiments:**		**266**

Table 5-2. ICSBEP evaluations with 9–21 wt% ^{235}U-enriched fuel, from DICE

Evaluation ID	# of cases	Listed Fuel wt% ^{235}U	Fuel type	Moderator	Spectrum
IEU-COMP-FAST-004	1	20.98	U Metal	Depleted Uranium	Fast
IEU-COMP-INTER-004	1	12.71	UF_4	None	Intermediate
IEU-COMP-INTER-005	1	16.27-16.35	U Metal, UO_2	Depleted Uranium	Intermediate
IEU-COMP-MIXED-002	5	11.60-18.93	UF_4	None	Mixed
IEU-COMP-THERM-002	6	17.00	UO_2	Graphite	Thermal
IEU-COMP-THERM-003	2	19.90	U-Zr-H	Graphite	Thermal
IEU-COMP-THERM-008	5	20.91	UO_2 TRISO particles	Graphite	Thermal
IEU-COMP-THERM-009	2	18.31	UO_2	Water	Thermal
IEU-COMP-THERM-010	1	17.00	UO_2	Graphite	Thermal
IEU-COMP-THERM-013	1	19.74	USi_2	Graphite, Water	Thermal
IEU-COMP-THERM-014	1	19.77	U Metal	Water	Thermal
IEU-MET-FAST-002	1	16.19	U Metal	Natural Uranium	Fast
IEU-MET-FAST-007	1	10.06	U Metal	Depleted Uranium	Fast
IEU-MET-FAST-012	1	16.79	U Metal	Depleted Uranium	Fast
IEU-MET-FAST-013	1	11.69	U Metal	Aluminum	Fast
IEU-MET-FAST-014	2	15.50-20.54	U Metal	Aluminum	Fast
IEU-MET-FAST-016	1	11.54	U Metal	Depleted Uranium	Fast
IEU-MET-FAST-020	9	20.05	U Metal	Copper	Fast
IEU-MET-FAST-021	1	20.05	U Metal	Natural Uranium	Fast
IEU-MET-FAST-022	4	20.05	U Metal	Copper	Fast
IEU-MET-INTER-001	3	20.05	U Metal	Copper	Intermediate
IEU-SOL-THERM-001	4	20.71	UO_2SO_4	Graphite	Thermal
IEU-SOL-THERM-004	1	14.67	UO_2SO_4	Beryllium Oxide	Thermal
LEU-COMP-THERM-022	7	9.83	UO_2	Water	Thermal
LEU-COMP-THERM-023	6	9.83	UO_2	Water	Thermal
LEU-COMP-THERM-024	2	9.83	UO_2	Water	Thermal
LEU-COMP-THERM-032	9	9.83	UO_2	Water	Thermal
LEU-COMP-THERM-103	2	19.84	U-Mo	Water	Thermal
LEU-SOL-THERM-003	9	10.07	$UO_2(NO_3)_2$	None	Thermal
LEU-SOL-THERM-004	7	9.97	$UO_2(NO_3)_2$	Water	Thermal
LEU-SOL-THERM-006	5	10.07	$UO_2(NO_3)_2$	Water	Thermal
LEU-SOL-THERM-007	5	9.97	$UO_2(NO_3)_2$	None	Thermal
LEU-SOL-THERM-008	4	9.97	$UO_2(NO_3)_2$	Concrete	Thermal
LEU-SOL-THERM-009	3	9.97	$UO_2(NO_3)_2$	Borated Concrete	Thermal
LEU-SOL-THERM-010	4	9.97	$UO_2(NO_3)_2$	Polyethylene	Thermal
LEU-SOL-THERM-012	2	9.98	$UO_2(NO_3)_2$	None	Thermal
LEU-SOL-THERM-013	1	9.98	$UO_2(NO_3)_2$	None	Thermal
LEU-SOL-THERM-016	7	9.97	$UO_2(NO_3)_2$	Water	Thermal
LEU-SOL-THERM-017	6	9.97	$UO_2(NO_3)_2$	None	Thermal
LEU-SOL-THERM-018	6	9.97	$UO_2(NO_3)_2$	Concrete	Thermal
LEU-SOL-THERM-019	6	9.97	$UO_2(NO_3)_2$	Polyethylene	Thermal
LEU-SOL-THERM-020	4	9.97	$UO_2(NO_3)_2$	Water	Thermal
LEU-SOL-THERM-021	4	9.97	$UO_2(NO_3)_2$	None	Thermal
LEU-SOL-THERM-022	4	9.97	$UO_2(NO_3)_2$	Borated Concrete	Thermal
LEU-SOL-THERM-023	9	9.97	$UO_2(NO_3)_2$	Water	Thermal
LEU-SOL-THERM-024	7	9.97	$UO_2(NO_3)_2$	Water	Thermal
LEU-SOL-THERM-025	7	9.97	$UO_2(NO_3)_2$	None	Thermal
MIX-MET-FAST-011	1	18.24	Pu and U metal	Graphite	Fast
Total number of evaluations:	**48**		**Total number of experiments:**		**182**

Outside of fuel enrichment, the most important characteristics to look for in the choice of critical experiments for validation are fuel form, moderator/reflector, and EALF. From the ARDP awardees reactor characteristics shown in Table 2-1, the relevant parameters are the presence of graphite as a moderator/reflector and the use of non-conventional fuel forms such as UCO or UN TRISO particle compacts, uranium fuel salts, and metallic uranium. Among the 182 experiments with fuel enrichments between 9 and 21 wt% ^{235}U listed in Table 5-2, 105 feature uranium solutions, not corresponding to any of the planned HALEU fuels. Those corresponding to some of the planned HALEU fuels include 39 uranium oxide and 27 uranium metal. Among the remaining experiments, 6 are for uranium tetrafluoride, having some relevance for the validation of transported UF_4 and UF_6, and some others include uranium hydride and uranium silicide. The evaluation that appears the most promising for UO_2 in TRISO particle fuel is IEU-COMP-THERM-008 (5 experiments in 1 evaluation), a pebble-bed critical facility with 20.91 wt% ^{235}U enriched TRISO particles moderated by graphite. The different fission spectra are covered in the available critical experiments with thermal, intermediate, and fast experiments, but the number of fast experiments is lower in the ICSBEP handbook because it primarily focuses on thermal spectrum systems for typical commercial water reactor fuel validation.

Other experiments with characteristics potentially relevant to HALEU fuel validation from advanced reactors without considering the uranium enrichment are shown in Table 5-3. Experiments listed in Table 5-1 or Table 5-2 were not replicated in Table 5-3. As seen in Table 5-3, 131 additional experiments from 15 different evaluations may potentially be applicable, depending on the advanced reactor fuel type to validate. In this table, 105 experiments listed are for UF_4 or UF_6 transportation, a few others concern space reactors, and the rest concern moderators or coolant of interest. Additionally, 173 evaluations and 739 experiments exist for uranium metal outside the 5–21 wt% ^{235}U enrichment range.

From this study, it can be concluded that there are still no or only a few experiments to validate HALEU fuel using TRISO particles in compacts or pebbles and/or uranium salts. Finally, no experiments exist using fuel specifically designed to target the burnt HALEU fuel range, which is necessary for the validation of the back end of the advanced reactors fuel cycle for spent fuel storage and transportation (e.g., spent TRISO particle pebbles, spent uranium salts).

Table 5-3. ICSBEP experiments outside the 5–21% ^{235}U fuel enrichment range sharing features with advanced reactor HALEU fuel designs, from DICE

Evaluation ID	# of cases	Listed Fuel wt% ^{235}U	Fuel type	Moderator	Spectrum	Link to HALEU Fuel Validation
HEU-COMP-MIXED-003	5	95.89	UO_2	Zirconium hydride	Mixed	Space reactor
HEU-COMP-THERM-016	6	89.48	U metal	Graphite	Thermal	Moderator
HEU-MET-FAST-075	5	82.43-93.23	U metal	Beryllium Oxide	Fast	Space reactor
HEU-MET-FAST-101	5	93.07	U metal and Pu metal	Beryllium Oxide	Fast	Space reactor
HEU-SOL-INTER-002	1	93.16	UF_6	Water	Intermediate	UF_6 transport
HEU-SOL-THERM-039	5	93.16	UF_6	Water	Thermal	UF_6 transport
IEU-COMP-INTER-003	9	37.5	UF_4	None, cellulose acetate plastic, or Lucite/Plexiglas	Intermediate	UF_6 transport
IEU-COMP-MIXED-001	4	29.83	UF_4	Polyethylene	Mixed	UF_6 transport
IEU-COMP-MIXED-003	7	37.5	UF_4	Lucite/Plexiglas	Mixed	UF_6 transport
IEU-COMP-THERM-001	25	29.83	UF_4	Polyethylene	Thermal	UF_6 transport
IEU-COMP-THERM-011	2	37.5	UF_4	Lucite/Plexiglas	Thermal	UF_6 transport
LEU-COMP-THERM-033	52	2-3	UF_4	Wax (C,H)	Thermal	UF_6 transport
MIX-COMP-FAST-004	1	0.22	UO_2 and Pu metal	Nickel and Sodium	Fast	Moderator
MIX-MET-FAST-006	3	0.42	Pu and depleted U	Lead	Fast	Lead-cooled fast reactor
PU-MET-INTER-004	1	N/A	Pu metal	Graphite	Intermediate	Lead-cooled fast reactor
Total number of evaluations:	**15**			**Total number of experiments:**	**131**	

5.2 EVALUATIONS IN THE IRPHE HANDBOOK

As described in recently published work [71], the International Reactor Physics Evaluation (IRPhE) project [72] also contains reactor physics experiments that are potentially relevant to HALEU fuel transportation validation. Though the evaluations in the IRPhE handbook focus primarily on reactor physics benchmarks and not on critical experiments, some of the evaluations include critical configurations of research and power reactors or experimental facilities that may be applicable. The main difference with the evaluations found in the ICSBEP Handbook is that critical configurations were not the goal of the benchmarks, so less attention might have been given to the uncertainty analysis, resulting in potentially higher benchmark experimental uncertainty. Some experiments are also present in both international handbooks and are not listed again for this subsection. The IRPhE handbook contains 897 experiments from 148 evaluations with criticality measurements and the derivation of a benchmark k_{eff} value that could potentially be used for HALEU fuel validation. Similarly to the previous section, the major relevant experiments (54 experiments in 15 evaluations) are shown in Table 5-4, from using the IRPhE Database and Analysis Tool (IDAT) [73], a tool similar to DICE from the ICSBEP. The IRPhE handbook contains more diverse fuel forms and moderators than the ICSBEP handbook, as those benchmarks mainly come from facilities testing innovative approaches to nuclear energy production. The most notable benchmarks are the HTR-10, the High-Temperature Test Reactor (HTTR), and PROTEUS for UO_2 in TRISO particles validation (20 experiments in 6 different evaluations, but four of them are from the PROTEUS research reactor, so it is really 3 facility-independent evaluations), and the Molten Salt Reactor Experiment (MSRE) for uranium salt validation (1 experiment in 1 evaluation). Those experiments all correspond to various HALEU fuel forms of interest, and some of them correspond to the enrichment range. Thus, these experiments look promising for validation, but their benchmark experimental uncertainty and C/E ratios can be very high for k_{eff} validation standards—as, for example, the MSRE benchmark has a 420 pcm keff uncertainty and a keff C/E ratio of 1.0215 [74]. This relatively low derived uncertainty with a very high C/E ratio shows that unknown unknowns exist in the benchmark, either in the evaluation or in the computational methods, so the analysts should consider whether or how to use this evaluation when performing HALEU fuel transport validation. Similar observations can be made with some of the other evaluations presented in Table 5-4. Other notable experiments come from (1) the Very High Temperature Reactor Critical assembly (VHTRC) evaluation, with 7 experiments using UO_2 Bi-structural Isotropic (BISO) particles—which is expected to be close enough for the validation of fuel types using TRISO particles, but the fuel particles are low-enriched (2 and 4 wt% ^{235}U)—or (2) the 20% enriched uranium metal fuel rods used in the Fast Critical Assembly (FCA) experiments of the Japan Atomic Energy Agency (JAEA) [75]. Some other experiments included in Table 5-4 are liquid metal cooled fast reactors (LMFRs) and LR(0)-VVER-RESR-003 [76], a zero-power reactor experiment with fluoride and graphite insertions for testing.

Table 5-4. Main characteristics of the IRPhE published experiments with potential use for the advanced reactor HALEU fuel transportation validation, from IDAT

Evaluation ID	# of cases	Listed Fuel wt% ^{235}U	Fuel type	Moderator/ Reflector/ Coolant	Spectrum	Link to HALEU Fuel Validation
VHTRC-GCR-EXP-001	7	2 and 4	UO_2 BISO particles	Graphite	Thermal	Fuel form, graphite
HTTR-GCR-RESR-001	8	3.4 - 9.9	UO_2 TRISO particles	Graphite	Thermal	Fuel form, graphite
PROTEUS-GCR-EXP-001	4	16.76	UO_2 TRISO particles	Graphite	Thermal	Enrichment, fuel form, graphite
PROTEUS-GCR-EXP-002	1	16.76	UO_2 TRISO particles	Graphite	Thermal	Enrichment, fuel form, graphite
PROTEUS-GCR-EXP-003	4	16.76	UO_2 TRISO particles	Graphite	Thermal	Enrichment, fuel form, graphite
PROTEUS-GCR-EXP-004	2	16.76	UO_2 TRISO particles	Graphite	Thermal	Enrichment, fuel form, graphite
HTR10-GCR-RESR-001	1	17	UO_2 TRISO particles	Graphite	Thermal	Enrichment, fuel form, graphite
MSRE-MSR-EXP-001	1	0.2 and 93	Uranium salt	Graphite and salts	Thermal	Fuel form, salts
LR(0)-VVER-RESR-003	17	3.3	UO_2	Water, graphite, salts	Thermal	Moderator, coolant
NRAD-FUND-RESR-001	2	19.75	U(20)-Zr-H	Graphite, water	Thermal	Enrichment, graphite
NRAD-FUND-RESR-002	2	19.75	U(20)-Zr-H	Graphite, water	Thermal	Enrichment, graphite
EBR2-LMFR-RESR-001	1	66.72	U metal	Stainless steel, sodium	Fast	Spectrum, moderator, coolant
JOYO-LMFR-RESR-001	2	0.2 and 23	MOX, depleted UO_2	Stainless steel, depleted U, sodium	Fast	Spectrum, moderator, coolant
ZPPR-LMFR-EXP-010	1	0.22	U_3O_8, Pu-U-Mo	Stainless steel, sodium	Fast	Spectrum, moderator, coolant
FCA-FUND-EXP-001	1	20	U metal	Depleted U	Fast	Enrichment
Total number of evaluations:	**15**			**Total number of experiments:**	**54**	

5.3 EXPERIMENT CORRELATION AND QUALITY

To ensure the best validation suite, it is necessary to have a high number of applicable experiments with experimental uncertainty as low as possible, but it is also important that those experiments come from the highest variety of experimental facilities possible to reduce the experimental correlations within evaluation and within facility [77]. Gathering the identified available experiments potentially applicable to HALEU transport validation from both ICSBEP and IRPhE handbooks, 616 experiments from 104 different evaluations were identified, but many of those evaluations come from the same facilities—meaning there could be many correlations within those experiments. For example, the 11 PROTEUS-GCR experiments from the 4 evaluations [78, 79, 80, 81] in the same PROTEUS facility and operated at the Paul Scherrer Institute (PSI) in Switzerland all have around 300–400 pcm uncertainty. The main uncertainty contributors between the four evaluations are common: the ^{235}U isotopic content, resulting in 250–300 pcm k_{eff} uncertainty depending on the evaluation, and the moderator pebble impurities, resulting in 80 to 170 pcm uncertainty depending on the evaluation. Those uncertainty values are similar and show that there is a correlation within the evaluations, so the resulting computational bias for all the experiments and evaluations from the same facility will be similar. Performing critical experiments applicable to advanced reactor HALEU fuel in additional critical facilities would decrease this correlation problem and increase the quality of the validation suite for computational bias and bias uncertainty derivations. Another potential issue already mentioned in the previous subsections is the quality of the evaluations. Some experiments were conducted decades ago, and some information is missing, leading to high experimental uncertainty. Another example is experiments from the IRPhE handbook, where the primary goal is not necessarily the critical configuration but other effects such as reactivity coefficients or power distributions, leading to high experimental uncertainty as well. From the experiments listed, additional review is necessary to judge the quality of the evaluations, similar to an effort already started by the Working Party on Nuclear Criticality Safety (WPNCS) subgroup 8 (SG-8); “Preservation of Expert Knowledge and Judgement Applied to Criticality Benchmarks” [82]. Another way to be sure of the quality of a critical experiment is by looking at the ORNL Verified, Archived Library of Inputs and Data (VALID) [83]. VALID is a project led by ORNL with the goal of creating high-quality, peer-reviewed sensitivity data files to be used in validation studies. From the list of potentially applicable experiments identified from DICE, only 44 out of 579 are already a part of the growing VALID collection, and none of the IRPhE experiments are in VALID. This is expected because VALID, like the ICSBEP, focuses on the validation of current commercial reactor fuel and is thus oriented to low-enriched uranium compound thermal types of experiments. To ensure the best quality validation study and the most accurate computational bias and bias uncertainty derivation possible, the number of those experiments added to VALID should be maximized to the extent possible.

5.4 DISCUSSION OF RELEVANT EXPERIMENTS/EVALUATIONS YET TO BE PUBLISHED IN THE ICSBEP AND IRPHE HANDBOOKS

Creating a critical and/or reactor physics evaluation worthy to be called a *benchmark* takes a great deal of time and money, and the process of doing so can be summarized in three major steps:

- Designing the experiment (months to years)
- Performing the experiment (weeks to months)
- Evaluating the experiment (months to years)

In the next subsections, some current experiments in different steps of this lengthy process are introduced, all potentially relevant to HALEU validation. Some of these experiments’ evaluations follow either the ICSBEP or IRPhE guidelines [84, 85], so they are expected to become high-quality and usable benchmarks for HALEU validation studies when completed. Some other experiments listed do not have clear plans yet for ICSBEP or IRPhE publications.

5.4.1 AGN-201M Reactor Benchmark – University of New Mexico, USA

The University of New Mexico's Aerojet General Nucleonics Model 201 (AGN-201M) reactor is one of four operating AGN-201 in the world. The core consists in 19.5 wt% enriched uranium microspheres coated with graphite and in polyethylene matrix, reflected by large graphite blocks. In 2021, a DOE Nuclear Energy University Program (NEUP) proposal was awarded to create a ICSBEP/IRPhE benchmark evaluation from critical experiments of this reactor [86]. This upcoming evaluation is interesting for HALEU validation because of the fuel enrichment and the presence of graphite. As there is no AGN-201M experiments in the handbooks, the experimental uncertainty cannot be estimated, so there is a possibility that it ends up being high for validation studies. The expected date of completion of this evaluation is 2025. One potential issue identified with the benchmark is a lack of characterization of the fuel.

5.4.2 IPEN/MB01 reactor conversion to 19.75 % metallic plates fuel – IPEN/MB-01 - Brazil

As noted in [71], in 2019, the IPEN/MB-01 reactor core in Sao Paulo, Brazil, was converted from typical low-enriched UO_2 rod-type fuel to 19.75 % U_3Si_2-Al plate-type fuel elements. This new core was created to perform critical experiments to validate the design of the future Brazilian Multipurpose Reactor (BMR), an upcoming research reactor to be built near Sorocaba, Brazil [87]. The IPEN/MB-01 research reactor is an extremely well characterized and trusted facility with 21 IRPhE and 18 ICSBEP evaluations published in the handbooks, and it can be expected that this new core will lead to new evaluations, although not officially announced. This new core is interesting for HALEU validation because of the fuel enrichment and the expected low experimental uncertainty due to the experience of the staff with the ICSBEP and IRPhE guidelines.

5.4.3 The Deimos Experiment – NCERC, USA

The Deimos experiment, designed by Los Alamos National Laboratory (LANL) to be conducted in the National Criticality Experiments Research Center (NCERC), will use HALEU fuel in the form of 19.9 wt% enriched TRISO particles embedded in cylindrical compacts and surrounded by large graphite parts. The experiment has been designed [88], but it has not yet been performed or evaluated. The HALEU fuel from the DEIMOS experiment was obtained from the Compact Nuclear Power Source (CNPS) experiment conducted at the Los Alamos Critical Experiments Facility [89]. The main goal of Deimos is to measure the temperature reactivity coefficient for HALEU fuel in a graphite matrix, but an ambient temperature critical configuration will also be evaluated as a basis point. There is no clear confirmation that this experiment will be published in the ICSBEP and/or IRPhE handbooks, but it would be highly beneficial to HALEU fuel validation as the only currently developed TRISO particle pebble-bed experiment. Given the experience of NCERC staff with critical experiments, the facility can be trusted to provide high-quality evaluation and adequate definition of uncertainties. One potential issue with the experiment is that the packing fraction of the compacts is about 60%, beyond the 40% packing fraction trending in the ARDP designs.

5.4.4 MARVEL Reactor – Idaho National Laboratory, USA

The Microreactor Applications Research Validation and Evaluation (MARVEL) reactor is to be built at INL and brought critical by December 2024 [71]. MARVEL is a sodium-potassium–cooled thermal microreactor fueled with standard commercial 19.75 wt% ^{235}U-enriched TRIGA uranium zirconium hydride fuel pins [90]. MARVEL's first goal is to demonstrate microreactor technologies, not necessarily to develop a benchmark, but a first critical evaluation is planned to be published in the IRPhE in the coming years. The reactor should provide additional data relevant for HALEU validation because of the fuel enrichment and the uranium metal fuel form.

5.4.5 ROSE Critical Facility – Joint Institute for Power and Nuclear Research, Belarus

In 2019, results from new critical experiments involving 21 wt% enriched UO_2 rods were presented [91]. The experiments were performed at the Rose facility by the National Academy of Science of Belarus in Sosny. The results presented show a benchmark uncertainty under 150 pcm for the four experiments. These measurements have not been developed into the strict ICSBEP or IRPhE benchmarks at this time, and it is unclear whether it is a plan for the future, but those experiments could be interesting for HALEU validation because of the fuel enrichment.

5.5 SUMMARY AND IDENTIFIED GAPS

In summary of the previous subsections, considering the available experiments from the ICSBEP and IRPhE handbooks as well as some critical experiments being currently designed, the following conclusions can be made:

- A high number of critical experiment evaluations are available within the HALEU enrichment range (5–20 wt%), from diverse facilities, and a few more are being developed, but more are needed with different HALEU fuel forms, as previously noted by the NRC, the industry, and US national laboratories [92, 93]. This statement is strengthened by previous ORNL preliminary validation studies showing that 20 wt% UF_6 and UO_2 fuels have enough applicable experiments for some transportation cases [94, 95, 96, 97]. Some of the applicable experiments do not correspond to 20 wt% enrichment and are LEU, showing that other parameters are important for similarity. The focus should be on performing experiments with different fuel forms such as TRISO particles compacts, uranium metal and uranium salts, and at different EALF (thermal and fast).
- A high number of thermal, intermediate, mixed and fast experiments are available.
- A low number of experiments with TRISO particle-based fuels or similar are available, some with questionable uncertainty and C/E ratios (PROTEUS), and one experiment is being developed (Deimos).
- Only one uranium salt experiment is available, with questionable uncertainty and C/E ratio (MSRE), and none are in development.
- A few HALEU fuel depletion studies exist, such as the AGR series for TRISO particles, but they are not evaluated, assembled, or curated to be used for validation [71]. A critical experiment could be designed from irradiated TRISO fuel particles and could be used to perform validation of burnt HALEU fuel storage and transportation.
- No critical experiments are available with burned HALEU fuel or validation of spent fuel storage and transportation.
- Only a few experiments identified as potentially relevant to HALEU are in VALID.
- Experimental correlations could be reduced by performing experiments in new facilities.
- Uncertainty and quality of evaluations can be increased by performing experiments in already trusted facilities but with new equipment, capitalizing on the experience of staff with the ICSBEP and IRPhE evaluations guidelines (SNL, NCERC, IPEN/MB-01).

6. CRITICAL EXPERIMENT FACILITIES

This section lists facilities in which critical experiments could be performed to enhance the HALEU fuel transport validation suite. Each facility is introduced with general information and important parameters to consider for potential future use as a HALEU fuel transport critical experiment. The list includes already established critical experiment facilities or research reactors with published work in the ICSBEP and/or IRPhE handbooks, but it also includes facilities with critical experiments records yet no published benchmarks; facilities that are designed but not built yet—as well as facilities that could perform critical experiments but in which such work is not within the current plans. The list of facilities was assembled from analysis of previous published experiments in the ICSBEP and IRPhE handbooks and from recent NEA working parties' efforts discussing criticality experiments facilities, such as a report summarizing the experimental needs for criticality safety [98] and a workshop on zero-power reactors [99]. The list is not exhaustive.

6.1 OPERATIONAL CRITICAL EXPERIMENT FACILITIES

6.1.1 NCERC – Los Alamos National Laboratory, USA

NCERC is a general-purpose criticality experiments facility located within the Device Assembly Facility (DAF) at the Nevada National Security Sites (NNSS) and operated by LANL since 2006, after being re-located from Technical Area 18 (TA-18). Missions of NCERC are mainly nuclear security, including nuclear criticality safety research and training, nuclear emergency response, and nuclear nonproliferation. NCERC has four critical assembly machines: Planet and Comet, vertical-lift machines [100, 101] where different fuel and moderators can be arranged; Godiva IV [102], a fast burst critical assembly using highly enriched U-Mo; and Flattop [103], a fast benchmark critical assembly with either HEU metal or delta-phase plutonium metal, surrounded by 1000 kg of natural uranium reflector. Some subcritical systems built by hand are also in NCERC, primarily used for training and radiation measurements. NCERC has an exemplary track record of published experiments in the ICSBEP handbook, with more than 40 evaluations and more forthcoming. From those four machines, both Planet and Comet could theoretically accommodate HALEU fuel validation experiments. As previously mentioned, NCERC is already working on the Deimos experiment that could benefit TRISO particle-like fuel validation. The issue with NCERC is its location within DAF, a hazard category 2 defense nuclear facility, so it is complex and costly to perform experiments there (very limited foreign national access, convoluted access for US citizens). Additionally, no water can be introduced, and uranium salt experiments seem complicated.

6.1.2 SPRF/CX facility – Sandia National Laboratories, USA

The Sandia Pulsed Reactor Facility – Critical Experiments (SPRF/CX) is located and operated by Sandia National Laboratories in Technical Area V. The laboratory is located within the Kirtland Air Force Base near Albuquerque, New Mexico. The facility provides a flexible, shielded location for performing critical experiments that employs different reactor core configurations and fuel types. The apparatus currently used for critical experiments has been in operation since 2007 and is an aluminum tank filled with water; it uses two different types of low-enriched UO_2 fuel rods (6.90 and 4.31 wt% enriched ^{235}U) with different diameters. As of 2023, 8 evaluations are published in the ICSBEP handbook, such as LEU-COMP-THERM-78 (LCT-78) [104] and LCT-102 [105]. Other efforts are ongoing to design new experiments, such as IER-304 [106] and IER-305 [107], and more. The facility is exceptionally well characterized, with very low experimental uncertainties around 100 pcm in k_{eff} in most published evaluations. HALEU fuel validation critical experiments could be performed in the SPRF/CX facility, either in the already existing aluminum water tank apparatus or in another newly designed apparatus that could be placed in a different shielded room of the facility. As the facility is within an Air Force base, its access is not convenient, but it is manageable.

6.1.3 ZED-2 – Chalk River Laboratories, Canada

The Zero Energy Deuterium (ZED-2) reactor is located at the Chalk River Laboratories site of the Canadian Nuclear Laboratories. ZED-2 is a versatile tank type, heavy water–moderated and graphite-reflected low-power research reactor that achieved first criticality in 1960. It was originally built to test the pressurized heavy water reactor program in Canada, but its highly configurable core was then used to achieve criticality with various fuels, such as natural uranium, MOX fuels, enriched and depleted UO_2, and uranium alloys—all with different coolants such as water, gases, and solid metals [108]. ZED-2 has 1 evaluation published in the ICSBEP handbook (LEU-MET-THERM-003 [109]) and 1 evaluation in the IRPhE handbook (ZED2-HWR-EXP-001 [110]), with more forthcoming. ZED-2 is currently funded to propose substitution measurements with HALEU fuel type components, such as TRISO particle fuels or molten fuel salts placed in its central region [111]. ZED-2 is a highly flexible facility that can accommodate a variety of measurements and assemblies, thanks to its flexible reactor safety case. ZED-2 would be a suitable location to perform critical experiments involving HALEU fuel types because of its flexibility, ongoing HALEU fuel research plans, and staff experience with ICSBEP/IRPhE evaluations.

6.1.4 New STACY – Japan Atomic Energy Agency, Japan

The Static Experiment Critical Facility (STACY) was a critical facility using low-enriched uranyl nitrate solution reaching first criticality in 1995, located at the Nuclear fuel Cycle safety Engineering research Facility (NUCEF) in the Tokai Research and Development Centre of the JAEA. STACY was used to study the criticality safety of uranium solutions treated in reprocessing plants and other facilities around the world. Critical experiments from the STACY led to more than 20 evaluations published in the ICSBEP handbook, such as LEU-SOL-THERM-011 [112]. In 2015, a STACY core reconfiguration effort was started to focus on decommissioning of the Fukushima Daiichi Nuclear Power Stations, involving molten fuel debris [113]. To do so, the critical facility is transitioning from the use of a uranium solution fuel to the use of 5 wt% ^{235}U enriched UO_2 fuel rods in a water tank. The re-configuration is almost complete, and critical experiments are planned to start in mid-2024 [114]. Capitalizing on the experience of JAEA staff operating STACY, a focus was placed on minimizing the experimental uncertainty of the future critical experiments performed at New STACY. The current critical experiment plans for new STACY include Japanese efforts as well as international collaborations with IRSN until 2025. The facility is seeking critical experiment opportunities, and it would be available to perform critical experiments using HALEU fuel forms after 2025.

6.1.5 IPEN/MB01 Research Reactor – Nuclear and Energy Research Institute, Brazil

The IPEN/MB-01 research reactor, located at IPEN/CNEN-SP (Nuclear and Energy Research Institute), in Sao Paulo, Brazil, reached criticality in 1988 and has been of major importance for Brazilian criticality and reactor physics research. Many different core configurations are possible (i.e., rectangular, square, and cylindrical), using low-enriched UO_2 fuel rods in a water tank. Versatility and flexibility were both considered when the reactor was designed. As mentioned previously, the IPEN/MB-01 research reactor is an extremely well characterized and trusted facility with 21 IRPhE and 18 ICSBEP evaluations published in the handbooks, such as IPEN(MB01)-LWR-RESR-001 [115], grouping a large number of critical and reactor physics experiments performed at the facility. More evaluations are forthcoming; these will use a different core with 19.75 wt% ^{235}U enriched uranium metal plates, corresponding to the HALEU enrichment range fuel [87]. The facility is very flexible and could be used to perform critical experiments involving other HALEU fuel forms.

6.2 UNIVERSITY RESEARCH REACTORS

6.2.1 Reactor Critical Facility – Rensselaer Polytechnic Institute, USA

The Reactor Critical Facility (RCF) is a zero-power research reactor owned and operated by the Rensselaer Polytechnic Institute (RPI) and built in 1956 in Schenectady, NY. The current configuration of the core uses 4.81% enriched UO_2 rods in a light water tank. Critical and reactor physics experiments were performed in the past few years at the RCF [116, 117], and some of them are evaluated [118], but none have been published to the ICSBEP nor IRPhE handbooks. The core is easily changeable, as displayed by the multi-physics (neutronics and thermal hydraulics) experiments conducted in 2018 [119], and it could be reconfigured to be used with HALEU fuel.

6.2.2 Illinois Microreactor Demonstration Project – University of Illinois Urbana-Champaign, USA

The university of Illinois Urbana-Champaign is collaborating with Ultra Safe Nuclear Corporation (USNC) to build one of their Micro Modular Reactor (MMR) Energy System microreactors on campus for power production [120]. The MMR microreactor uses 19.75 wt% ^{235}U enriched oxycarbide fuel in TRISO particles, cooled with helium gas. The goal of this project is power production, but it could eventually be used as a benchmarking facility for HALEU fuel. There is currently no planned date for the reactor to be built and operated.

6.2.3 Molten Salt Nuclear Reactor Research – Abilene Christian University, USA

The Abilene Christian University is collaborating with Texas A&M, Georgia Tech, and the University of Texas at Austin in an effort funded by Natura Resources, LLC to form the Nuclear Energy eXperimental Testing Research Alliance (NEXTRA). From this collaboration, a molten salt reactor is planned to be built in Abilene by 2025 [121], with an application for a construction permit already submitted to the NRC in 2020 [122]. This reactor is planned to be operated with HALEU in FLiBe salt. The goal of this project is to develop advanced reactor licensing experience and demonstrate molten salt chemistry management [123], but it is one of the only planned facilities involving uranium salts, so its use as a benchmarking facility should be pursued.

6.2.4 NextGen MURR – University Missouri, USA

The Missouri University Research Reactor (MURR) is the most powerful university research reactor in the United States, operating at 10 MW since 1966. The core consists of HEU aluminide fuel elements plates placed in a water tank reflected by beryllium and graphite. MURR operations led to two published evaluations in the ICSBEP handbook related to subcritical neutron noise measurements [124, 125]. In 2023, the University of Missouri announced an initiative to build a new and larger research reactor called NextGen MURR, planned to be 20 MW and to use low-enriched fuel [126] and beryllium reflector. NextGen MURR is expected to be operational by 2033. The goal of this project is mainly production of radioisotopes, but it could eventually be used as a benchmarking facility for HALEU fuel.

6.2.5 Kyoto University Critical Assembly – Kyoto University, Japan

The Kyoto University Critical Assembly (KUCA) is used to perform critical, subcritical, and reactor physics experiments at the Kyoto University in Japan [127]. The core is highly configurable, with the possibility of using wet or dry core. Recent efforts are ongoing to replace the highly enriched fuel with low enriched fuel, but some capabilities are expected to be lost in the process [128].

6.3 OTHER FACILITIES

Other notable facilities where critical experiments for HALEU transportation validation could be performed are listed in this subsection.

- The Vulcan Experimental Nuclear Study (VENUS), a reactor operated by SCK CEN at Mol, Belgium, with three evaluations published in the IRPhE handbook, such as VENUS-LWR-EXP-003 [129] .
- LR-0, a zero-power reactor operated by the Nuclear Research Institute Řež plc at Husinec, Czech Republic, with a few ICSBEP and IRPhE evaluations published, such as LR(0)-VVER-RESR-003 previously introduced [76], and more forthcoming, with notable FLiBe experiments.
- The RSV Tapiro, acronym coming from TAratura Rapida Potenza ZerO (Fast pile Calibration at Zero Power), is a research reactor operated by the Italian National Agency for New Technologies, Energy and Sustainable Economic Development (ENEA), located in Rome, Italy, without published benchmarks but with notable lead-cooled advanced reactor studies [130].
- CROCUS, a zero-power reactor operated by Ecole Polytechnique Federale (EPFL) in Lausanne, Switzerland, with one evaluation published in the IRPhE handbook as CROCUS-LWR-RESR-001 [131].
- Two additional facilities are currently being built at INL, with no critical benchmark planned so far [132]. The goal of the Demonstration of Microreactor Experiments (DOME) test bed facility at INL is to provide advanced reactor companies a demonstration platform flexible enough to test different microreactor designs. DOME is set out to repurpose EBR II (a sodium-cooled reactor that operated from 1964–1994) by the DOE's National Reactor Innovation Center (NRIC). DOME's construction started in 2021 and should be ready by 2026. Its first users should be eVinci by Westinghouse, the Pylon D1 by USNC, and the Kaleidos Battery by Radiant Industries. The other INL facility, Laboratory for Operation and Testing in the U.S. (LOTUS), is a separate test bed that will host smaller reactor experiments to support the development of advanced reactors. Its first anticipated user may be the Molten Chloride Reactor Experiment (MCRE) being developed by Southern Co. and TerraPower.
- The University Training and Research Reactor (UTR), located in Kindai University in Japan, is aimed at providing training for the university students and is currently being re-configured to use LEU fuel [128].
- Other university research reactors such as TRIGA reactors using uranium metal fuel should be mentioned as other potential critical facilities to use for HALEU fuel transport validation.

6.4 SUMMARY

The most promising critical facilities and research reactors to potentially perform critical experiments for the validation of HALEU fuels mentioned in the section are summarized in Table 6-1. The main characteristics and the pros and cons of each are listed. This table shows that the facilities with the highest number of advantages and lowest number of disadvantages—and thus seem the most logical—are the SPRF/CX at SNL for a facility within the United States and Zed-2 in Chalk River Laboratories in Canada for a facility outside the United States. Both of these facilities could be used to develop high-quality critical experiments and with an estimated lead time of less than a few years to publish an evaluation in the ICSBEP handbook.

Table 6-1. Summary of facilities identified to potentially perform HALEU fuel type critical experiments.

Facility	Type	Organization	Location	Status of operations	Advantages	Disadvantages
NCERC	Critical experiment facility	Los Alamos National Laboratory	USA	Operational	Inside USA, dedicated critical experiment facility, TRISO particle experiment already ongoing, extensive staff experience with designing critical experiments and ICSBEP and IRPhE evaluation process	Hazard category 2 facility, no water allowed, time and money consuming, highly utilized currently
SPRF/CX facility	Critical experiment facility	Sandia National Laboratories	USA	Operational	Inside USA, dedicated critical experiment facility, room to install new critical machines, extensive staff experience with designing critical experiments and ICSBEP and IRPhE evaluation process	Facility in an air force base, no current critical machine to easily accommodate new HALEU fuel types outside of a water tank, highly utilized currently, potential staff addition needed
ZED-2	Critical experiment facility	Chalk River Laboratories	Canada	Operational	Dedicated critical experiment facility, HALEU fuel research already ongoing, staff experience with designing critical experiments and ICSBEP and IRPhE evaluation process, facility availability for international collaborations	Outside USA
New STACY	Critical experiment facility	Japan Atomic Energy Agency	Japan	Operational mid 2024	Dedicated critical experiment facility, staff experience with designing critical experiments and ICSBEP and IRPhE evaluation process, facility availability for international collaborations	Outside USA, not yet operational so delays could occur
IPEN/MB01 research reactor	Critical experiment facility	Nuclear and Energy Research Institute	Brazil	Operational	Dedicated critical experiment facility, extensive staff experience with designing critical experiments and ICSBEP and IRPhE evaluation process	Outside USA, no communicated plans for international collaboration
Reactor Critical Facility	University research reactor	Rensselaer Polytechnic Institute	USA	Operational	Inside USA, flexible reactor	Facility is not in a ICSBEP or IRPhE evaluation
Illinois Microreactor Demonstration Project	University research reactor	University of Illinois Urbana	USA	Licensing, not built	TRISO-like fuel	Not built yet, no flexibility, potentially not suitable for benchmarking
Molten Salt Nuclear Reactor Research	University research reactor	Abilene Christian University	USA	Licensing, not built	Uranium salt fuel	Not built yet, no flexibility, potentially not suitable for benchmarking
NextGen MURR	University research reactor	University of Missouri	USA	Licensing, not built	Modern upgrade	Not built yet, low flexibility, potentially not suitable for benchmarking
Kyoto University Critical Assembly	University research reactor	Kyoto University	Japan	Core upgrades in progress	Modern upgrade	Not built yet, potential loss of flexibility and capabilities

7. THERMAL SCATTERING LAW NUCLEAR DATA

7.1 INTRODUCTION

The licensing of transportation packages for fresh or spent fuel necessitates the comprehensive availability of nuclear data, encompassing various types of radiation particles and spanning a wide spectrum of energies, to support accurate computational prediction of k_{eff}. One specific category of relevant nuclear data is notably temperature-dependent and referred to as the thermal neutron scattering law (TSL), known as S(α, β). These data are used to simulate the interactions of thermal neutrons—that is, those with energies at or below 5–10 eV—with other materials in the model.

Thermal neutrons possess wavelengths comparable to the interatomic distances within solids, typically on the order of few angstroms. Moreover, the energy of thermal neutrons closely aligns with that of excitations within a scattering medium such as phonons in a solid. Consequently, thermal neutrons undergo inelastic scattering, involving the exchange of neutron energy and momentum through the creation or annihilation of phonons in solids. It is crucial to emphasize that, unlike other nuclear reactions in which the interaction occurs between the incident particle and a target nucleus, thermal neutron scattering involves interactions with an aggregate of atoms in solids or molecules in liquids. In other words, the thermal motion of atoms or molecules in the scattering medium can no longer be ignored and atoms cannot be assumed to be free. As a result, a thorough understanding and accurate calculations of the TSL necessitate a profound comprehension of the dynamics of the atoms within the scattering medium.

The inelastic thermal neutron double differential scattering cross sections, $d^2\sigma_{iel}/d\Omega dE_s$, is defined as

$$\frac{d^2\sigma_{iel}}{d\Omega dE'} = \frac{1}{4\pi}\frac{k_s}{k_i}\{\sigma_c S(\vec{Q},\omega) + \sigma_{inc}\, S_s(\vec{Q},\omega)\}, \tag{1}$$

where σ_{iel} is the inelastic scattering cross section, $\hbar\omega$ represents the energy transferred to (phonon creation) or from (phonon annihilation) the scattering medium, and $\hbar\,\vec{Q}$ represents the momentum transfer. σ_c and σ_{inc} are the bound atom coherent and incoherent scattering cross-sections, respectively. $S(\vec{Q},\omega)$ is called the thermal neutron scattering function [133, 134, 135]. It contains two terms:

$$S(\vec{Q},\omega) = S_s(\vec{Q},\omega) + S_d(\vec{Q},\omega), \tag{2}$$

where the self-scattering function, $S_s(\vec{Q},\omega)$, accounts for the non-interference (incoherent) effects, whereas the distinct scattering function, $S_d(\vec{Q},\omega)$, accounts for the interference (coherent) effects. It is worth noting that the Eq. (1) is composed of two parts: the first part is nuclear, which depends on the nuclear spin and is represented by the bound scattering cross-sections. It measures the undistorted properties of the scattering medium. The second part is atomic, which is represented by the scattering function and measures the spontaneous fluctuation of the scattering medium. That is, the scattering function of a scattering medium at a given temperature contains information about the dynamics of that system.

It is common to replace the $S(\vec{Q},\omega)$ (has a dimension of [time]) with a dimensionless one known as the *thermal scattering law*, $S(\alpha,\beta)$ [133, 136, 137], through the relation

$$S(\vec{Q},\omega) = \frac{\hbar e^{-\beta/2}}{k_B T}\, S(\alpha,\beta), \tag{3}$$

$$\frac{d^2\sigma_{iel}}{dE'd\Omega} = \frac{1}{4\pi k_B T}\sqrt{\frac{E'}{E}}e^{-\beta/2}\left(\sigma_c\, S(\alpha,\beta) + \sigma_{inc}\, S_s(\alpha,\beta)\right), \quad (4)$$

where α and β are dimensionless parameters that represent the momentum and energy transfer, respectively.

7.2 EVALUATION, PROCESSING, AND TRANSPORT CODE CAPABILITIES

The use of nuclear data in radiation transport codes requires consideration of the complex interplay among the measurement, evaluation, tabulation, processing, and representation of the various necessary interaction probabilities and distributions. Generally, the measurement, evaluation, and tabulation steps result in the release of nuclear data libraries such as ENDF, JEFF, JENDL, etc. These released data files contain evaluated data in specific formats designed to balance the fidelity of the reconstructed data with the constraints of the disk space and processing speed of computers. The formats are constantly reviewed, maintained, and updated to provide evaluators and users with the necessary data to perform state-of-the-art simulations. Various computer codes are used in the evaluation of TSLs, though in some cases the evaluation codes are included within processing code systems.

The released evaluated data must also be processed for use in radiation transport codes. The processing step translates the data from the format used in the evaluated library to one that can be more readily accessed by the transport codes. This step invests computational effort in processing the data so that the transport codes can operate more quickly and efficiently in using the data. As with the evaluated data formats, there is an ongoing connection between processing and transport codes to ensure that all necessary data are available in the appropriate formats for use in the transport codes. This connection can and frequently does influence evaluation formats and inherently the evaluation techniques available to evaluators. Ultimately, changes or improvements in nuclear data evaluation and representation must be implemented carefully throughout the entire nuclear data tool chain, and it is not always evident which step in the process is limiting for the deployment of a new or updated data representation scheme.

The following three subsections provide details about available, commonly used computer codes for generating TSLs, processing nuclear data, and performing radiation transport simulations. Each of these steps is essential to the deployment of advanced reactor technologies and the fabrication, transportation, and storage infrastructure needed to support them.

7.2.1 TSL Generation Codes

TSL generation codes are the first of the three types of codes discussed, as the file must be generated before the data are processed for, finally, use in radiation transport simulations. There are other codes further upstream used to determine some of the inputs for these evaluation codes, most notably the phonon density of states (PDOS), but those codes are not described here. These are codes that are used to develop the TSLs that are included in the released data libraries.

7.2.1.1 LEAPR/NJOY

The above equation is used in the LEAPR module of the NJOY code [138] and is built-in based on the so-called *incoherent approximation*, where the S_d term is neglected (i.e., $S_d = 0$). That is, $\frac{d^2\sigma_{iel}}{dE'd\Omega}$ given by Eq. (4) is rewritten as

$$\frac{d^2\sigma_{iciel}}{dE'd\Omega} = \sigma_{iciel}(E, E', T) = \frac{\sigma_c+\sigma_{inc}}{4\pi k_B T}\sqrt{\frac{E'}{E}}e^{-\beta/2}S_s(\alpha,\beta), \quad (5)$$

where σ_{iciel} stands for incoherent inelastic scattering cross section. There are many assumptions and approximations used to formulate and simplify the calculations of the $S_s(\alpha,\beta)$. It is assumed that the incoherent intermediate function has a Gaussian-like shape (Gaussian approximation), the solid interatomic forces are harmonic, only one kind of atom is present in the solid, the solid has one atom per unit cell, the unit cell has a cubic symmetry, and the vibrational modes of the crystal are described by a continuous spectrum, the PDOS, $\rho(\beta)$ [139]. Under these assumptions, the self-scattering function is written as

$$S_s(\alpha,\beta) = \frac{1}{2\pi}\int_{-\infty}^{\infty} e^{i\beta t}e^{-\gamma^2(t)}dt\,, \quad (6)$$

where *t* is time in units of $\hbar/k_B T$, and

$$\gamma^2(t) = \alpha\int_{-\infty}^{\infty}\frac{\rho(\beta)\left(1-e^{i\beta t}\right)e^{-\beta/2}}{2\beta sinh(\beta/2)}d\beta. \quad (7)$$

As seen from the above equation, in addition to the α and β grids, the only input needed is $\rho(\beta)$ so that LEAPR can generate $S_s(\alpha,\beta)$ at different temperatures in ENDF-6 File 7 format that can be processed using the THERMR module of the NJOY system. THERMR is discussed in more detail in Section 7.2.2.2.

In addition to calculation of the thermal scattering law, LEAPR utilizes $\rho(\beta)$ and the crystal structure information to calculate the coherent elastic scattering (known as Bragg's scattering), $\sigma_{cel}(E,\mu)$, only for some hexagonal (graphite, Be and BeO) and cubic (Al, Pb, and Fe) structures and also calculates the incoherent elastic scattering σ_{icel} for all solids using an analytical term. Regarding thermal neutron scattering from liquids such as water, LEAPR employs a solid-type spectrum for rotational and vibrational modes combined with a diffusion term.

7.2.1.2 NCrystal

NCrystal covers a broad spectrum of physics, encompassing coherent and incoherent elastic scattering alongside inelastic scattering across a diverse array of materials: powders, mosaic single crystals, layered single crystals, and liquids. Its expansive data library includes crucial materials relevant to neutron scattering facilities. Additionally, it performs small-angle neutron scattering (SANS) calculations using a spherical model and computes the dynamic structure factor, employing cubic symmetry or the Debye temperature [140, 141].

As mentioned earlier, within the ENDF-6 format, the elastic section stores either coherent elastic or incoherent elastic cross sections exclusively. The NCrystal+NJOY tool resolves this limitation by introducing the mixed elastic format, which suggests storing both coherent and incoherent elastic cross sections successively within the elastic section, mimicking their individual storage formats. Presently, this new format is not supported in MCNP, but a modified version of OpenMC has been developed to accommodate it.

7.2.1.3 OCLIMAX

OCLIMAX employs density functional theorem (DFT) calculations akin to NJOY to calculate inelastic and elastic cross sections [142]. However, it is distinguished by various capabilities; notably, it computes the coherent one-phonon distinct scattering function $S_d^1(\alpha, \beta)$. Unlike LEAPR, which approximates the dynamical structure factor using an incoherent approach for a cubic structure with one atom per unit cell, OCLIMAX precisely calculates this factor by utilizing polarization vectors for all atoms across any crystal symmetry and corresponding phonon frequencies, offering a more comprehensive assessment. Additionally, OCLIMAX generates inelastic neutron spectra for instruments like VISION and ARCS, allowing users to compare their computed spectra with experimental data. Moreover, it employs a Gaussian resolution function to determine scattering intensity, facilitating the comparison of the measured and calculated scattering functions.

7.2.1.4 FLASSH

Another code similar to OCLIMAX is the FLASSH code system [143]. It can perform many of the same kinds of calculations as OCLIMAX, but it also contains several post-processing capabilities to generate ENDF6-format files. However, a considerable drawback is that this tool is not publicly available, and this causes challenges in the TSL community.

7.2.2 Processing Codes

Processing codes are the next step in the process and are correspondingly described next. These codes perform the necessary step of processing the released data files to generate libraries that are usable in radiation transport codes. This reformatting of data may seem like a zero-value-added step, but it facilitates accelerated data use within the transport codes, reducing run time for end users.

7.2.2.1 AMPX

AMPX is a modular code package of computer programs used to provide continuous-energy (CE), multigroup (MG), and covariance data libraries for radiation transport and sensitivity/uncertainty (S/U) analysis packages in SCALE [144]. It also helps creating covariance data for uncertainty calculations and provides tailored depletion, activation, and decay data for ORIGEN. AMPX is an essential part of the SCALE code system, distributed along with its functionalities.

7.2.2.2 THERMR/NJOY

THERMR produces coherent and incoherent cross sections and scattering (energy-to-energy) matrices for free or bound scatterers in the thermal energy range. ACER prepares libraries in ACE (A Compact ENDF) format for the LANL CE Monte Carlo code MCNP, described in Section 7.2.3.2. The ACER module is supported by subsidiary modules for the different classes of the ACE format. All types of cross sections are represented on a union grid for linear interpolation. It is worth mentioning that a thermal kernel evaluation may include data to represent “coherent” elastic or “incoherent” elastic, and it always contains “incoherent” inelastic scattering, $S_s(\alpha,\beta)$.

7.2.2.3 FUDGE

Lawrence Livermore National Laboratory (LLNL) maintains a nuclear data processing code, FUDGE [145]. In the context of this report, FUDGE is primarily of interest as the preferred processing code for the Generalised Nuclear Database Structure (GNDS) [146]. GNDS is important here because this new data format will allow covariance data to be included with TSL evaluations or files. In the broader context, FUDGE is used to process evaluated nuclear data for use with the COG 3D Monte Carlo Transport code used at LLNL.

7.2.3 Transport Codes

7.2.3.1 SCALE

The SCALE software suite, developed and maintained by Oak Ridge National Laboratory (ORNL), encompasses a diverse range of interconnected modules catering to reactor physics, criticality safety, radiation shielding, and fuel cycle analysis [147]. Criticality safety analyses are performed with the KENO V.a, KENO-VI, or Shift 3D Monte Carlo transport codes. KENO V.a uses a restricted geometry package that facilitates fast neutron tracking for systems that can be represented with a small number of shapes. KENO-VI uses a generalized geometry package using linear and quadratic shapes, allowing significantly greater geometric complexity to be represented compared to that offered by KENO V.a. Shift has been implemented in SCALE, supporting both the KENO V.a and KENO-VI geometry descriptions.

All three Monte Carlo transport codes support either CE or MG neutron transport calculations. The CE treatment enables precise representation of physics, notably in characterizing thermal scattering using free gas and $S(\alpha,\beta)$ data. $S(\alpha,\beta)$ data are used for neutron energies below 10 eV. The MG transport calculations rely on cross section processing in the SCALE module XSProc to generate problem-dependent MG cross sections. The main component of XSProc is CENTRM, which solves the energy-dependent neutron spectrum in a representative 1D unit cell using the discrete ordinates method or a 2D unit cell using the method of characteristics. CENTRM predominantly employs the free gas model for most nuclides, except for materials with specific thermal scattering laws defined in the ENDF/B nuclear data files. The Monte Carlo transport codes use $S(\alpha,\beta)$ data below 5 eV.

7.2.3.2 MCNP

The MCNP code, or Monte Carlo N-Particle, handles the transport of diverse particles—charged (e.g., electrons, ions) and uncharged (e.g., neutrons, photons)—up to energies of 1 TeV/nucleon [148]. It employs collision physics, variance reduction methods, and pseudo-random number sampling to simulate particle transport through specified geometries. MCNP is developed and maintained by LANL.

Using tabulated nuclear and atomic data, MCNP models the physics governing each particle collision during transport. Specifically for neutrons, isotope-specific nuclear data are commonly represented in a CE format, covering all potential reaction channels, including various secondary-particle production mechanisms.

7.3 SENSITIVITY/UNCERTAINTY CAPABILITIES

Sensitivity analysis provides a unique perspective on system performance by quantifying how the system responds to changes in input processes. In the context of neutron transport simulations, calculating crucial outputs such as k_{eff}, reaction rates, and reactivity coefficients demands an array of input parameters, such as material compositions, system geometry, temperatures, and neutron cross-section data. Considering the complexity of nuclear data and its evaluation, understanding how neutron transport models react to cross-section data is an invaluable resource for analysts.

Uncertainty quantification plays a pivotal role in identifying potential sources of computational biases and highlighting parameters essential for validating the code. Formats and procedures are already established for representing covariances for various types of ENDF reaction data. The character of thermal neutron scattering data demands an uncertainty quantification approach that will necessarily differ from historical methodologies. Transport codes such as SCALE calculate sensitivity to the 1D scattering sensitivity, but not directly to the TSL. Covariance data are available for all neutron files including thermal scattering law data (though these covariances are identical to the neutron sub-library covariance files), but not for the two-dimensional S(α,β) data. As of this writing, no published ENDF evaluations include covariance data for TSL or its corresponding scattering cross sections. Moreover, a standardized approach for generating or preserving covariance data related to TSLs has not been established. Nonetheless, ongoing initiatives such as the GNDS and the Working Party on International Nuclear Data Evaluation Cooperation (WPEC) subgroup 42/44/48 are actively exploring thermal scattering covariances. Recent endeavors have focused on the assessment of covariances in thermal neutron scattering concerning moderators such as H_2O, D_2O, and graphite [149, 150, 151].

There are two primary neutron transport codes developed in the United States that contain S/U capabilities: SCALE and MCNP. The radiation transport capabilities of both codes are discussed in Section 7.2.3. A more focused discussion of their S/U capabilities is provided here.

7.3.1 SCALE/TSUNAMI

Sensitivity coefficients for criticality safety analyses are calculated using the TSUNAMI-3D sequence within SCALE using adjoint perturbation theory, as discussed in [152]. Both KENO V.a and KENO-VI geometries are supported in TSUNAMI-3D. Three different sensitivity calculation methods are deployed in SCALE 6.2 and 6.3 [147]: one for MG calculations and two for CE calculations. A brief summary of each method is presented here, but the details are not relevant to this discussion. The details are available in the references. TSUNAMI-1D and -2D sequences are also available to calculate sensitivities but are rarely relevant for criticality safety assessments; TSUNAMI-1D can be used effectively in analyzing homogenous 1D systems. All TSUNAMI methods calculate the sensitivity of k_{eff} to the 1D elastic scattering, MT 2, and inelastic scattering, MT 4 [147].

The MG sensitivity calculation methodology involves explicit calculations of forward and adjoint fluxes. These fluxes, or flux moments in 3D, are combined in the SAMS module to calculate the sensitivity coefficients. The BONAMI-ST module is used to calculate the “implicit” sensitivity contribution resulting from MG cross section processing. The MG method is used in TSUNAMI-1D and TSUNAMI-2D and is also available for use in TSUNAMI-3D.

The two CE sensitivity calculation methodologies are only available in TSUNAMI-3D. One method is the iterated fission probability (IFP) approach, and the other is the contributon-linked eigenvalue sensitivity/uncertainty estimation via track-length importance characterization (CLUTCH) method. Both methods perform the sensitivity calculation within a single forward k_{eff} calculation, but the methods differ in the proxy used for the importance function. In the MG method, the adjoint k_{eff} calculation explicitly provides the importance estimate. The IFP method uses an estimate of the progeny of each reaction in the asymptotic neutron population as a measure of importance [153]. The CLUTCH method tabulates an importance function on a spatial mesh, referred to as F*(r), that estimates the importance of fission chains beginning in a particular region of space [154].

Sensitivity and uncertainty analysis tools are also available in SCALE primarily via the TSUNAMI-IP sequence. TSUNAMI-IP combines nuclear covariance data with sensitivity coefficients to determine the nuclear data-induced uncertainty in the system k_{eff} value. This uncertainty quantification can be used for a number of purposes, including similarity assessment. The primary metric for S/U-based similarity assessment of critical benchmark experiments and safety application systems is the integral index c_k, which is a correlation coefficient based on the data-induced uncertainty [152].

Finally, SCALE contains a statistical analysis package for validation of criticality safety calculations called the Validation Analysis Data Evaluation Resource (VADER). VADER implements trending and non-trending analysis techniques, including both parametric and nonparametric approaches, referenced in validation guidance documents [155, 156].

7.3.2 MCNP/Whisper

Sensitivity coefficients can be calculated by providing one or more KSEN DATA cards. These cards specify the sensitivities to be calculated. The sensitivities can be calculated for specific nuclides, reactions, and/or energy bins. The default behavior is to calculate the energy-integrated sensitivity to the total cross section for each nuclide in the problem. MCNP sensitivity calculations are performed using the IFP methodology. Sensitivities can be calculated for elastic and inelastic scattering, MT 2 and 4 respectively, or for the "total scattering law," the "elastic scattering law," and the "inelastic scattering law." These "scattering law" sensitivities are specific to the 2D scattering data in the TSL. Various editing options are provided, but the ability to perform analysis on these results is limited by a lack of post-processing tools.

Whisper is a statistical analysis package developed at LANL to support nuclear criticality safety validation [157]. It leverages sensitivity profile data, coupled with covariance files related to select similar benchmarks, to determine calculational margin and a baseline margin of subcriticality (MOS) to establish an upper subcritical limit (USL) specific to the application. The calculational margin is determined via a nonparametric method based on the extreme value theorem.

7.4 AVAILABLE TSL FILES IN ENDF/B-VIII.1

Table 7-1 lists the TSL files that will be available in ENDF/B-VIII.1. (Preliminary TSL listing from early-access to ENDF 8.1 library.) The file names are grouped according to their purpose of use (moderator, fuel, filter, etc.), though there is no unique way to group them. Regarding the group of filters and structural materials, one could also argue that some of these materials could be used as moderators. Likewise, some moderators (e.g., graphite, Be-metal, BeO) can be used as filters or structural materials. In Table 7-1, "sd" refers to the definition in Equation 2, and "5p," "10p," and "100p" refer to ^{235}U abundance.

Table 7-1. Material number (MAT) and name for available TSL files in ENDF/B-VIII.1 (Preliminary TSL listing from early-access to ENDF 8.1 library)

MAT	Moderators	MAT	Metallic Hydrides
H /Water/Ice		5	H in YH_2
1	H in H_2O (liquid)	7	H in ZrH
50	O in H_2O (ice (Ih))	3001	Zr in ZrH_2
10	H in H_2O (ice (Ih))	3002	H in ZrH_2
51	O in D_2O (liquid)	3006	Zr in ZrHx
11	D in D_2O (liquid)	3007	H in ZrHx
2	para-Hydrogen	3011	Ca in CaH_2
3	ortho-Hydrogen	3013	^{1}H in CaH_2
12	para-Deuterium	3014	^{2}H in CaH_2
13	ortho-Deuterium	3031	^{7}Li in ^{7}LiH-mixed
Beryllium Compounds		3032	H in ^{7}LiH-mixed
26	Be (metal)	3034	^{7}Li in ^{7}LiD-mixed
204	Be+sd	3035	D in ^{7}LiD-mixed
27	Be in BeO	58	Zr in ZrH
46	O in BeO	55	Y in YH_2
28	Be in Be_2C	**MAT**	**Filters/Structural**
1021	C in Be_2C	112	Mg (metal)
Graphite		53	Al (metal)
30	crystalline graphite	56	Fe (metal)
301	Graphite + sd	59	Si
31	reactor-grade graphite (10% porosity)	49	beta-phase SiO_2
320	reactor-grade graphite (20% porosity)	3016	Si in SiO_2-alpha
32	reactor-grade graphite (30% porosity)	3017	O in SiO_2-alpha
Polymers		43	Si in SiC
33	CH_4 (liquid methane)	44	C in SiC
34	CH_4 (solid methane)	1051	C in CF_2
37	H in CH_2 (polyethylene)	1052	F in CF_2
39	H in $C_5O_2H_8$ (lucite)	3048	H in HF
40	C_6H_6 (benzene)	3047	F in HF
41	H in Paraffinic Oil	1001	Zr in ZrC
42	H in C_7H_8 (toluene)	1002	C in ZrC
1042	H in Mesitylene-Phase II	3052	Al in Al_2O_3
1011	C in C_8H_8	3053	O in Al_2O_3
1012	H in C_8H_8	**MAT**	**FLiBe**
1501	O in $C_5O_2H_8$	4001	F in FLiBe
1502	C in $C_5O_2H_8$	4002	Be in FLiBe
		4003	Li in FLiBe

MAT	Fuel	MAT	Fuel
71	N in UN	8205	U in UO_2-5p
72	U in UN	8210	U in UO_2-10p
75	U in UO_2	8248	U in UO_2-HALEU
45	O in UO_2	8249	U in UO_2-HEU
76	U in UC	8255	O in UO_2-5p
71	N in UN	8260	O in UO_2-10p
8000	U-metal	8297	O in UO_2-100p
8010	U-metal-10p	8298	O in UO_2-HALEU
8099	U-metal-HEU	8299	O in UO_2-HEU
8105	U in UC-5p	8305	U in UN-5p
8110	U in UC-10p	8310	U in UN-10p
8147	U in UC-100p	8347	U in UN-100p
8148	U in UC-HALEU	8348	U in UN-HALEU
8149	U in UC-HEU	8349	U in UN-HEU
8150	C in UC	8355	N in UN-5p
8155	C in UC-5p	8360	N in UN-10p
8160	C in UC-10p	8397	N in UN-100p
8197	C in UC-100p	8398	N in UN-HALEU
8198	C in UC-HALEU	8399	N in UN-HEU
8199	C in UC-HEU	8540	H in UH_3

7.5 THERMAL MODERATOR DATA ASSESSMENTS

7.5.1 Introduction

Table 7-2 highlights the design features of the thermal reactors summarized in Table 2-1, and it adds the SMR-160, an ARDP design featuring LEU fuel. The table also includes fuel and moderator/reflector materials and planned fuel enrichment values. Below are some notes about these materials:

1. All thermal reactors use TRISO particle fuel except SMR-160, which will use UO_2/UO_2-Gd_2O_3.
2. The TRISO fuel kernel could be uranium oxycarbide (UCO or $UC_{0.5}O_{1.5}$) or UN.
3. Two different moderators will be used in these reactors: graphite or water, but metal hydrides (YH_x or ZrH_x) are of some interest, so discussion on these is presented as well
4. KP-FHR will use FLiBe as a coolant, but it also moderates.

Table 7-2: Material features of the thermal-spectrum ARDP designs

Reactor	Company	Materials	Enrichment of ^{235}U
Xe-100	X-Energy	Moderator: Pebble Reflector: Graphite Fuel: TRISO particle (UCO)	HALEU
KP-FHR	Kairos Power	Moderator: Pebble (Pyrolytic Graphite), FLiBe Reflector: Graphite Fuel: TRISO particle(UCO) Coolant: FLiBe	15.5 wt%
eVinci	Westinghouse	Moderator: Graphite Fuel: TRISO particle (UCO)	19.75 wt%
BANR	BWXT	Moderator: Graphite Fuel matrix: SiC Cladding: Graphite Fuel: TRISO particle (UN)	19.75 wt%
SMR-160	Holtec International	Moderator and coolant: Water Fuel: UO_2/UO_2-Gd_2O_3 Cladding: Zirconium Alloy	4.95 wt%
Horizontal Compact High-Temperature Gas Reactor	MIT	Moderator: Graphite Fuel: TRISO particle ($UC_{0.5}O_{1.5}$)	Unknown; likely HALEU for TRISO particles

7.5.2 Available TSL Files and Measurements

Table 7-3 summarizes the available TSL files, corresponding differential, and double differential scattering cross-section measurements (Differential Meas.), transmission cross section measurements (Integral Meas.) and availability of benchmarking experiments for the main moderators including FLiBe coolant. In addition, other moderators (Be, BeO, MgO, SiC, and Be_2C) that could be used in composite form [158] are included.

Table 7-3: Summary of available TSL ENDF files and corresponding available differential, integral (cross sections) measurements as well as benchmark experiments

Material	Avail. TSL ENDF files	Differential Meas.	Integral Meas.	IRPhE Benchmark Experiments
Graphite	Yes	[159, 160, 161, 162, 163, 164, 165]	[166, 167, 168] [169, 170, 171, 172]	Yes
H_2O	Yes	[173, 174, 175, 176]	[177, 178, 179]	Yes
$ZrH_{1.6}$, & ZrH_2	Yes	[180] [181, 182]	[183, 184]	Yes
YH_2	Yes	[185] [186]	[187, 188, 189]	No
FLiBe	Yes	No	No	No
Be metal	Yes	[190]	[190, 191]	Yes, using HEU
BeO	Yes	No	[191]	Yes, using HEU
MgO	No	No	[192, 193]	Yes, using HEU
3C-SiC	Yes	No	No	No
Be_2C	Yes	No	No	No

7.5.3 Available Validation Data and Assessment of Data

7.5.3.1 Graphite

Crystalline graphite (e.g., highly oriented pyrolytic graphite) is highly anisotropic and has a density that is close to the theoretical density of 2.26 g/cm^3. Nuclear graphite has a complicated mesostructure and consists of filler material, a binder phase, and pores. Nuclear graphite also has a lower density due to its porosity, and is isotropic in nature [163]. Within the nuclear graphite structure, thermal neutrons undergo three different types of scattering: inelastic scattering, elastic scattering (called Bragg diffraction), and SANS. The latter interaction is caused by pores, voids, and cracks in nuclear graphite. It is worth mentioning that nuclear graphite porosity has no effect on graphite inelastic scattering; in other words, it does not affect the graphite lattice dynamics (phonons). The SANS cross section is temperature independent and is much higher than the inelastic scattering cross section. However, different graphite grades have different microstructures (porosity, pore size, cracks, etc.); thus, they show significant variations in the total cross section due to the variations in the SANS cross sections.

Neutron thermalization in graphite has been studied extensively both computationally and experimentally. The thermal scattering law of graphite has been measured since the late 1950s using triple-axis spectrometry [159, 160, 161, 162]. Recently, the scattering function and phonon density of states were measured using ORNL's Spallation Neutron Source (SNS) for different types of graphite [163, 164, 165]. The agreement between measured scattering function and calculated ones is excellent when including the coherent one-phonon contribution (^1S_d) [194]. The total scattering cross section is measured for both highly oriented pyrolytic graphite and nuclear graphite [167, 166, 168]. Excellent agreement between measured data of highly oriented pyrolytic graphite and calculated cross section was achieved when including the coherent one-phonon contribution (s_d^1) [163].

SANS cross sections for different types of nuclear graphite have been measured via transmission experiments [165, 169, 170, 171, 172]. Very recently, the SANS cross section was implemented in the MCNP code to investigate the influence of SANS on criticality calculations [164]. The table below lists the benchmarking experiments having graphite as neutron moderators and fuel enrichments between 5 and 19.75 wt% ^{235}U and includes neutron fluxes lower than 0.625 eV [72].

The Monte Carlo technique was employed to generate the scattering law covariance matrix through sampling an initial phonon frequency spectrum of graphite from first principles. This approach shows how this information can be propagated to compute uncertainties related to both differential and integral inelastic scattering cross sections [151]. Table 7-4 provides a summary of the graphite benchmark experiments detailed in the IRPhE 2021 handbook [72], where the fuel enrichment is in the 5–19.75 wt% ^{235}U range, and Figure 7-1 shows the C/E and portion of flux < 0.625 eV for each case.

Table 7-4. Graphite benchmark experiments in the 5–19.75 wt% ^{235}U enrichment range

Case Identification	# Matching Cases	Case Identification	# Matching Cases
HTR10-GCR-RESR-001	1	PROTEUS-GCR-EXP-001	4
HTTR-GCR-RESR-001	1	PROTEUS-GCR-EXP-002	1
HTTR-GCR-RESR-002	5	PROTEUS-GCR-EXP-003	4
HTTR-GCR-RESR-003	2	PROTEUS-GCR-EXP-004	2

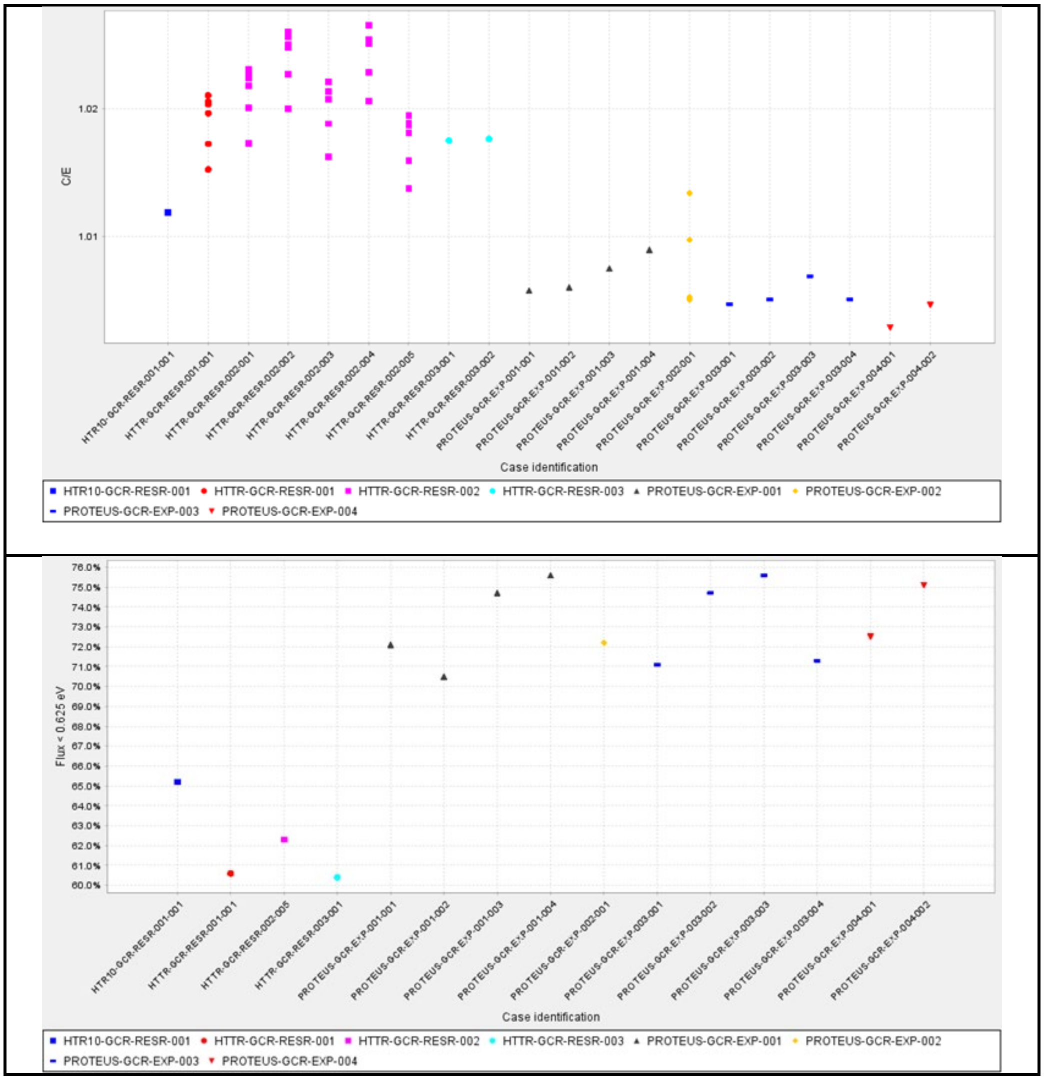

Figure 7-1: C/E (top) and flux percentage < 0.625 eV (bottom) for graphite cases, from IDAT [72, 73]

7.5.3.2 Light Water

There are several measurements of light water double-differential scattering cross sections [173, 174, 175, 176] as well as total cross sections [177, 178, 179]. Recently, the full-frequency spectrum was measured at different pressures using the SEQUOIA spectrometer at SNS [195]. The current S(α,β) (ENDF/B-VIII.1) for light water is for H in H_2O and was based on classical molecular dynamics using the TIP4P/2005f water potential known as the *CAB model* to calculate the frequency spectrum [196]. The internal vibrations were modeled using two discrete oscillators for the bending mode at 205 meV and for the stretching mode at 415 meV at all temperatures. The oxygen atom is treated as a free gas. Compared to previous evaluations, significant improvement was accomplished in terms of the calculated double differential and total inelastic scattering cross sections, and very good agreement with the corresponding measured data was achieved [194]. In addition, an analytical methodology to produce the covariance matrix associated with the CAB model parameters was developed and implemented in integral calculations on MISTRAL-1 and MISTRAL-2 configurations carried out in CEA Cadarache's EOLE critical facility [150]. Table 7-5 provides a summary of the light water benchmarking experiments detailed in the IRPhE 2021 handbook [72], where the fuel composition in the 5–19.75 wt% ^{235}U, and Figure 7-2 shows the C/E and flux (< 0.625 eV) for each case.

Table 7-5: Water benchmark experiments in the 5–19.75 wt% ^{235}U enrichment range

Case Identification	# Matching Cases	Case Identification	# Matching Cases
NRAD-FUND-RESR-001	2	OTTOHAHN-PWR-RESR-001	1
NRAD-FUND-RESR-002	2	PBF-FUND-RESR-001	2

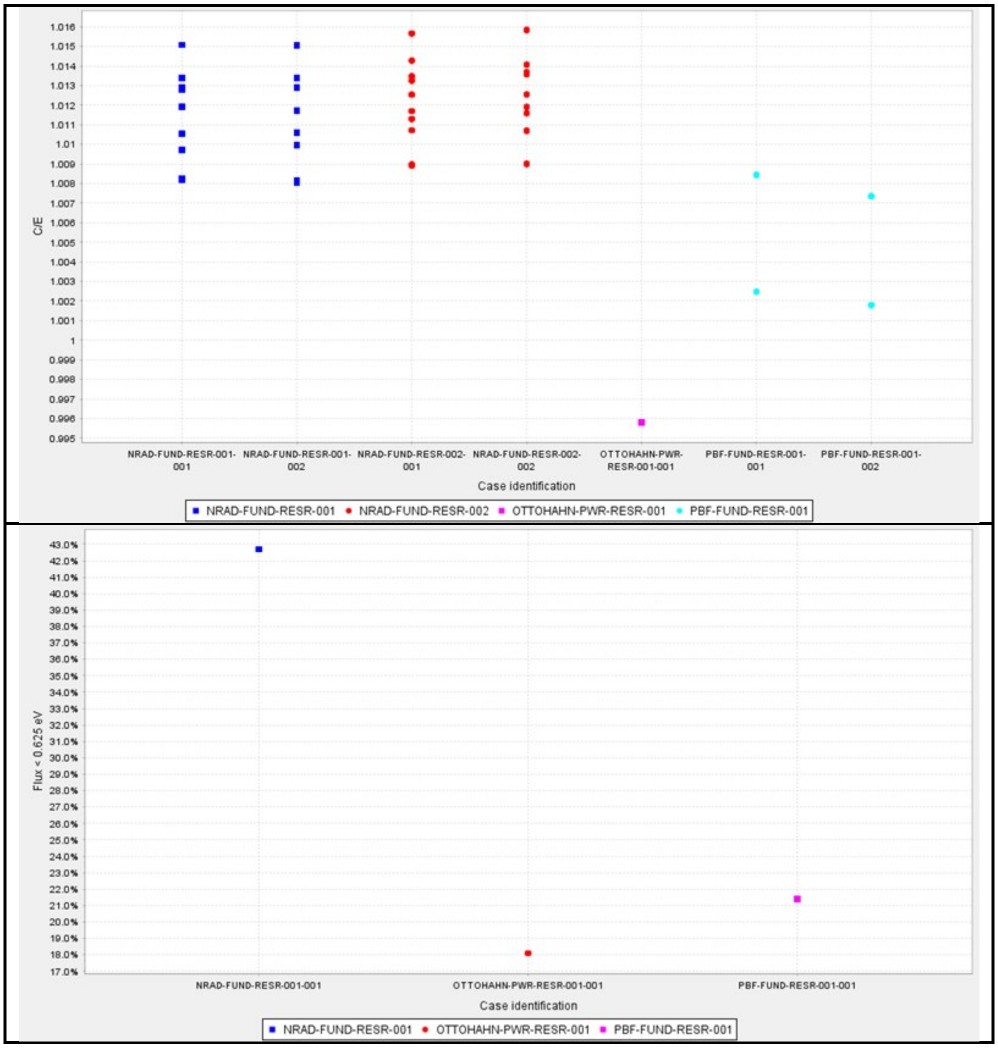

Figure 7-2: C/E (top) and flux percentage < 0.625 eV (bottom) for light water cases, from IDAT [72, 73]

7.5.3.3 ZrH_x

The latest ENDF/B-VIII.1 library contains three TSL files for hydrogen and zirconium in zirconium hydride. These are:

i) H and Zr in ZrH_2 (approximated face-centered cubic [FCC] crystal structure)
ii) H and Zr in ZrH_2 (body-centered tetragonal, ε–phase)
iii) H and Zr in $ZrH_{1.5}$ (fluorite structure, δ-phase)

The TSL file for the approximated FCC structure was based on the central force model with four atomic force constants proposed by Slaggie [197]. In this model, the body-centered tetragonal lattice structure of ZrH_2 (ε phase) was approximated by a face-centered cubic lattice. The atomic force constants were obtained by fitting both specific heat and neutron data whereas the phonon frequency spectrum was obtained by means of a root sampling technique.

Recently, first-principles calculations were employed to calculate the phonon density of states of the ε-phase and δ-phase [198]. These evaluations included the coherent elastic scattering, which was not included in the previous evaluations using the FCC crystal structure (ENDF/B-VIII.0 and earlier). The calculated phonon densities of states of both phases are in good agreement with the measured corresponding PDOSs [180]. The differential and double differential cross sections for ZrH_2 are in reasonable agreement with neutron scattering measurements [181, 182]. The total cross section for the $ZrH_{1.5}$ agrees well with neutron transmission measurements [183, 184].

The 2021 IRPhE handbook shows two benchmarking experiments including zirconium hydride as a part of fuel. These are NRAD-FUND-RESE-001 and -002, in which the fuel is a mixture of uranium (19.75 wt % ^{235}U), erbium (0.9 wt %), and zirconium hydride ($ZrH_{1.6}$). Only NRAD-FUND-RESR-001 has a 42.7% flux below 0.625 eV. It is worth mentioning that there is another benchmarking experiment TRIGA-FUND-RESR-001 in which the fuel is a mix of uranium and $ZrH_{1.6}$; however, the fuel enrichment is 20 wt % (i.e., > 19.75 wt %). Figure 7-3 shows the C/E ratio for these NRAD-FUND-RSER-001.

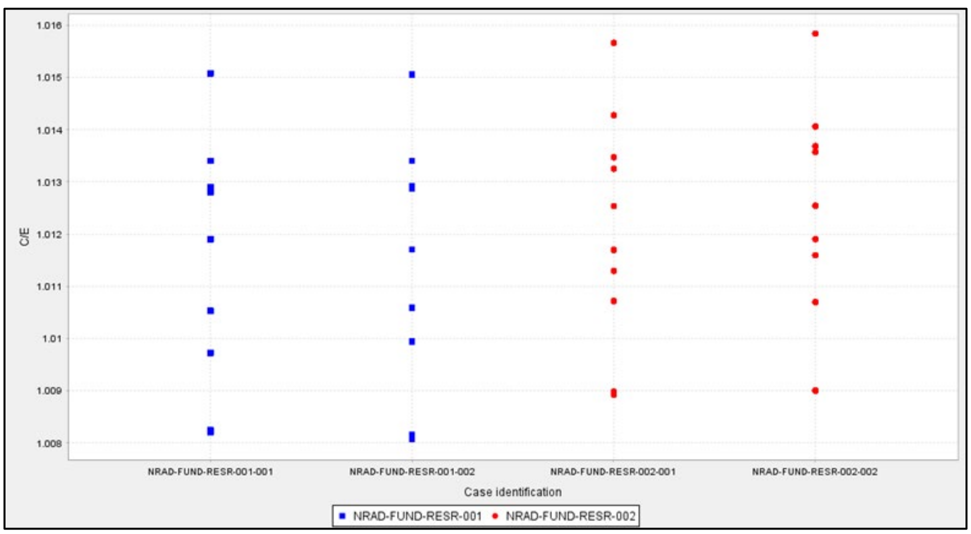

Figure 7-3: $ZrH_{1.6}$ C/E for NRAD-FUND-RESR-001, from IDAT [72, 73]

7.5.3.4 YH_x

Recently, yttrium hydride has attracted much interest in the thermal scattering law community as a high-temperature moderator for microreactor concepts because of its superior hydrogen retainment capacity at high temperatures. Ab initio lattice dynamics were used to calculate the partial phonon density of states of hydrogen in YH_2 and Y in YH_2 and to generate S(α,β) [199]. Excellent agreements were achieved between the calculated and measured heat capacity [200] and the calculated and measured total scattering cross section of hydrogen in $YH_{1.9}$ and $YH_{1.88}$ [189, 187]. In addition to thermal scattering law evaluation for stoichiometric YH_2, the thermal scattering law of YH_{2-x} (x:0.09–0.69) was also generated using ab initio lattice dynamics. For the validation of this work, the quasi-harmonic approximation was used to calculate the thermal expansion of YH_2 and the heat capacity at constant pressure [201]. In addition, measurements of the total thermal neutron cross section measurements $YH_{1.68}$ and $YH_{1.85}$ at room temperature using incident neutron energies between 0.0005 eV and 3 eV were performed [188]. The measurements of the double differential scattering cross section and scattering intensity spectra were conducted using the SEQUOIA spectrometer and the VISION instrument at SNS at 5 and 295 K for YH_x (x = 1.62, 1.74, 1.85, 1.90) [186]. It is only YH_2 that have TSL ENDF files. No benchmarking experiments are available for yttrium hydride.

7.5.3.5 FLiBe

FLiBe is a liquid formed by fusing crystalline LiF and BeF_2 salts at temperatures exceeding 732 K. It has the chemical formula Li_2BeF_4. FLiBe has outstanding properties such as chemical stability at high temperatures, a high moderating ratio, and high heat capacity. FLiBe has been proposed as a coolant, moderator, and heat storage medium in thermal neutron–driven nuclear reactors [202]. The thermal neutron scattering law for liquid FLiBe was calculated using the molecular dynamics (MD) model [202, 203]. Neither measured differential scattering data nor measured total scattering cross section measurements are available to validate the calculations. Also, no benchmarking experiments are available for FLiBe. However, the MD model calculations of FLiBe density, viscosity, and diffusion coefficients of lithium and fluorine in FLiBe show good agreement with corresponding measured data.

7.5.3.6 Beryllium Metal

Metallic beryllium has a hexagonal closed pack structure with two atoms per unit cell. Beryllium has a strong coherent scattering cross section. The current version of ENDF/B-VIII.1 includes two libraries: the first is based only on the incoherent approximation, whereas the second includes the contribution of the coherent one phonon scattering (i.e., ^1S_d), which was included in ENDF/B-VIII.0 [194]. The ab initio lattice dynamics [204] were used to generate the phonon density of states. Excellent agreements were observed between the calculated scattering law and the measured one [191], as well as between the calculated total scattering cross section and the measured one, especially when including the ^1S_d term [190]. There are two benchmark evaluations [68] that use beryllium as a moderator, listed in Table 7-6. Because of the high enrichment of ^{235}U, the measured, calculated, and C/E figures for these cases are not shown.

Table 7-6. Beryllium metal benchmark experiments with potential suitability for thermal energies

Case Identification	# Matching Cases	Fuel Enrichment (wt% ^{235}U)	Neutron Spectrum Energy
HEU-MET-THERM-025	2	93.40	Calculated flux percentage (<0.625) using three energy groups data is 5% for case 1 and 17.9% for case 2.
HEU-MET-THERM-026	27	80	No spectra data available in database

7.5.3.7 Beryllium Oxide

Beryllium oxide (BeO) is a ceramic compound that has a wurtzite structure with six atoms per unit cell. ENDF/B-VIII.1 includes two libraires; the first is for beryllium in BeO and the second one is for oxygen in BeO. Ab initio lattice dynamics were used to calculate the scattering function in the incoherent approximation. Very good agreement between the calculated total cross section and the measured one in the Bragg scattering region [191, 194] was observed. This evaluation improves upon the beryllium in BeO evaluation in ENDF/B-VIII.0 [194] by updating the mass and free atom cross section of oxygen to be those of the naturally weighted atom and using experimental lattice parameters in the calculation of the coherent elastic scattering cross section. The contribution of coherent one-phonon scattering is *no*t included in case of BeO as those of graphite and beryllium metal. One benchmarking experiment HEU-MET-THERM-027 [68] with 14 cases performed in 1950s is available for BeO with flux percentage (<0.625 eV) between 7.4 and 37.4%. However, the ^{235}U enrichment is 93.6%; therefore, the measured, calculated, and C/E figures for these cases are not shown.

7.5.3 Magnesium Oxide

There is no TSL ENDF file available for the MgO. However, Al-Qasir et al. [137] studied neutron thermalization within MgO through first principles lattice dynamics calculations. Their study revealed a remarkable alignment between the calculated and measured phonon dispersion relations [205]. Good agreement was also observed between the calculated and measured total cross sections at both 77 K and 300 K [192, 193]. However, there is some discrepancy that might be attributed to the presence of boron in the sample used in the transmission measurement. As a result, ENDF files for the thermal scattering laws of magnesium in MgO and oxygen in MgO were crafted and submitted to the Cross Section Evaluation Working Group for assessment, aiming for potential incorporation into the ENDF database. Only one benchmarking experiment, HEU-MET-THERM-009 [68], includes MgO as a separator: 32.2% of the flux is < 0.625 eV, the ^{235}U enrichment is 93.23%, and the measured, calculated, and C/E figures for these cases are not shown.

7.5.4 Silicon Carbide

The 3C-SiC (zinc blend structure) ENDF structure TSL file was calculated in the incoherent approximation using ab initio lattice dynamics [194]. The calculated phonon dispersion relations show very good agreement with measured data [206]. Unfortunately, there are no differential nor integral cross sections measurements. In addition, no benchmarking experiments are available for SiC.

7.5.3 Beryllium Carbide

Beryllium carbide (Be_2C) has an antifluorite cubic structure. The inelastic scattering cross sections were evaluated in the incoherent approximation using the beryllium and carbon phonon density of states. Unfortunately, there are no differential or integral cross sections to compare with. In addition, no benchmarking experiments are available for SiC. As of this writing, there is no published work documenting the generation of the TSL calculations used for the ENDF/B-VIII.1 evaluation. However, a previous similar analysis was done and published earlier using the same supercell size of 328 atoms and a unit cell lattice constant of 4.342 Å [207]. Good agreement was obtained between the calculated and measured heat capacity.

8. CONCLUSIONS

This report serves as a survey of current information as of early 2024 to consider in the prioritization of critical benchmarks for commercial-scale HALEU-based fuel cycles. It is intended as a starting point for a conversation between industry, NRC, DOE, national labs, and other parties, not an ending point. The overarching goal of the DNCSH project which has funded this work, is to enable rapid review of HALEU-based fuel cycle applications at NRC, for both front-end and back-end aspects, according to 10 CFR part 70 and 71, by addressing potential nuclear data or validation basis gaps which would be uncovered during application review at the NRC. It is our hope that these efforts also lead to valuable data that industry may use in the safety basis for optimized, commercial-scale operations.

One of the first questions to ask is which technologies to consider, and as a starting point, technologies related to DOE awards have been considered in this report, covered in Chapter 2. Even with this subset of all available technologies, the diversity in fuel forms, moderators, reflectors, and configurations is clear. Of particular deviation relative to current commercial reactor technology, are the variety of TRISO particle fuel compacts, advanced moderating materials such as yttrium hydride, liquid-fueled reactors, and small/micro reactors.

Small/micro reactors are interesting from a critical benchmark perspective. It is well-known that reducing core size increases neutron leakage and therefore optimized moderators/reflectors will yield large gains in efficiency. Development of state-of-the-art moderators and reflector materials, at best, coincides with the development of corresponding nuclear data evaluations. Critical benchmarks can only occur after the new material exists. An advantage of the small/micro size is a central, factory-based assembly which leads to transportation of a partially or fully assembled core from factory to plant. For criticality analysis during transportation, if exemptions for consideration of water in-leakage is pursued, it is likely the spectrum will be intermediate where there is a known lack of critical benchmarks. If water in-leakage is considered, the margin to critical may be small, and having a solid validation basis will be required.

Chapter 3 of this report introduced fuel cycle facilities and Chapter 4, transportation packages. Critical benchmarks to support commercial-scale HALEU-based fuel cycles are both are within the scope of the DNCSH project. Transportation packages have been initially prioritized somewhat, as facilities often have the option to use geometry and spacing to increase margin. For optimal transportation, there are fewer natural solutions. Decreasing the amount of material transported per package or per conveyance both have direct economic impacts and potentially safety impacts as there may be an argument that a large number of conveyances transporting small amounts of material increases the chance of an event. The industry has already licensed packages for LEU+ for the current LWR fleet which, by definition, are at commercial-scale. For most advanced reactors, more general-purpose containers would need to be used, which necessarily limit the amount of fuel to be transported and do not achieve what we would envision as commercial-scale.

Chapter 5 performed a survey of HALEU benchmarks in both ICSBEP and IRPhE handbooks. Modern validation basis assessments use similarity techniques which require an “application model” to compare to the suite of benchmark experiments. Therefore, it is impossible without these application models to fully assess the validation gaps that may exist. A key area of future work is to define application models that cover both front-end and back-end commercial-scale activities to clearly identify gaps. Ideally this is done in a way to be generic, and fairly simple, without the structural complexity needed for true transportation or storage designs. Only the neutronic characteristics are important for the validation basis assessment. However, with that said, it does appear there are numerous potentially applicable benchmarks to HALEU-based fuel cycles. Some key conclusions from that section are:

- A high number of thermal, intermediate, mixed, and fast experiments are available.

- The focus should be on performing experiments with different fuel forms such as TRISO particle compacts, uranium metal, and uranium salts across different EALF (thermal and fast).
- No critical experiments are available with burned HALEU fuel for validation of spent fuel storage and transportation.

Chapter 6 covered the suitability of critical benchmark facilities around the world, for which there are limited capabilities. Within the US, there is only SPRF/CX and NCERC. The Canadian ZED-2 facility may also be attractive for relevant benchmarks. Note that even if there are existing benchmarks which are shown to be applicable, new data points are likely valuable, especially when the existing benchmarks are from pre-2000s. Table 6-1 features a detailed discussion of each facility.

Chapter 7 covered nuclear data, focusing on the thermal neutron scattering law data which is relevant for any thermal systems, typical for hypothetical accident conditions used in criticality safety. Nuclear data is fundamental input to all criticality safety calculations and validation basis assessments. Also, as part of the application review process, NRC must assess the nuclear data and codes used by the applicant, as well as their analysis models. Therefore, we also seek to avoid future scenarios where, for example, an applicant would have designed an exotic moderator and used a nuclear data library in their analysis which did not include explicit TSL data for that moderator, falling back on a "free gas" treatment. The effect of this approximation both directly on k_{eff} and on the validation basis assessment must be understood. This section shows the scarcity of new TSL data that is available in recent versions of ENDF/B, i.e., the soon-to-be released ENDF/B VIII.1. For certain materials, it may be necessary for the NRC to recommend a more recent ENDF/B, and additional margin might be needed if a company utilizes a previous release of ENDF/B. The main result of the section is highlighting the need for experimental verification for modern graphite, YHx, FLiBe, and SiC data.

9. ACKNOWLEDGEMENTS

This work was funded by the U.S. Department of Energy, Office of Nuclear Energy and would not be possible without the support and collaboration with DOE-NE, the U.S. HALEU Consortium, and the U.S. Nuclear Regulatory Commission (NRC).

10. REFERENCES

[1] R. J. A. Yarmuth, "Inflation Reduction Act of 2022, H.R. 5376," 2022. [Online]. Available: https://www.congress.gov/bill/117th-congress/house-bill/5376.

[2] U.S. Nuclear Regulatory Commission, "Uranium Enrichment," December 2020. [Online]. Available: https://www.nrc.gov/materials/fuel-cycle-fac/ur-enrichment.html.

[3] U.S. DOE, "Advanced Reactor Demonstration Program," [Online]. Available: https://www.energy.gov/ne/advanced-reactor-demonstration-program.

[4] U.S. DOE, "Infographic for the Advanced Reactor Demonstration Program," [Online]. Available: https://www.energy.gov/ne/articles/infographic-advanced-reactor-development.

[5] TerraPower, "Natrium(TM) Reactor and Integrated Energy Storage," [Online]. Available: https://www.terrapower.com/our-work/natriumpower/. [Accessed 2 Jan 2024].

[6] TerraPower, "Natrium Fuel Cycle: Environmental Impacts," 16 August 2022. [Online]. Available: https://adamswebsearch2.nrc.gov/webSearch2/main.jsp?AccessionNumber=ML22227A204.

[7] TerraPower, "Natrium Fuel and Control Assembly Qualification," 25 January 2023. [Online]. Available: https://adamswebsearch2.nrc.gov/webSearch2/main.jsp?AccessionNumber=ML23066A331.

[8] TerraPower, "The Demonstration Project," [Online]. Available: https://natriumpower.com/wyoming/. [Accessed 2 January 2024].

[9] Nuclear Engineering International, "TerraPower awards contracts for Natrium Reactor Demonstration Project," *Nuclear Engineering International,* 16 August 2023.

[10] X-energy, "Xe-100," [Online]. Available: https://x-energy.com/reactors/xe-100. [Accessed 2 January 2024].

[11] X-Energy, "Overview of X-Energy's 200 MWth Xe-100 Reactor," 13 January 2021. [Online]. Available: https://www.nationalacademies.org/documents/embed/link/LF2255DA3DD1C41C0A42D3BEF0989ACAECE3053A6A9B/file/DCB77DCC95AEF75D0CA6FE9C717CAA34436F7817D15A?noSaveAs=1. [Accessed 2 January 2024].

[12] X-energy, "Xe-100 Topical Report: TRISO-X Pebble Fuel Qualification Methodology," 2021. [Online]. Available: https://www.nrc.gov/docs/ML2124/ML21246A289.pdf.

[13] X-Energy, "X-energy's TRISO-X Selects Oak Ridge Horizon Center for First Commercial Advanced Reactor Fuel Fabrication Facility in North America," 2022.

[14] Kairos Power, "Kairos Power Company Overview," October 2022. [Online]. Available: https://kairospower.consultation.ai/assets/pdf/Kairos_Power_Overview_Oct_2022.pdf.

[15] Kairos Power, "Kairos Power Atlas Fuel Fabrication Facility Pre-Application Meeting," 14 December 2021. [Online]. Available: https://www.nrc.gov/docs/ML2202/ML22028A086.pdf.

[16] Kairos Power, "Hermes Design Overview," 21 April 2022. [Online]. Available: https://www.nrc.gov/docs/ML2210/ML22105A581.pdf.

[17] Kairos Power, "Kairos Power Overview," 13 January 2021. [Online]. Available: https://www.nationalacademies.org/documents/embed/link/LF2255DA3DD1C41C0A42D3BEF0989ACAECE3053A6A9B/file/D3D9A732063C494A395EBC28DE77E71FB8519D7BFFF4?noSaveAs=1.

[18] Kairos Power, "Safety Evaluation Related to the Kairos Power LLC Construction Permit Application for the Hermes Test Reactor," June 2023. [Online]. Available: https://www.nrc.gov/docs/ML2315/ML23158A268.pdf.

[19] Westinghouse, "Principal Design criteria Topical Report (Non-Proprietary)," 28 June 2023. [Online]. Available: https://adamswebsearch2.nrc.gov/webSearch2/main.jsp?AccessionNumber=ML23179A199.

[20] Westinghouse, "Westinghouse eVinciTM Micro-Reactor," May 2021. [Online]. Available: https://www.nationalacademies.org/documents/embed/link/LF2255DA3DD1C41C0A42D3BEF0989ACAECE3053A6A9B/file/D9FCB39F5BE1C7A68DF05DEE6E3EF2018B4EBDB36F21?noSaveAs=1.

[21] Westinghouse, "eVinci Miroreactor Principal Design Criteria Topical Report NRC Pre-submittal Meeting," 22 June 2023. [Online]. Available: https://adamswebsearch2.nrc.gov/webSearch2/main.jsp?AccessionNumber=ML23165A156.

[22] Westinghouse, Bruce Power, "Executive Summary of the eVinci(TM) Micro-Reactor," October 2021. [Online]. Available: https://www.brucepower.com/wp-content/uploads/2021/10/210283A_WestinghouseBPMicroReactor_ExecutiveSummary_R000.pdf?__hstc=253552982.1605bb6ce919979b982676322b14664a.1635794433559.1635794433559.1635794433559.1&__hssc=253552982.1.1635794433560&__hsfp=342969.

[23] Idaho National Laboratory, "Final Environmental Assessment for the Molten Chloride Reactor Experiment (MCRE) Project," August 2023. [Online]. Available: https://www.energy.gov/sites/default/files/2023-08/final-ea-2209-molten-chloride-reactor-2023-08.pdf.

[24] TerraPower, "Development of TerraPower's Molten Chloride Fast Reactor (MCFR) to Enable Low-Cost, Economy-Wide Decarbonization," 21 May 2021. [Online]. Available: https://local.ans.org/savriv/wp-content/uploads/2021/06/SR-ANS-Brief_distributed.pdf.

[25] BWX Technologies, "BWXT's Advanced Nuclear Reactor (BANR)," 11 January 2021. [Online]. Available: https://www.nationalacademies.org/documents/embed/link/LF2255DA3DD1C41C0A42D3BEF0989ACAECE3053A6A9B/file/DD7F72C500641846CD3FC86C8D19F97B8889C926B7DE?noSaveAs=1.

[26] BWX Technologies, "Terrestrail Micro RX - BWXT Advanced Nuclear Reactor (BANR)," [Online]. Available: https://www.bwxt.com/what-we-do/advanced-technologies/terrestrial-micro-rx. [Accessed 2 January 2024].

[27] BWX Technologies, "BWXT Advanced Nuclear Reactor (BANR) Regulatory Update," 6 June 2023. [Online]. Available: https://adamswebsearch2.nrc.gov/webSearch2/main.jsp?AccessionNumber=ML23156A226.

[28] BWX Technologies, "BWXT to Manufacture HALEU Feedstock for Advanced Reactors," 30 August 2023. [Online]. Available: https://www.bwxt.com/news/2023/08/30/BWXT-to-Manufacture-HALEU-Feedstock-for-Advanced-Reactors-.

[29] Advanced Reactor Concepts, "ARC-100 Technical Summary," August 2023. [Online]. Available: https://www.arc-cleantech.com/uploads/ARC-100%20Technical%20Overview%20August%2023_FINAL.pdf.

[30] General Atomics Electromagnetic Systems, "Fast Modular Reactor Source Term Methodology," 31 October 2023. [Online]. Available: https://adamswebsearch2.nrc.gov/webSearch2/main.jsp?AccessionNumber=ML23317A093.

[31] W. Stewart, E. Velez-Lopez, R. Wiser and K. Shirvan, "Economic solution for low carbon process heat: A horizontal, compact high temperature gas reactor," *Applied Energy,* vol. 304, 2021.

[32] Centrus Energy Corporation, "Centrus Makes First HALEU Delivery to U.S. Department of Energy," 7 November 2023. [Online]. Available: https://www.centrusenergy.com/news/centrus-makes-first-haleu-delivery-to-u-s-department-of-energy/. [Accessed 2 January 2024].

[33] Centrus Energy Corporation, "Centrus Completes Construction and Initial Testing of HALEU Demonstration Cascade, Expects to Begin Production by End of 2023," 9 February 2023. [Online]. Available: https://www.centrusenergy.com/news/centrus-completes-construction-and-initial-testing-of-haleu-demonstration-cascade-expects-to-begin-production-by-end-of-2023/. [Accessed 2 January 2024].

[34] Centrus Energy Corporation, "Oklo Teams Up with Centrus to Produce U.S.-based Fuel Supply to Support the Commercialization of Advanced Fission," 17 November 2021. [Online]. Available: https://www.centrusenergy.com/news/oklo-teams-up-with-centrus-to-produce-u-s-based-fuel-supply-to-support-the-commercialization-of-advanced-fission/.

[35] Centrus Energy Corporation, "TerraPower and Centrus expand efforts to commercialize domestic HALEU production," 17 July 2023. [Online]. Available: https://www.centrusenergy.com/news/terrapower-and-centrus-expand-efforts-to-commercialize-domestic-haleu-production/.

[36] World Nuclear News, "Urenco USA announces HALEU activities," 6 February 2019. [Online]. Available: https://world-nuclear-news.org/Articles/Urenco-USA-announces-HALEU-activities.

[37] Urenco USA, "UUSA's Leadership Team Visits Santa Fe," 10 February 2023. [Online]. Available: https://urencousa.com/news/sustainability/2023/uusas-leadership-team-visits-santa-fe.

[38] Kairos Power, "Twitter," 9 Februrary 2023. [Online]. Available: https://twitter.com/KairosPower/status/1623722413317038080. [Accessed 2 January 2024].

[39] Ultra Safe Nuclear Corporation, "USNC - Factories," [Online]. Available: https://www.usnc.com/factory/. [Accessed 24 January 2024].

[40] BWX Technologies, "BWXT Starts Production of TRISO Fuel for First U.S. Generation IV Microreactor," 7 December 2022. [Online]. Available: https://www.bwxt.com/news/2022/12/07/BWXT-Starts-Production-of-TRISO-Fuel-for-First-US-Generation-IV-Microreactor. [Accessed 2 January 2024].

[41] BWX Technologies, "BWXT to Provide Nuclear Reactor Engine and Fuel for DARPA Space Project," 26 July 2023. [Online]. Available: https://www.bwxt.com/news/2023/07/26/BWXT-to-Provide-Nuclear-Reactor-Engine-and-Fuel-for-DARPA-Space-Project. [Accessed 2 January 2024].

[42] BWX Technologies, "BWXT Subsidiary Awarded $428 Million Contract for Uranium Conversion and Purification Services," 10 April 2023. [Online]. Available: https://www.bwxt.com/news/2023/04/10/BWXT-Subsidiary-Awarded-428-Million-Contract-for-Uranium-Conversion-and-Purification-Services. [Accessed 2 January 2024].

[43] General Electric, "Global Nuclear Fuel and TerraPower Announce Natrium Fuel Facility," 21 October 2022. [Online]. Available: https://www.ge.com/news/press-releases/global-nuclear-fuel-and-terrapower-announce-natrium-fuel-facility. [Accessed 2 January 2024].

[44] Nuclear Engineering International, "Orano plans extension of uranium enrichment capacity," 13 September 2023. [Online]. Available: https://www.neimagazine.com/news/newsorano-plans-extension-of-uranium-enrichment-capacity-11143485/.

[45] C. Hatch, "U.S. researchers fabricate commercial grade uranium dioxide HALEU fuel," Idaho National Laboratory, 20 November 2023. [Online]. Available: https://inl.gov/feature-story/u-s-researchers-fabricate-commercial-grade-uranium-dioxide-haleu-fuel/. [Accessed 2 January 2024].

[46] U.S. Nuclear Regulatory Commission, "New Fuels Licensing Activities," 7 July 2023. [Online]. Available: https://www.nrc.gov/materials/new-fuels/licensing-activities.html. [Accessed 2 January 2024].

[47] U.S. Nuclear Regulatory Commission, "Certificate of Compliance No. 9380, Rev. 2," 26 January 2023. [Online]. Available: https://adamswebsearch2.nrc.gov/webSearch2/main.jsp?AccessionNumber=ML23024A176. [Accessed 2 January 2024].

[48] U.S. Nuclear Regulatory Commission, "Certificate of Compliance, No. 9319, Rev. 14," 6 February 2023. [Online]. Available: https://adamswebsearch2.nrc.gov/webSearch2/main.jsp?AccessionNumber=ML23033A348.

[49] U.S. Nuclear Regulatory Commission, "Certificate of Compliance No. 9309, Rev. 14," 24 July 2023. [Online]. Available: https://adamswebsearch2.nrc.gov/webSearch2/main.jsp?AccessionNumber=ML23199A315.

[50] U.S. Nuclear Regulatory Commission, "Certificate of Compliance No. 9372, Rev. 4," 23 October 2023. [Online]. Available: https://adamswebsearch2.nrc.gov/webSearch2/main.jsp?AccessionNumber=ML23291A360.

[51] U.S. Nuclear Regulatory Commission, "Certificate of Compliance No. 9390, Rev. 3," 6 February 2024. [Online]. Available: https://adamswebsearch2.nrc.gov/webSearch2/main.jsp?AccessionNumber=ML24032A320.

[52] U.S. Nuclear Regulatory Commission, "Certficate of Compliance No. 9388, Rev. 0," 27 March 2023. [Online]. Available: https://adamswebsearch2.nrc.gov/webSearch2/main.jsp?AccessionNumber=ML23083B978.

[53] U.S. Nuclear Regulatory Commission, "Certificate of Compliance No. 9342, Rev. 18," 12 april 2023. [Online]. Available: https://adamswebsearch2.nrc.gov/webSearch2/main.jsp?AccessionNumber=ML23093A076.

[54] U.S. Nuclear Regulatory Commission, "Certificate of Compliance No. 9315, Rev. 16," 5 january 2021. [Online]. Available: https://adamswebsearch2.nrc.gov/webSearch2/main.jsp?AccessionNumber=ML21005A252.

[55] R. Hall, B. J. Marshall and W. A. Wieselquist, "Assessment of Existing Transportation Packages for Use with HALEU," Oak Ridge National Laboratory, Oak Ridge, TN, 2020.

[56] Westinghouse, "Application for Certificate of Compliance for the Traveller PWR Fuel Shipping Package, Revision 3," 24 January 2023. [Online]. Available: https://adamswebsearch2.nrc.gov/webSearch2/main.jsp?AccessionNumber=ML23020A925.

[57] Framatome, "Application for Certificate of Compliance for the MAP Series of PWR Fuel Shipping Packages," 30 March 2021. [Online]. Available: https://adamswebsearch2.nrc.gov/webSearch2/main.jsp?AccessionNumber=ML21090A324.

[58] Global Nuclear Fuel, "RAJ-II Safety Analysis Report, Rev. 11," September 2022. [Online]. Available: https://adamswebsearch2.nrc.gov/webSearch2/main.jsp?AccessionNumber=ML22266A190.

[59] Framatome, "Framatome TN-B1 Docket No. 71-9372 Safety Analysis Report," 31 January 2023. [Online]. Available: https://adamswebsearch2.nrc.gov/webSearch2/main.jsp?AccessionNumber=ML23031A217.

[60] Nuclear Engineering International, "HALEU fuel transport packaging," 12 January 2023. [Online]. Available: https://www.neimagazine.com/features/featurehaleu-fuel-transport-packaging-10510222/.

[61] NAC International, "NAC International Selected to Join Energy Department HALEU Consortium," 18 May 2023. [Online]. Available: https://www.nacintl.com/insights/nac-international-selected-to-join-energy-department-haleu-consortium.

[62] NAC International, "OPTIMUS® - OPTIMUS® Transport Packagings Brochure," [Online]. Available: https://www.nacintl.com/solutions/transportation/transportation-systems/optimus. [Accessed 2 January 2024].

[63] Orano, "Urenco and Orano sign consortium agreement to develop 30B-X cylinder for LEU+ and HALEU fuel transport," 2023. [Online]. Available: https://www.orano.group/usa/en/our-news/news-releases/2023/urenco-and-orano-sign-consortium-agreement-to-develop-30b-x-cylinder-for-leu-haleu-fuel-transport. [Accessed 2 January 2024].

[64] Orano, "Safety Analysis Report for the DN30-X Package, Rev. 3," 23 November 2022. [Online]. Available: https://adamswebsearch2.nrc.gov/webSearch2/main.jsp?AccessionNumber=ML22327A183.

[65] Orano, "Application for Certificate of Compliance for the Versa-Pac Shipping Package," December 2021. [Online]. Available: https://adamswebsearch2.nrc.gov/webSearch2/main.jsp?AccessionNumber=ML21356B710.

[66] Orano, "Expanded Double Capacity Approved for Orano Versa-Pac 55 Transport Package for LEU+ and HALEU," 5 September 2023. [Online]. Available: https://www.orano.group/usa/en/our-news/news-releases/2023/expanded-double-capacity-approved-for-orano-versa-pac-55. [Accessed 2 January 2024].

[67] Consolidated Nuclear Security, LLC, "Safety Analysis Report,Y-12 National Security Complex, Model ES-3100 Package with Bulk HEU contents," 16 June 2022. [Online]. Available: https://adamswebsearch2.nrc.gov/webSearch2/main.jsp?AccessionNumber=ML24060A099.

[68] J. B. Briggs, L. Scott and A. Nouri, "International Criticality Safety Benchmark Evaluation Project," *Nuclear Science and Engineering,* vol. 145, no. 1, pp. 1-10, 2003.

[69] J. D. Bess, et al., "Intrinsic value of the international benchmark projects, ICSBEP and IRPhEP, for advanced reactor development," *Frontiers in Energy Research,* vol. 11, 2023.

[70] A. Nouri, P. Nagel, J. B. Briggs and T. Ivanova, "DICE: Database for the International Criticality Safety Benchmark Evaluation Program Handbook," *Nuclear Science and Engineering,* vol. 145, no. 1, p. 11–19, 2003.

[71] M. D. DeHart, J. D. Bess and G. Ilas, "Review of Candidates for a Validation Data Set for High-Assay Low-Enrichment Uranium Fuels," *Journal of Nuclear Engineering,* vol. 4, pp. 602-624, 2023.

[72] J. B. Briggs and J. Gulliford, "An Overview of the International Reactor Physics Experiment Evaluation Project," *Nuclear Science and Engineering,* vol. 178, no. 3, p. 269–279, 2014.

[73] I. Hill, N. Soppera and M. Bossant, "IDAT: The International Handbook of Evaluated Reactor Physics Benchmark Experiments Database and Analysis Tool," *Nuclear Science and Engineering,* vol. 178, no. 3, pp. 280-294, 2014.

[74] D. Shen, et al., "Molten-Salt Reactor Experiment (MSRE) Zero-Power First Critical Experiment with U-235 (MSRE-MSR-EXP-001)," in *International Handbook of Evaluated Reactor Physics Benchmark Experiments*, OECD Nuclear Energy Agency, Paris, France, NEA/NSC/DOC(2006)1, 2019.

[75] M. Fukushima, K. Tsujimoto, S. Okajima and H. J., "FCA IX-7 Assembly Experiments: 20% Enriched Uranium Metal Core Surrounded by Depleted Uranium Metal Blanket (FCA-FUND-EXP-001)," in *International Handbook of Evaluated Reactor Physics Benchmark Experiments*, OECD Nuclear Energy Agency, Paris, France, NEA/NSC/DOC(2006)1, 2006.

[76] M. Kostal, et al., "VVER-1000 Physics Experiments Hexagonal Lattices (1.275 Pitch) of Low Enriched U(3.3 WT.% U235)O2 Fuel Assemblies in Light Water with Graphite and Fluoride Salt Insertions in Central Assembly (LR(0)-VVER-RESR-003)," in *International Handbook of Evaluated Reactor Physics Benchmark Experiments*, Organisation for Economic Co-operation and Development, Nuclear Energy Agency, Paris, France, NEA/NSC/DOC(2006)1, 2019.

[77] F. Fernex, et al., "Impact of Correlations Between Experiments on the Evaluation of Bias due to Nuclear Data by Assimilation Methodologies," in *Proceedings of the 12th International conference on Nuclear Criticality Safety 2023 (ICNC 2023), Sendai, Japan, October 2-5*, 2023.

[78] J. D. Bess, et al., "HTR-PROTEUS Pebble Bed Experimental Program Cores 1, 1A, 2, and 3: Hexagonal Close Packing with a 1:2 Moderator-to-fuel Pebble Ratio (PROTEUS-GCR-EXP-001)," in *International Handbook of Evaluated Reactor Physics Benchmark Experiments*, OECD Nuclear Energy Agency, Paris, France, NEA/NSC/DOC(2006)1, 2013.

[79] J. D. Bess, et al., "HTR-PROTEUS Pebble Bed Experimental Program Core 4: Random Packing with a 1:1 Moderator-to-fuel Pebble Ratio (PROTEUS-GCR-EXP-002)," in *International Handbook of Evaluated Reactor Physics Benchmark Experiments*, OECD Nuclear Energy Agency, Paris, France, NEA/NSC/DOC(2006)1, 2013.

[80] J. D. Bess, et al., "HTR-PROTEUS Pebble Bed Experimental Program Cores 5, 6, 7, & 8: Columnar Hexagonal Point-on-point Packing with a 1:2 Moderator-to-fuel Pebble Ratio (PROTEUS-GCR-EXP-003)," in *International Handbook of Evaluated Reactor Physics Benchmark Experiments*, OECD Nuclear Energy Agency, Paris, France, NEA/NSC/DOC(2006)1, 2013.

[81] J. D. Bess, et al., "HTR-PROTEUS Pebble Bed Experimental Program Cores 9 & 10: Columnar Hexagonal Point-on-point Packing with a 1:2 Moderator-to-fuel Pebble Ratio (PROTEUS-GCR-EXP-004)," in *International Handbook of Evaluated Reactor Physics Benchmark Experiments*, OECD Nuclear Energy Agency, Paris, France, NEA/NSC/DOC(2006)1, 2013.

[82] W. Wieselquist, et al., "Initial Efforts Organizing WPNCS SG-8: Preservation of Expert Knowledge and Judgement Applied to Criticality Benchmarks," *Transactions of the American Nuclear Society,* vol. 123, pp. 895-897, 2020.

[83] W. J. Marshall and R. B. T., "The SCALE Verified, Archived Library of Inputs and Data-VALID," in *Proceedings of the American Nuclear Society Nuclear Criticality Safety Division Conference, 2013 (NCSD 2013)*, Wilmington, NC, USA, September 29 – October 03, 2013.

[84] OECD Nuclear Energy Agency, "Document Content and Format Guide for the International Criticality Safety Benchmark Evaluation Project (ICSBEP) (Critical and Subcritical Measurements)," Organisation for Economic Co-operation and Development, Nuclear Energy Agency, Paris, France, NEA/NSC/DOC(95)03, 2021.

[85] A. Yamaji, "Evaluation guide for the International Reactor Physics experiments evaluation project (IRPhEP)," OECD Nuclear Energy Agency, Paris, France, EA/NSC/DOC(2013)2, 2013.

[86] R. Davis, et al., "Developing a High-Fidelity Benchmark of the University of New Mexico's AGN-201M Reactor," in *Proceedings of the American Nuclear Society Nuclear Criticality Safety Division Conference 2022 (NCSD 2022)*, Anaheim, CA, USA, June 12 – 16, 2022.

[87] A. Dos Santos, et al., "New Plate-Type Core of the IPEN/MB-01 Research Reactor Facility for Validation of RMB Project," in *Proceedings of the Research Reactors: Addressing Challenges and Opportunities to Ensure Effectiveness and Sustainability*, Buenos Aires, Argentina, 25–29 November, 2019.

[88] T. Cutler, et al., "The Deimos experiment: Advanced Reactor Testbed," *Transactions of the American Nuclear Society,* vol. 128, pp. 498-501, 2023.

[89] G. E. Hansen, et al., "Critical Experiments in Support of the CNPS Program," LA-UR-88-2272, Los Alamos National Laboratory, Los Alamos, NM, 1988.

[90] Nuclear News, "INL's MARVEL could demonstrate remote operation on a micro scale," 13 January 2021. [Online]. Available: https://www.ans.org/news/article-2537/inls-marvel-could-demonstrate-remote-operation-on-a-micro-scale/. [Accessed 4 January 2024].

[91] S. Sikorin, et al., "Benchmark Evaluation of Water-Moderated Hexagonal Lattices 21% Enriched UO2 Fuel Rods at "ROSE" Critical Facility," in *Proceedings of the 11th International conference on Nuclear Criticality Safety 2019 (ICNC 2019)*, Paris, France, September 15-20, 2019.

[92] J. Jarrell, "A Proposed Path Forward for Transportation of High-Assay Low-Enriched Uranium," INL/EXT-18-51518, Idaho National Laboratory, Idaho Falls, Idaho, 2018.

[93] N. Hall, X. He, Y. M. Pan and L. P., "Information Gaps and Potential Information Needs Associated with Transportation of Fresh (Unirradiated) Advanced Reactor Fuel Types," prepared for U.S. Nuclear Regulatory Commission, Center for Nuclear Waste Regulatory Analyses, San Antonio, Texas, 2020.

[94] B. T. Rearden, et al., "Initial Investigations of the Criticality Safety Validation Basis for HALEU Transportation," *Transactions of the American Nuclear Society,* vol. 120, p. 17–520, 2019.

[95] E. M. Saylor, A. Lang, W. J. Marshall and R. Hall, "Analysis of the 30B UF6 Container for Use with Increased Enrichment," ORNL/TM-2021/2043, Oak Ridge National Laboratory, Oak Ridge, Tennessee, 2021.

[96] W. J. Marshall, et al., "Initial Application of TSUNAMI for Validation of Advanced Fuel Systems," in *Proceedings of the 11th International conference on Nuclear Criticality Safety 2019 (ICNC 2019)*, Paris, France, September 15-20, 2019.

[97] R. A. Hall, W. J. Marshall, E. Eidelpes and B. M. Hom, "Assessment of Critical Experiment Benchmark Applicability to a Large-Capacity HALEU Transportation Package Concept," *Nuclear Science and Engineering,* vol. 195, pp. 310-319, 2021.

[98] C. Percher and G. Kenzie, "Experimental Needs for Criticality Safety Purposes," Nuclear Energy Agency, Nuclear Science Committee, Working Party on Nuclear Criticality Safety (WPNCS), NEA/NSC/R/M(2022)6, Paris, France, 2023.

[99] O. Buss and E. Poplavskaia, "NSC/WPRS Workshop on Zero Power Reactors "The demise of zero power reactors: From concern to action", Summary Record," Nuclear Energy Agency, Nuclear Science Committee, Working Party on Scientific Issues and uncertainty analysis of Reactors Systems (WPRS), NEA/NSC/WPRS/M(2023)4, Fontenay-aux-Roses, France, 2023.

[100] R. Sanchez, et al., "A New Era of Nuclear Criticality Experiments: The First 10 Years of Planet Operations at NCERC," *Nuclear Science and Engineering,* vol. 195, pp. S1-S16, Supplement 1, 2021.

[101] N. Thompson, et al., "A New Era of Nuclear Criticality Experiments: The First 10 Years of Comet Operations at NCERC," *Nuclear Science and Engineering,* vol. 195, pp. S17-S36, Supplement 1, 2021.

[102] J. Goda, et al., "A New Era of Nuclear Criticality Experiments: The First 10 Years of Godiva IV Operations at NCERC," *Nuclear Science and Engineering,* vol. 195, pp. S55-S79, Supplement 1, 2021.

[103] D. Hayes, et al., "A New Era of Nuclear Criticality Experiments: The First 10 Years of Flattop Operations at NCERC," *Nuclear Science and Engineering,* vol. 195, pp. S37-S54, Supplement 1, 2021.

[104] G. A. Harms, "Water Moderated Square-Pitched U(6.90)O2 Fuel Rod Lattices with 0.52 Fuel-to-Water Volume Ratio (LEU-COMP-THERM-078)," in *International Handbook of Evaluated*

Reactor Physics Benchmark Experiments, OECD Nuclear Energy Agency, Paris, France, NEA/NSC/DOC(2006)1, 2013.

[105] D. E. Ames, G. A. Harms and L. N., "Pitch Variation Experiments in Water-Moderated Square-Pitched U(6.90)O2 Fuel Rod Lattices with Fuel to Water Volume Ratios Spanning 0.08 to 0.67 (LEU-COMP-THERM-102)," in *International Handbook of Evaluated Criticality Safety Benchmark Experiments*, OECD Nuclear Energy Agency, Paris, France, NEA/NSC/DOC(95)03/IV, 2021.

[106] M. N. Dupont, D. Ames, G. Harms, W. J. Marshall and P. M. T., "Integral Experiment Request 554 CED-2 Summary Report," ORNL/TM-2023/3124, Oak Ridge National Laboratory, Oak Ridge, Tennessee, 2023.

[107] N. Leclaire, "Design of experiments involving molybdenum in SNL SPRF/CX facility," IRSN/2020-000464, Institut de Radioprotection et de Sûreté Nucléaire, Fontenay-aux-Roses, France, 2020.

[108] J. E. Atfield, B. Sur and Y. L. R., "Canda's ZPR Experience: ZED-2," in *Presented at the NEA/NSC/WPRS Workshop on Zero Power Reactors "The demise of zero power reactors: From concern to action,"*, Fontenay-aux-Roses, France, June 22-23 June, 2023.

[109] J. E. Atfield, G. B. Wilkin, A. Colton and F. B., "ZED-2 Reactor: Natural-Uranium Metal Fuel Assemblies in Heavy-Water (LEU-MET-THERM-003)," in *International Handbook of Evaluated Criticality Safety Benchmark Experiments,*, OECD Nuclear Energy Agency, Paris, France, NEA/NSC/DOC(95)03/IV, 2012.

[110] J. Atfield, et al., "28-Element Natural UO2 Fuel Assemblies in ZED-2 (ZED2-HWR-EXP-001)," in *International Handbook of Evaluated Reactor Physics Benchmark Experiments*, OECD Nuclear Energy Agency, Paris, France, NEA/NSC/DOC(2006)1, 2011.

[111] D. G. Watts, et al., "Physics Modeling for Conceptual Designs of Proposed Experiments in the ZED-2 Critical Facility for Testing SMR-Type Fuels," *Journal of Nuclear Engineering and Radiation Science,* vol. 8, no. 3, 2022.

[112] S. Sato, K. Tonoike, H. Okuno and P. G., "STACY: 80-cm-diameter Cylindrical Tank of 6%-Enriched Uranyl Nitrate Solutions (LEU-SOL-THERM-011)," in *International Handbook of Evaluated Criticality Safety Benchmark Experiments*, OECD Nuclear Energy Agency, Paris, France, NEA/NSC/DOC(95)03/IV, 2009.

[113] H. Sono, et al.,, "Modification of the STACY Critical Facility for Experimental Study on Fuel Debris Criticality Control," in *Nakajima, K. (eds) Nuclear Back-end and Transmutation Technology for Waste Disposal*, Tokyo, Japan, Springer, 2015, pp. 261-268.

[114] S. Gunji, "Status of New STACY," in *Status of New STACY," Presented at the NEA/NSC/WPRS Workshop on Zero Power Reactors "The demise of zero power reactors: From concern to action"*, Fontenay-aux-Roses, France, June 22-23, 2023.

[115] A. Dos Santos, et al., "Reactor Physics Experiments in the IPEN/MB-01 Research Reactor Facility (IPEN(MB01)-LWR-RESR-001)," in *International Handbook of Evaluated Reactor Physics Benchmark Experiments*, OECD Nuclear Energy Agency, Paris, France, NEA/NSC/DOC(2006)1, 2013.

[116] M. N. Dupont, M. D. Eklund, P. F. Caracappa and W. Ji, "Experimental Measurements of Isothermal Reactivity Coefficient and Temperature-dependent Reactivity Changes with Associated Uncertainty Evaluations," *Progress in Nuclear Energy,* vol. 118, pp. 103-131, 2020.

[117] M. N. Dupont, M. D. Eklund, P. F. Caracappa and W. Ji, "Inversion Point of the Isothermal Reactivity Coefficient with Increasing System Temperature in a Heterogeneous Core Lattice of a Light Water Reactor," *Nuclear Science and Engineering,* vol. 197, pp. 2884-2901, 2023.

[118] M. D. Eklund, P. J. Kowal, M. N. Dupont and W. Ji, "Evaluation of Temperature-Dependent Critical Experiments at the Walthousen Reactor Critical Facility for Benchmark Development," *Annals of Nuclear Energy,* vol. 180, 2023.

[119] M. N. Dupont, M. D. Eklund, P. F. Caracappa and W. Ji, "Development of Critical Experiments to Provide Validation Data for Multiphysics Coupling Codes," *Annals of Nuclear Energy,* vol. 128, pp. 256-267, 2019.

[120] Nuclear, Plasma & Radiological Engineering at the University of Illinois Urbana-Champaign, Ultra Safe Nuclear Corporation, "Illinois Microreactor Demonstration Project," [Online]. Available: https://npre.illinois.edu/about/illinois-microreactor-project. [Accessed 2024 4 January].

[121] R. Walton, "Abilene Christian University Taking Lead in Molten Salt Nuclear Reactor Research," Energy Tech, 22 September 2023. [Online]. Available: https://www.energytech.com/renewables/article/21274229/abilene-christian-university-taking-lead-in-molten-salt-nuclear-reactor-research. [Accessed 4 January 2024].

[122] U.S. Nuclear Regulatory Commission, "MSRR – Abilene Christian University Application," 19 May 2023. [Online]. Available: https://www.nrc.gov/reactors/non-power/new-facility-licensing/msrr-acu.html. [Accessed 4 January 2024].

[123] D. Haas and K. Clarno, "UTES – Building a Molten Salt Research Reactor in Texas by 2025," 7 September 2022. [Online]. Available: https://www.youtube.com/watch?v=Fi8DhmXZXS8. [Accessed 4 January 2024].

[124] E. D. Blakeman, T. E. Valentine, R. M. Westfall and W. T., "Water Moderated U(93.15 wt. %) Aluminum Research Reactor Fuel Element Subcritical Noise Measurements (SUB-HEU-MET-THERM-001)," in *International Handbook of Evaluated Criticality Safety Benchmark Experiments*, OECD Nuclear Energy Agency, Paris, France, NEA/NSC/DOC(95)03/II, 2006.

[125] E. D. Blakeman, T. E. Valentine, R. M. Westfall, W. T. and J. Gulliford, "Water Moderated U(93.15 wt. %) Aluminum Research Reactor Fuel Element Subcritical Noise Measurements with Strong Neutron Absorbing Materials (SUB-HEU-MET-THERM-002)," in *International Handbook of Evaluated Criticality Safety Benchmark Experiments*, OECD Nuclear Energy Agency, Paris, France, NEA/NSC/DOC(95)03/II, 2007.

[126] University of Missouri, "Design and development of the next generation University of Missouri Research Reactor," University of Missouri Request for Qualifications RFQ#23101, University of Missouri, Columbia, MO, 2023.

[127] C. H. Pyeon and K. Morioka, "Nuclear Data-Induced Uncertainty of Criticality in Solid-Moderated and Solid-Reflected Cores with Highly Enriched Uranium Fuel at Kyoto University Critical Assembly," *Nuclear Science and Engineering,* vol. 196, no. 10, p. 1147–1160, 2022.

[128] C. H. Pyeon, "Status of Critical Assembly (KUCA) and Training Reactor (UTR) in Japan," in *NEA/NSC/WPRS Workshop on Zero Power Reactors "The demise of zero power reactors: From concern to action"* , Fontenay-aux-Roses, France, June 22-23, 2023.

[129] Ellis A. N. , and Dean V., "VENUS-3 PWR UO2 Core 3-Dimensional Benchmark Experiment," in *International Handbook of Evaluated Reactor Physics Benchmark Experiments*, Organisation for Economic Co-operation and Development, Nuclear Energy Agency, Paris, France, NEA/NSC/DOC(2006)1, 2009.

[130] F. Valentina, et al., "Neutrons propagation in Lead: a feasibility study for experiments in the RSV TAPIRO fast research reactor," *EPJ Web of Conferences,* vol. 284, 2023.

[131] U. Kasemeyer, et al., "Benchmark on Kinetics Parameters in CROCUS," in *International Handbook of Evaluated Reactor Physics Benchmark Experiments*, Organisation for Economic

Co-operation and Development, Nuclear Energy Agency, Paris, France, NEA/NSC/DOC(2006)1, 2007.

[132] Powermag, "DOE Picks Nuclear Designs for First Microreactor Experiments at INL's New Test Bed," 23 October 2023. [Online]. Available: https://www.powermag.com/doe-picks-nuclear-designs-for-first-microreactor-experiments-at-inls-new-test-bed/.

[133] G. I. Bell and S. Glasstone, Nuclear Reactor Theory, New York, NY: Van Nostrand Reinhold Company, 1970.

[134] G. L. Squires, Introduction to the Theory of Thermal Neutron Scattering, Cambridge: Cambridge University Press, 1978.

[135] I. Al-Qasir, V. Gillette and A. Qteish, "Thermal neutron scattering kernels for uranium mono-nitride: A potential advanced tolerant fuel candidate for light water reactors," *Annals of Nuclear Energy,* vol. 127, pp. 68-78, 5 2019.

[136] R. E. Macfarlane, "New Thermal Neutron Scattering Files for ENDF/B-VI Release 2," *LA-12639-MS, Los Alamos National Laboratory,* 1994.

[137] I. Al-Qasir, N. Jisrawi, V. Gillette and A. Qteish, "Thermal neutron scattering cross sections of beryllium and magnesium oxides," *Annals of Nuclear Energy,* vol. 87, no. N/A, 2016.

[138] R. E. Macfarlane, D. W. Muir, R. M. Boicourt and A. C. Kahler, "The NJOY Nuclear Data Processing System," LA-UR-12-27079, Los Alamos National Labaratory, 2012.

[139] I. Al-Qasir, "Thermal Neutron Scattering in Graphite," PhD Dissertation, North Carolina State University, 2007.

[140] K. Ramić, J. I. M. Damian, T. Kittelmann, D. D. D. Julio, D. Campi, M. Bernasconi, G. Gorini and V. Santoro, "NJOY+NCrystal: An open-source tool for creating thermal neutron scattering libraries with mixed elastic support," *Nuclear Inst. and Methods in Physics Research, A,* vol. 1027, p. 166227, 2022.

[141] X.-X. Cai and T. Kittelmann, "NCrystal: A library for thermal neutron transport," *Computer Physics Communications,* vol. 246, p. 106851, 2020.

[142] Y. Q. Cheng and A. J. Ramirez-Cuesta, "Calculation of the Thermal Neutron Scattering Cross-Section of Solids Using OCLIMAX," *Journal of chemical theory and computation,* vol. 16, no. 8, pp. 5212-5217, 8 2020.

[143] N. Fleming, C. Manring, B. Laramee, J. Crozier, E. Lee and A. Hawari, "FLASSH 1.0: Thermal Scatterling Law Evaluation and Cross-Section Generation for Reactor Physics Applications," *Nuclear Science and Engineering,* vol. 197, no. 8, pp. 1887-1907, 2023.

[144] D. Wiarda, et al., "AMPX-6: A Modular code System for Processing ENDF/B Evaluations," Oak Ridge National Laboratory, ORNL/TM-2016/43, 2016.

[145] C. Mattoon, B. Beck and G. Gert, "Managing and Processing Nuclear Data Libraries with FUDGE," in *15th International Conference on Nuclear Data for Science and Technology (ND2022)*, Sacremento, California, 2023.

[146] Working Party on Nuclear Data Evaluation Cooperation, "Specifications for the Generalised Nuclear Database Structure (GNDS)," Organization for Economic Cooperation and Development Nuclear Energy Agency, Paris, France, 2020.

[147] W. A. Wieselquist, R. A. Lefebvre, Eds., "SCALE 6.3.1 User Manual," UT-Battelle, LLC, Oak Ridge National Laboratory, ORNL/TM-SCALE-6.3.1, Oak Ridge, TN, 2023.

[148] C. J. Werner, et al, "MCNP6.2 Release Notes," Los Alamos National Laboratory, report LA-UR-18-20808, 2018.

[149] C. W. Chapman, G. Arbanas, A. I. Kolesnikov, L. Leal, Y. Danon, C. Wendorff, K. Ramić, L. Liu and F. Rahnema, "Methodology for Generating Covariance Data of Thermal NeutronScattering Cross Sections," *Nuclear Science and Engineering,* vol. 195, pp. 13-32, 2021.

[150] J. P. Scotta, G. Noguère and J. I. M. Damian, "Generation of the 1H in H2O neutron thermal scattering law covariance matrix of the CAB model," *EPJ Nuclear Sci. Technol.,* vol. 4, p. 32, 2018.

[151] J. Holmes, A. Hawari and M. Zerkle, "A Phonon-Based Covariance Methodology for ENDF S(α, β) and Thermal Neutron Inelastic Scattering Cross Sections," *NUCLEAR SCIENCE AND ENGINEERING,* vol. 184, p. 84 –113, 2016.

[152] B. T. Rearden, M. L. William, M. A. Jessee, D. E. Mueller and D. A. Wiarda, "Sensitivity and Uncertainty Analysis Capabilities in SCALE," *Nuclear Technology,* vol. 174, no. 2, pp. 236-288, 2011.

[153] B. C. Kiedrowski and F. B. Brown, "Adjoint-Based k-Eigenvalue Sensitivity Coefficients to Nuclear Data Using Continuous-Energy Monte Carlo," *Nuclear Science and Engineering,* vol. 174, no. 3, pp. 227-244, 2013.

[154] C. M. Perfetti, B. T. Rearden and W. R. Martin, "SCALE Continuous-Energy Eigenvalue Sensitivity Coefficient Calculations," *Nuclear Science and Engineering,* vol. 182, no. 3, pp. 332-353, 2016.

[155] J. C. Dean and R. W. Tayloe, Jr, "Guide for Validation of Nuclear Criticality Safety Calculational Methodology," US Nuclear Regulatory Commission, Washington, D.C., 2001.

[156] J. J. Lichtenwalter, S. M. Bowman, M. D. DeHart and C. M. Hopper, "Criticality Benchmark Guide for Light-Water-Reactor Fuel in Storage and Transportation," US Nuclear Regulatory Commission, Washington, D.C., 1997.

[157] B. Kiedrowski, "User Manual for Whisper (v1.0.0), Software for Sensitivity- and Uncertainty Based Nuclear Criticality Safety Validation," LA-UR-14-26436, 2014.

[158] L. Snead, D. Sprouster, B. Cheng, et al., "Development and potential of composite moderators for elevated temperature nuclear applications," *Journal of Asian Ceramic Societies,* vol. 10, no. 1, pp. 9-32, 2022.

[159] F. Carvalho, "Inelastic Scattering of Thermal Neutrons in Graphite," *Nuclear Science and Engineering,* vol. 34, no. 3, pp. 224-236, 12 1968.

[160] P. A. Egelstaff, "The slow-neutron cross-section of graphite," *Journal of Nuclear Energy (1954),* vol. 5, no. 2, pp. 203-209, 1 1957.

[161] W. L. Whittemore, "Differential Neutron Thermalization. Annual Summary Report, October 1, 1965 through September 30, 1966. GA-7439, General Dynamics Corporation, General Atomic Division," San Diego, California, 1967.

[162] W. L. Whittemore, "Neutron Scattering by Reactor-Grade Graphite," *Nuclear Science and Engineering,* vol. 33, no. 1, pp. 31-40, 7 1968.

[163] I. I. Al-Qasir, Y. Cheng, J. Y. Lin, A. A. Campbell, G. Sala, K. Ramic, F. F. Islam, A. Qteish, B. Marsden, D. L. Abernathy and M. B. Stone, "Neutron thermalization in nuclear graphite: A modern story of a classic moderator," *Annals of Nuclear Energy,* vol. 161, p. 108437, 2021.

[164] K. Ramic, et al., "SCALE/MCNP testing of ENDF/VIII.1 TSLs for Graphite Thermal Reactor Benchmarks," Nuclear Data Week 2023 - Cross Section Evaluation Working Group (CSWEG) Meeting, 16 November 2023. [Online]. Available: https://indico.bnl.gov/event/18701/contributions/82620/.

[165] A. Kimura, S. Endo and S. Nakamura, "Total and Double Differential Scattering Cross-Section Measurements of Isotropic Graphite," in *Wonder 2023: 6th International Workshop on Nuclear Data Evaluation for Reactor Applications*, Aix-en-Provence, France, June 5-9, 2023.

[166] A. Steyerl and W. D. Trüstedt, "Experiments with a neutron bottle," *Zeitschrift für Physik,* vol. 267, no. 5, pp. 379-388, 10 1974.

[167] D. J. Hughes and R. B. Schwartz, Neutron Cross Sections, Tech. Rep. BNL-325;, 2nd ed., Brookhaven National Labaratory, Upton, NY, USA, 1958.

[168] B. I. Shamasundar, "Investigation of neutron thermalization in polycrystalline moderators," PhD Dissertation, Georgia Institute of Technology, 1974.

[169] S. Petriw, J. Dawidowski and J. Santisteban, "Porosity effects on the neutron total cross section of graphite," *Journal of Nuclear Materials,* vol. 396, no. 2-3, pp. 181-188, 1 2010.

[170] V. M. G. Josa, J. Dawidowski, J. R. Santisteban, F. Malamud and R. G. Oliveira, "Model for neutron total cross-section at low energies for nuclear grade graphite," *Nuclear Inst. And Methods in Physics Resarch, A,* Vols. 780,, pp. 27-32, 2015.

[171] J. I. Robledo, J. Dawidowski, J. I. M. Damián, G. Škoro, C. Bovo and G. Romanelli, "Measurement of neutron total cross sections at the VESUVIO spectrometer," *Nuclear Inst. And Methods in Physics Resarch, A,* vol. 971, p. 164096, 2020.

[172] C. D. Bowman, D. C. Bowman, T. Hill, J. Long, A. P. Tonchev, W. Tornow, F. Trouw, S. Vogel, R. L. Walter, S. Wender and V. Yuan, "Measurements of Thermal Neutron Diffraction and Inelastic Scattering in Reactor-Grade Graphite," *Nucl. Sci Eng.,* vol. 159, pp. 182-189, 2008.

[173] F. Bischoff, et al., "Low Energy Neutron Inelastic Scattering (LENIS) in Linear Accelerator Project Progress Report, Technical Report RPI-328-27," 1967.

[174] A. G. Novikov and A. A. Van'kov, "Temperature Dependence of the General Spectrum for Water," *Journal of Structural Chemistry,* vol. 31, pp. 77-85, 1990.

[175] M.-C. Bellissent-Funel, et al., "Incoherent Quasielastic Neutron Scattering From H2O and Aqueous ZnCl2 Solutions," *Molecular Physics,* vol. 52, no. 6, pp. 1479-1486, 1984.

[176] J. R. Beyster, et al., "Integral Neutron Thermalization, Annual Summary Report, October 1, 1964 through September 30, 1965, 'I USAEC Report GA-6824, General Atomic Division," General Dynamics Corporation, November 1, 1965.

[177] K. Zaitsev, "The Total Cross Sections of the Interaction of Ultracold Neutrons with H2O and D2O," *Soviet Atomic Energy,* Vols. 70,, p. 238, 1991.

[178] S. B. Stepanov, V. E. Zhitarev, F. M. Zelenyuk and V. Ya. Krasil'nikov, "Temperature dependence of total cold neutron cross section in light water and benzne," *Soviet Atomic Enerfgy,* vol. 37, p. 1094, 1974.

[179] S. B. Stepanov and V. E. Zhitarev, "Total cross section for the interaction of cold neutrons with water," *Soviet Atomic Energy,* vol. 41, p. 743, 1976.

[180] J. G. Couch, O. K. Harling and L. C. Clune, "Structure in the Neutron Scattering Spectra of Zirconium Hydride," *Phys. Rev. B,* vol. 4, p. 2675–2681, 1971.

[181] S. Kornbichler, "Bestimmung der Diffusionskonstanten D(E0,T) und <Dv(T)> Thermischer Neutronen in H2O, Phenylen, ZrH1.92 und D2O durch Messung der Streuwinkelverteilungen. II. Zirkonhydrid und Schweres Wasser," *Nukleonik,* vol. 78, p. 281, 1965.

[182] S. N. Purohit, "Inelastic neutron scattering in metal hydrides, UC and UO2, and applications of the the scattering law," in *Neutron Thermalization and Reactor Spectra, Vol. I*, 1967.

[183] W. L. Whittemore, "Neutron interaction in zirconium hydride," GA-4490, General Atomics, 1964.

[184] U. Schmidt, " Untersuchung der wasserstoff- und deuteriumschwingungen in metalhydriden, -hydrodeuteriden und -deuteriden mittles totaler neutronen- wirkunsquerschnitte," *ATKE,* vol. 12, p. 385, 1967.

[185] J. J. Rush, H. E. Flotow, D. W. Connor and C. L. Thaper, "Vibration Spectra of Yttrium and Uranium Hydrides by the Inelastic Scattering of Cold Neutrons," *J. Chem. Phys. ,* vol. 45, pp. 3817-3825, 1966.

[186] C. W. Chapman, X. Hu, G. Arbanas, A. I. Kolesnikov, Y. Cheng and a. L. Daemen, "Thermal Neutron Scattering Measurements of YHx for the Transformational Challenge Reactor," *Transactions of the American Nuclear Society,* vol. 122, pp. 783-786, 2020.

[187] K. Brand, "Total Neutron Cross Sections of Chemical Bound Protons and Deuterons in Some Metal Hydrides and Deuterides," *Atomkernenergie,* vol. 17, pp. 113-120, 1971.

[188] D. Fritz, et al., "Total thermal neutron cross section measurements of yttrium hydride from 0.0005 - 3 eV," *Annals of nuclear energy,* vol. 181, p. 109475, 2023.

[189] P. Vorderwisch and K. Wasserroth, "Total Neutron-Proton Scattering Cross Section of Yttrium Hydrid," *Atomkernenergie,* vol. 14, p. 370, 1969.

[190] G. M. Borgonovi, "Coherent Scattering Law for Polycrystalline Beyrllium," USAEC Report GA-9364 , General Atomic Division, 1969.

[191] D. J. Hughes and R. B. Schwartz, "Neutron cross sections," Tech. Rep. BNL-325, Brookhaven National Laboratory, Upton, NY, USA. Second Edition., 1958.

[192] S. Holmryd and D. Connor, "SiO2(Quartz), MgO, PbF2, and Bi as low-pass neutron velocity filters," *Review of Scientific Instruments,* vol. 40, no. 1, pp. 49-56, 1969.

[193] P. Thiyagarajan, R. Crawford and D. Mildner, "Neutron Transmission of a Single-Crystal MgO Filter," *Journal of Applied Crystallography,* vol. 31, no. 6, pp. 841 - 844, 1998.

[194] D. A. Brown, et al., "ENDF/B-VIII.0: The 8th Major Release of the Nuclear Reaction Data Library with CIELO-project Cross Sections, New Standards and Thermal Scattering Data," *Nuclear Data Sheets,* vol. 148, pp. 1-142, 2018.

[195] V. Jaiswal, L. Leal and A. I. Kolesnikov, "Analysis of the time-of-flight neutron scattering cross-section data for light," *EPJ Web of Conferences ,* vol. 239, p. 14007, 2020.

[196] J. I. M. Damián, J. R. Granada and D. C. Malaspina, "CAB models for water: A new evaluation of the thermal neutron scattering laws for light and heavy water in ENDF-6 format," *Annals of Nuclear Energy,* vol. 65, pp. 280-289, 2014.

[197] E. L. Slaggie, "Central Force Lattice Dynamical Model for Zirconium Hydride,," General Atomic report GA-8132, July 1967.

[198] J. L. Wormald, M. L. Zerkle and J. C. Holmes, "Generation of the TSL for zirconium hydrides from ab initio methods," *Journal of Nuclear Engineering ,* vol. 2, no. 2, pp. 105-113, 2021.

[199] M. L. Zerkle and J. C. Holmes, "A Thermal Neutron Scattering Law for Yttrium Hydride," *EPJ Web of Conferences,* vol. 146, p. 13005, 2017.

[200] H. E. Flotow, D. W. Osborne and K. Otto, "Heat Capacities and Thermodynamic Functions of YH2 and YD2 from 5° to 350°K and the Hydrogen Vibration Frequencies," *The Journal of chemical physics,* vol. 36, no. 4, pp. 866-872, 1962.

[201] V. K. Mehta, M. W. D. Cooper, R. B. Wilkerson, D. Kotlyar and S. C. Vogel, "Evaluation of Yttrium Hydride (δ-YH2-x) Thermal Neutron Scattering Laws and Thermophysical Properties," *Nuclear Science and Engineering,* vol. 195, p. 5 · 563, 2021.

[202] Y. Zhu, *Analysis of Neutron Thermalization in Liquid FLiBe,* PhD Dissertation, North Carolina State University, 2018.

[203] Y. Zhu, C. A. Manring and A. I. Hawari, "Thermal Scattering Law ENDF Libraries for Liquid FLiBe," *EPJ Web of Conferences,* vol. 247, p. 09023, 2021.

[204] J. Wormald and A. Hawari, "Thermal Neutron Scattering Law Calculations using Ab Initio Molecular Dynamics," *EPJ Web of Conferences,* vol. 146, p. 13002, 2017.

[205] M. Sangster, G. Peckham and D. Saunderson, "Lattice dynamics of magnesium oxide," *Journal of Physics C: Solid State Physics,* vol. 3, no. 5, p. 1026, 1970.

[206] Y. Zhu, "Thermal Neutron Scattering Cross Sections for Silicon Carbide," Master Thesis, North Carolina State Univeristy, 2014.

[207] B. Hehr and A. Hawari, "Generation of Thermal Neutron Scattering Libraries for Beryllium Carbide," in *Proceedings of the 1st International Nuclear and Renewable Energy Conference (INREC10)*, Amman, Jordan,, March 21-24, 2010.